

UNCLASSIFIED

AD 414886

DEFENSE DOCUMENTATION CENTER

FOR

SCIENTIFIC AND TECHNICAL INFORMATION

CAMERON STATION, ALEXANDRIA, VIRGINIA



UNCLASSIFIED

NOTICE: When government or other drawings, specifications or other data are used for any purpose other than in connection with a definitely related government procurement operation, the U. S. Government thereby incurs no responsibility, nor any obligation whatsoever; and the fact that the Government may have formulated, furnished, or in any way supplied the said drawings, specifications, or other data is not to be regarded by implication or otherwise as in any manner licensing the holder or any other person or corporation, or conveying any rights or permission to manufacture, use or sell any patented invention that may in any way be related thereto.

CATALOGED BY DDC

AS AD No. 414886

414886

ASD-TDR 63-633

APPLIED RESEARCH ON HIGH RESOLUTION CAMERA TUBES

TECHNICAL DOCUMENTARY REPORT NO. ASD-TDR 63-633

August 1963

Electronic Technology Division
AF Avionics Laboratory
AERONAUTICAL SYSTEMS DIVISION
Air Force Systems Command
Wright-Patterson Air Force Base, Ohio

Project No. 4156, Task No. 415605

Prepared under Contract No. AF33(657)-7939

by

Electron Tube Division
RADIO CORPORATION OF AMERICA
Lancaster, Pennsylvania

Authors: S. Grey, P. Herold, J. B. Lurie, P. C. Murray, O. J. Zoemelis

NOTICES

When Government drawings, specifications, or other data are used for any purpose other than in connection with a definitely related Government procurement operation, the United States Government thereby incurs no responsibility nor any obligation whatsoever; and the fact that the Government may have formulated, furnished, or in any way supplied the said drawings, specifications, or other data, is not to be regarded by implication or otherwise as in any manner licensing the holder or any other person or corporation, or conveying any rights or permission to manufacture, use, or sell any patented invention that may in any way be related thereto.

Qualified requesters may obtain copies of this report from the Defense Documentation Center (DDC), (formerly ASTIA), Arlington Hall Station, Arlington 12, Virginia.

This report has been released to the Office of Technical Services, U. S. Department of Commerce, Washington 25, D. C. , for sale to the general public.

Copies of this report should not be returned to the Aeronautical Systems Division unless return is required by security considerations, contractual obligations, or notice on a specific document.

ASD-TDR 63-633

APPLIED RESEARCH ON HIGH RESOLUTION CAMERA TUBES

TECHNICAL DOCUMENTARY REPORT NO. ASD-TDR 63-633

August 1963

**Electronic Technology Division
AF Avionics Laboratory
AERONAUTICAL SYSTEMS DIVISION
Air Force Systems Command
Wright-Patterson Air Force Base, Ohio**

Project No. 4156, Task No. 415605

Prepared under Contract No. AF33(657)-7939

by

**Electron Tube Division
RADIO CORPORATION OF AMERICA
Lancaster, Pennsylvania**

**Authors: S. Grey, P. Herold, J. B. Lurie, P. C. Murray,
O. J. Ziemelis**

ABSTRACT

Image orthicons with structured targets were tested using a new cycled test set which separates the functions of exposure and read-out by a selected time interval. Resolution of image orthicons, when cycled in a manner corresponding to slow scan read-out, has exceeded 50 percent sine-wave response at 500 TV lines/inch. Possible means of increasing resolution toward the contract objective of 1500 TV lines/inch are discussed.

Electron gun resolution, measured at high velocity, was nearly doubled during the year. Improvement was achieved by smoothing the mixed carbonate cathode coating.

The procedure used to process targets is explained in detail.

Towards the end of 1962 the procedure used to process targets was revised. These revisions resulted from the gradual evaluation of testing and methods procedures. The revised procedure is explained in detail.

The processing procedure for "enlarged pore targets" is explained in detail.

Tubes fabricated with integral mesh plug type targets made with Positop resist showed a considerable reduction in dark current. The processing procedure of targets made with Positop resist is explained in detail.

PUBLICATION REVIEW

Publication of this technical documentary report does not constitute Air Force approval of the reports findings or conclusions. It is published only for the exchange and stimulation of ideas.

TABLE OF CONTENTS

SECTION I: ASTRO-ELECTRONICS DIVISION, PRINCETON, N. J.
CONTRIBUTION

	<u>Page</u>
I. INTRODUCTION	1
II. IMAGE ORTHICON EVALUATION	2
A. Resolution	2
1. Experimental Evaluation of the Resolution of the Image Orthicon Image Section	3
2. Analytical Evaluation of Structured Target Resolution	5
3. The Field Effect on a Glass Image Orthicon Target	11
4. Low Velocity Beam Bending	15
5. Analytical Value of Image Orthicon Resolution	18
6. Measured Image Orthicon Resolution	19
B. Signal-to-Noise Ratio of Image Orthicons	21
C. Target Signal Erasure	22
D. Target Signal Decay	27
III. ELECTRON GUNS AND BEAMS	28
A. Effect of Energy Spreads on Resolution	31
B. Experimental Results	33
1. Resolution of Electron Beams From Smoothed Oxide Cathodes	33
2. Resolution of Electron Beams From Smoothed Cathodes-Low Velocity	34
3. Life Tests of Smoothed Cathode Electron Guns	44

TABLE OF CONTENTS (CONT'D.)

	<u>Page</u>
4. Performance Evaluation of BN Cathodes	44
5. Matrix Cathodes	46
6. Gun Geometry Variations	46
C. Electron Trajectory Studies	47
D. Digital Computer Program for Plotting Electron Trajectories	54
E. Positive Grid Guns	56
F. Experimental Guns	60
1. Smoothed Cathode on Passive Nickel Base	60
2. Cesium-Plasma Hollow-Cathode Image Orthicon Gun	62
3. Point Cathode Image Orthicon Gun	63
4. Hydrogen Activation of Image Orthicon Cathodes	65
G. High Beam Current Life Tests	65
IV. TEST EQUIPMENT	66
A. Life Test Rack and Power Supply	66
B. Cycled Operation Equipment	66
1. Functional Block Diagram (D1681064), Figure 23	68
2. Exposure Generator (C1680361), Figure 24	71
3. Delay and Sequence Controls I and II (D1681050 and D1681061) Figures 25a and 25b	71
4. Read Generator (D1681052), Figure 26	71
5. Algebraic Adders (C1680330), Figure 27	71

TABLE OF CONTENTS (CONT'D.)

	<u>Page</u>
6. Horizontal Keying Control (C1680324), Figure 28	77
7. Beam and Photocathode Drivers (C1680331 and A220174), Figures 29a and 29b	77
8. Vertical Deflection Generator (B224641 and A220173), Figures 30a and 30b	81
9. Horizontal Deflection Generator (C1680333), Figure 31	81
10. Voltage Adapter and Beam Signal Control (B224657), Figure 32	81
11. Power Supplies (C1680342), Figure 33	86
12. Power Supply (B224527), Figure 34	86
V. DISCHARGE DEPOSITION OF INCLUSION-FREE ALUMINUM TARGET BLANKS	86

TABLE OF CONTENTS (CONT'D.)

SECTION II: ELECTRON TUBE DIVISION, LANCASTER, PA.
CONTRIBUTION

	<u>Page</u>
Summary of Work Performed From 1 December 1961 to 1 December 1962	
I. INTEGRAL MESH PLUG TYPE TARGETS	90
A. Processing of Targets Using Old Procedure	90
1. Preparation of Sheet Aluminum	90
2. Anodizing	91
3. Generation of Collector Mesh and Al ₂ O ₃ Mesh	91
4. Plating of Ni Plugs	92
5. Preparation for Mounting	93
6. Mounting	93
7. Firing	94
B. Processing of Targets Using the Revised Procedure	95
1. Preparation of Sheet Aluminum	95
2. Anodizing	97
3. Generation of Collector Mesh and Al ₂ O ₃ Mesh	99
4. Plating of Ni Plugs	101
5. Preparation for Mounting	102
6. Mounting	104
7. Firing	104
II. SUMMARY OF PROCESSING	106
III. ENLARGED PORE TARGETS	108

TABLE OF CONTENTS (CONT'D.)

	<u>Page</u>
Summary of Work Performed From 1 December 1962 to 31 March 1963	
I. INTEGRAL MESH PLUG TYPE TARGETS MADE WITH POSITOP RESIST	110
A. Processing of Targets Using Positop Resist	111
1. Preparation of Sheet Aluminum	111
2. Anodizing	111
3. Generation of Collector Mesh and Al_2O_3 Mesh	111
4. Production of Dense Al_2O_3 Plugs	112
5. Preparation for Mounting	113
6. Mounting	113
7. Firing	113

List of Figures

<u>Fig. No.</u>	<u>Title</u>	<u>Page</u>
1	$\frac{1}{N_e}$ as a Function of $\frac{1}{\sqrt{VPC}}$ for 5820A image Section	4
2	Nickel Plug and Alumina Window Targets	6
3	Effect of a Raster on Typical Plug Sine-Wave Response	8
4	Two Scanning Modes for Plug Targets	9
5	Reduction of the Field Effect After Several Scans	12
6	Sine-Wave Responses in 5820 Glass Target Image Orthicon	16
7	Signal-to-Noise Ratio of F2 as a Function of Photocathode Illumination	23
8a	Monitor Display of Image Orthicon F2 Target with Integral Mesh Potential at +2.5 Volts	24
8b	Monitor Display of Image Orthicon F2 Target with Integral Mesh Potential at -2.5 Volts	25
8c	Monitor Display of Underscanned Portion of Alumina Window Target of Image Orthicon F2	26
9a	Amplitude of Initial Readout Pulse as a Function of Delay for Integral Mesh Targets	29
9b	Amplitude of Initial Readout Pulse as a Function of Delay for Several Image Orthicons	30
10a	Standard Cathode Surface	35
10b	Princeton Resprayed Cathode Surface	36
10c	Smoothed Cathode Surface	37

List of Figures (Cont'd.)

<u>Fig. No.</u>	<u>Title</u>	<u>Page</u>
11	Photo of Coining Tool	38
12	Photo of Smoothing Tool	39
13	Smoothing Operation	40
14	Sine-Wave Response of Image Orthicon Guns	41
15	Image Orthicon Gun Resolution as a Function of Beam Current	42
16	Resolution of Image Orthicon Guns as a Function of Operating Time	45
17	Relation Between N_e and I_{G2}/I_B	49
18	Radius of Arrival at Limiting Aperture (r_A) as a Function of Starting Radius (r_K)	50
19	5820A Electron Gun	52
20	Gun Diagrams for Computer Input	53
21	Electron Paths Computed in the Standard Gun	55
22	Cycled Image Orthicon Equipment-Block Diagram	69
23	Block Diagram-Pulse and Digital Circuitry	70
24	Exposure Generator	72
25a & b	Delay and Sequence Controls I and II	73, 74
26	Read Pulse Generator	75

List of Figures (Cont'd.)

<u>Fig. No.</u>	<u>Title</u>	<u>Page</u>
27	Algebraic Adders	76
28	Horizontal Keying Control	78
29a & b	Beam and Photocathode Drivers (C1680331 and A220174)	79, 80
30a & b	Vertical Deflection Generator (B224641 and A220173)	82, 83
31	Horizontal Deflection Generator	84
32	Voltage Adapter and Beam Signal Control	85
33	Low Voltage Power Supplies	87
34	Power Supply	88
35a, b	Cross-section of a 1000 Line Per Inch Target	98
36	Electrodiolysis of an Alumina Target	103
37	Expanded Monitor Picture of Target Made From 60 Minute Chromic Acid Anodized Film Operated in an Image Orthicon	107

List of Tables

No.	Title	Page
1	Image Section N_e as a Function of Photocathode Voltage	3
2	Resolution of Image Orthicons with Structured Targets	19
3	Resolution, with Life, of Image Orthicon Guns	44
4	Depth of Focus Measurements	58
5	Resolution, with Life, of Tube H-8643-9	61

ASD-TDR 63-633

SECTION I: ASTRO-ELECTRONICS DIVISION, PRINCETON,
N. J. CONTRIBUTION

I. INTRODUCTION

The material presented in this report is a summary of work performed from 1 December 1961 through 31 March 1963. Section I of this report summarizes the work effort performed by RCA Astro-Electronics Division, Princeton, New Jersey and Section II is a summary of the work effort performed by RCA Electron Tube Division, Lancaster, Pennsylvania.

The work being performed on this contract is in part a continuation of research performed on positive-grid electron guns in the last phases of Contract AF33(616)-6682. The new work effort to be accomplished under this contract is concerned with cathode, electron gun and electron beam problems; and with the development of a system for cycled operation of a camera tube of the image orthicon type. It is also a continuation of work in developing a target structure consistent with the requirements for a high sensitivity camera tube capable of 1500 television lines per inch at 50 percent sine-wave response over a 2" x 2" format and signal-to-noise ratio of 100.

Manuscript released by the authors, August 1963, for publication as an ASD Technical Documentary Report.

II. IMAGE ORTHICON EVALUATION

The properties of image orthicons which have been evaluated are those related to resolution, signal-to-noise ratio, signal decay and signal erasure. The resolution of each of the component apertures in the image orthicon has been analysed. Since the resolution of the complete image orthicon depends on the cascaded aperture responses of its components, the response of the complete tube can be calculated from the response of the components. Measured response of image orthicons with structured targets does not approach the calculated values. This discrepancy is an area of continuing investigation.

Signal-to-noise ratio has been measured for an image orthicon with a structured target containing thin alumina windows as the storage elements. Signal-to-noise ratios exceeding 40 db have been measured recently in a bandwidth of 20 megacycles. This high ratio is good evidence that the structured target with integral mesh can meet the signal storage objectives of this contract.

Decay of readout amplitude and resolution of several image orthicons has been measured for intervals of up to 4 seconds between exposure and readout. It has been found that structured targets perform satisfactorily. This result indicates that slow scan readout is a practical mode of operation for image orthicons containing structured targets.

Nearly complete signal erasure during readout has been found to be impractical. If beam current is optimized for resolution and signal-to-noise ratio a large residual signal remains. Complete erasure, therefore, requires an erasure field between readout and exposure. All of these factors related to image orthicon performance are discussed in detail in the following sections.

A. Resolution

The resolution of an image orthicon is determined by the cascaded aperture responses of its several components. The components contributing to the image orthicon response which have been studied are the following:

1. Image Section
2. Structured Target
3. Field Effect
4. Electron Beam

The aperture response of each of these is treated analytically or experimentally in this section. The cascaded response of these components gives a predicted resolution far exceeding that obtained experimentally. This indicates that the effect of unidentified apertures has not been considered. One possibility now being investigated is the bending and defocusing of the beam by the potential distribution on the target. The response of the known apertures is discussed first.

1. Experimental Evaluation of the Resolution of the Image Orthicon Image Section

The image section of the image orthicon consists of the photocathode surface, the image section target surface, and the accelerating region between these surfaces. A point on the photocathode is focused at the target by adjusting the magnetic field and photocathode voltage so that electrons traverse one complete cyclotron loop during their time-of-flight from the photocathode to the target.

A complete and comprehensive study of the image section was given in an earlier report (Ref. 1). Resolution data from that study are repeated in Table 1 below. These data are used to derive the curve in Figure 1.

Table 1: Image Section N_e (Ref. 2) as a
Function of Photocathode Voltage

Photocathode Voltage	Resolution N_e
150 volts	458 TV lines/inch
200	631
300	770
400	936
500	1276
600	1125
700	1329

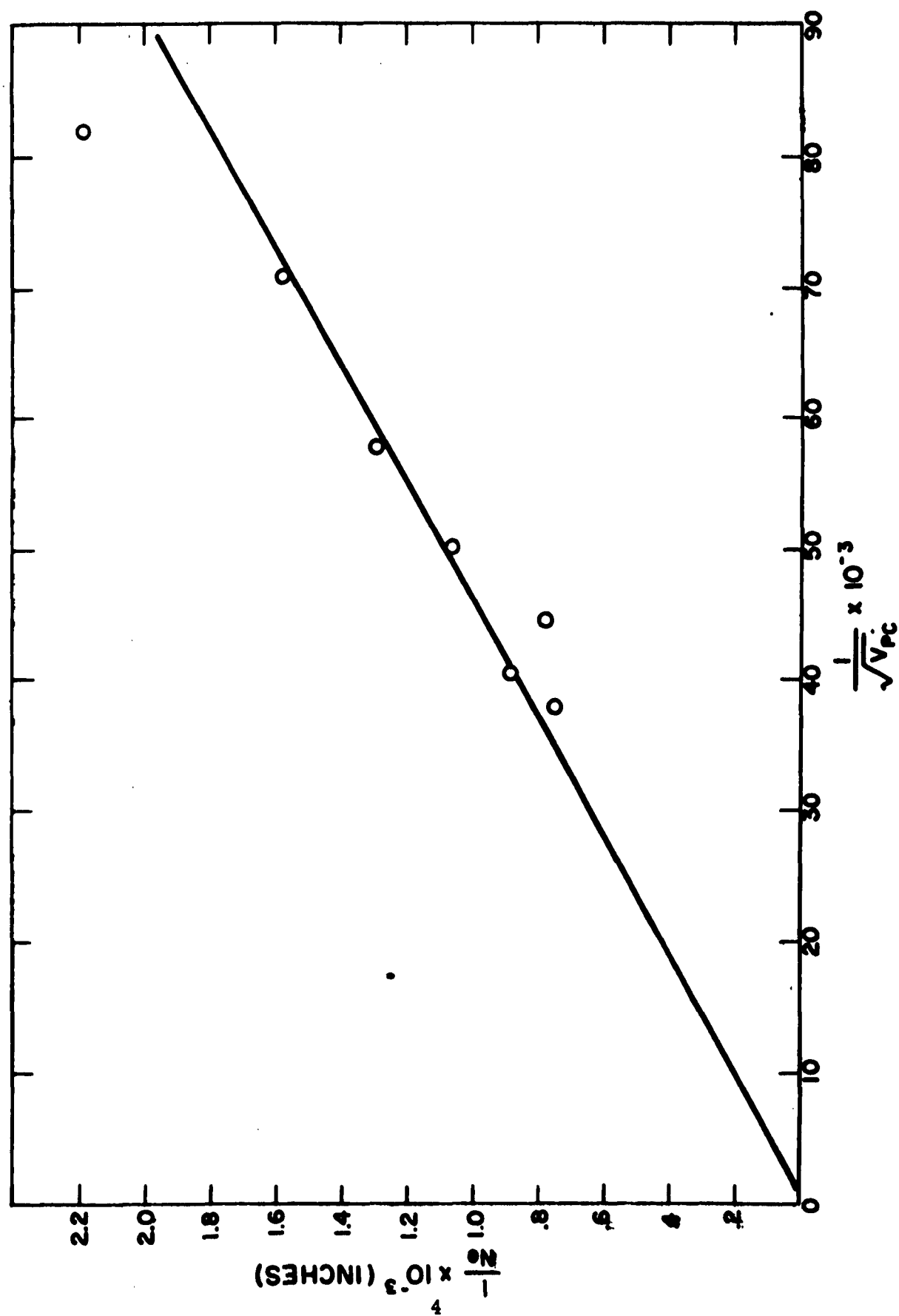


FIG. 1 $\frac{1}{N_e}$ AS A FUNCTION OF $\frac{1}{\sqrt{V_{pc}}}$ FOR 5820 A IMAGE SECTION

The co-ordinates of this curve have been chosen so that the ordinate is proportional to spot size at the target. A straight line drawn through the origin and the data points gives the spot size as a function of $\frac{1}{\sqrt{V}}$, where V is the voltage between photocathode and target. For sufficiently high voltages V, the emission velocity of the photoelectrons may be neglected in time of flight calculations. In that case the abscissa is proportional to time of flight. In other cases this curve cannot be used to predict resolution as a function of V unless the image section in question is the same length as the one for which the curve is drawn.

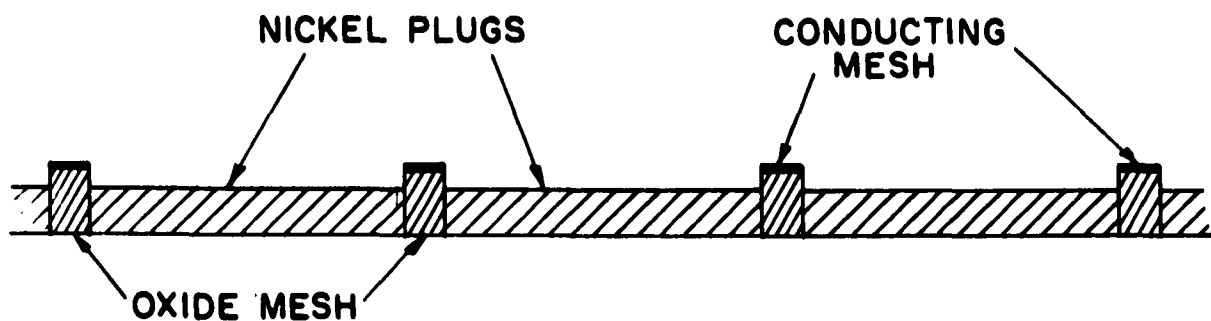
Normal image orthicon photocathode voltages range between 400 and 540 volts. For the 5820 image section presently in use, the value of N_e for the photocathode to target aperture process exceeds 1000 TV lines per inch. This figure will be used later to calculate the overall image orthicon performance.

2. Analytical Evaluation of Structured Target Resolution

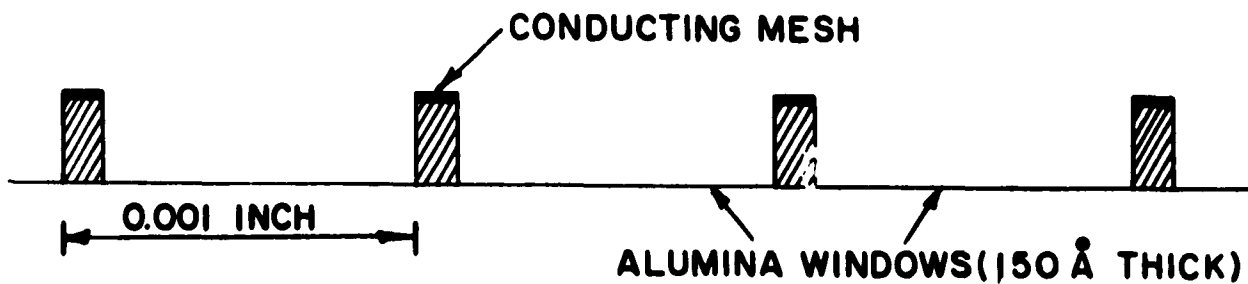
Image orthicons with two types of structured targets have been evaluated experimentally. Both targets have an alumina supporting structure or framework and an integral nickel mesh on the image section side of the target. The essential difference between the two targets is the nature of the charge storage element. One target uses nickel plugs as storage elements while the other uses thin alumina windows. Drawings of these targets are shown in Figure 2.

The proximity of the mesh to the charge storing element results in high capacitance for these target structures as compared to conventional targets. This high capacitance is necessary to attain the contract objective of a high signal-to-noise ratio.

Because the nickel plugs are good electrical conductors, the calculation of the sine-wave response of this target is mathematically more straightforward than a similar



(a) NICKEL PLUG INTEGRAL MESH TARGET



(b) ALUMINA WINDOW INTEGRAL MESH TARGET

FIG. 2 NICKEL PLUG AND ALUMINA WINDOW TARGETS

calculation for the target with alumina windows. The analytical treatment of an alumina-window target would involve assumptions concerning the position and mobility of the stored charges.

In the nickel-plug target the signal is derived by the electron beam scanning the beam side of the plugs. The nickel plugs are highly conducting but are well insulated from one another by the alumina supporting structure of the target. Measurements presented later show that charges remain on the plugs without loss to the mesh or neighboring plugs for a number of seconds. The evidence lends validity to the analytical treatment of plug target resolution given below.

The calculation of the plug target sine-wave response was performed by considering the target as two apertures in cascade^(Ref. 3). The first aperture is the plug, which is treated as a square aperture of uniform transmittance. The assumption of uniform transmittance is equivalent to assuming that the scanning beam sees an equipotential surface on each plug. Therefore, this calculation takes into account the field effect discussed below. Computations were made for the two cases: scanning parallel to a side of the square and scanning parallel to a diagonal of the square. The second aperture is the raster effect of the mesh which superimposes a carrier wave on the signal. The presence of the mesh limits the line numbers which may be transmitted by the system to values less than or equal the raster constant, n_r , which in this case is the number of plugs per unit length. The sine-wave response of the mesh is unity for $0 \leq N \leq n_r$. The effect of a mesh, or other two dimensional raster, on a sine-wave response of a typical plugs is shown in Figure 3.

To calculate the sine-wave response of a plug one assumes that a point charge placed on the photocathode side of the plug will spread over the element in such a way that the entire plug surface is an equipotential. When the scanning direction is perpendicular to the mesh structure the element is a square aperture. If its side is "a" (see Figure 4a), the sine-wave response is given by $r \tilde{\Psi}(N) = \frac{\sin(\pi Na/2)}{\pi Na/2}$.

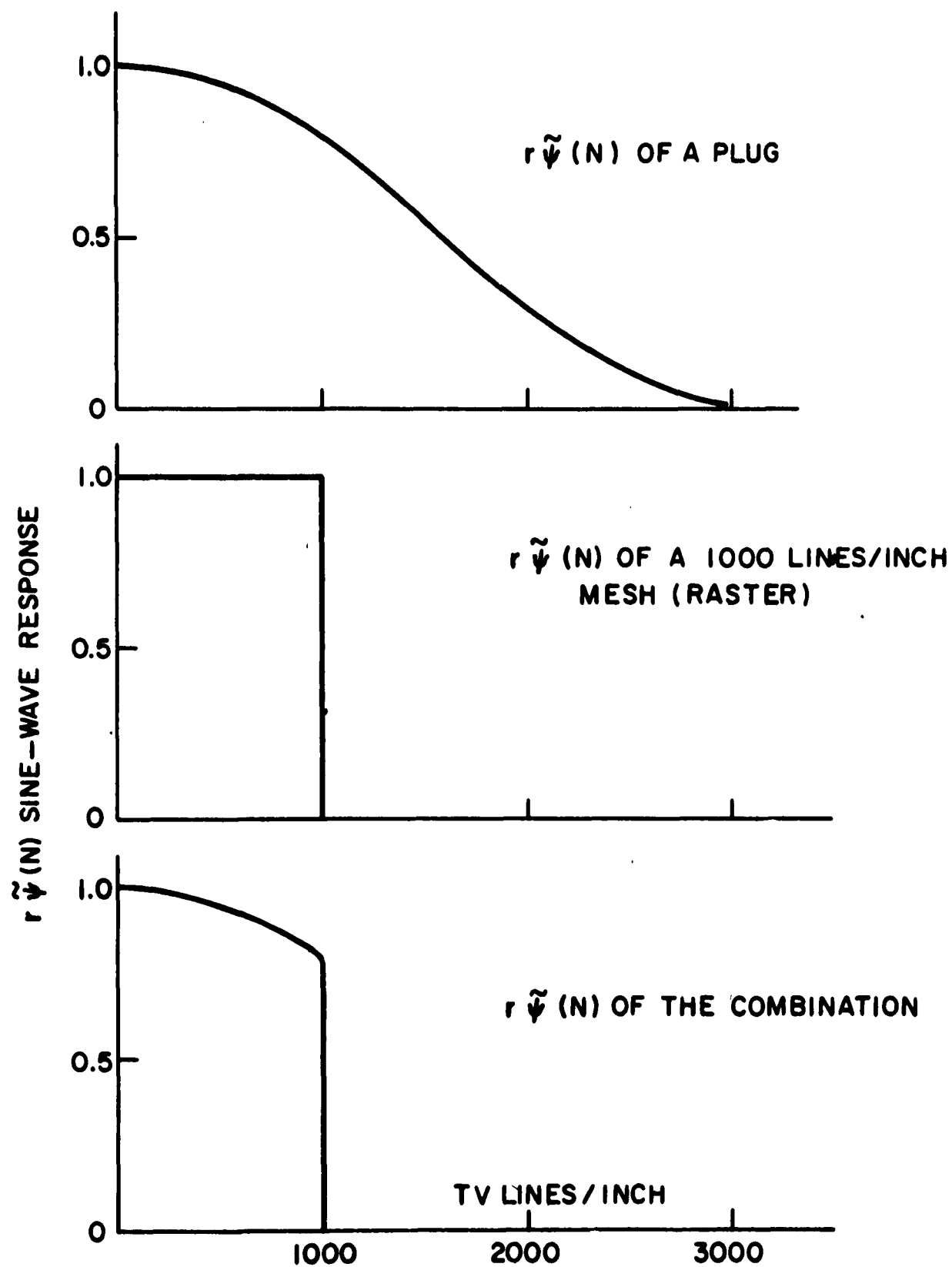
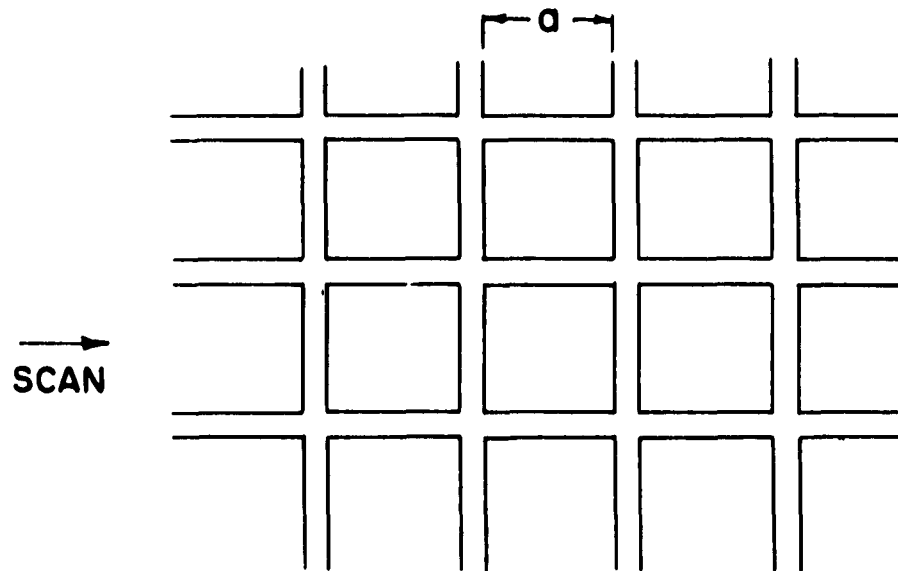
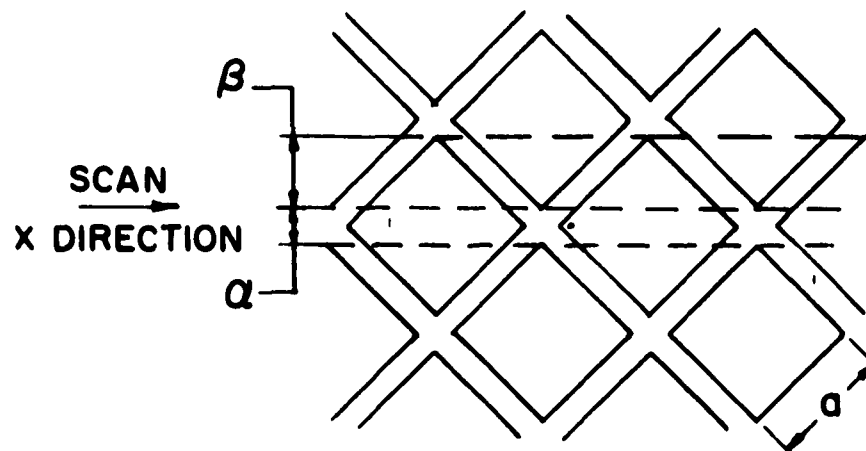


FIG.3 EFFECT OF A RASTER ON TYPICAL PLUG SINE-WAVE RESPONSE



(a) DIAGRAM SHOWING SCAN PERPENDICULAR TO MESH



(b) DIAGRAM FOR CALCULATING RASTER CONSTANT FOR DIAGONAL SCAN

FIG.4 TWO SCANNING MODES FOR PLUG TARGETS

The value of N_e for the target is given by:

$$N_e = \int_0^{n_r} (r \tilde{\Psi}(N))^2 dN$$

where $r \tilde{\Psi}(N)$ is the sine-wave response of the plug. The mesh is taken into account by making the upper limit on the integral n_r instead of infinity. The result for plugs of side $a = 0.0009$ inches in a 1000 line/inch mesh is $N_e = 820$ TV lines/inch.

In a more commonly used scanning mode the beam scans at an angle of 45° to the mesh direction. In this case the line transmittance is:

$$T(x) = \begin{cases} 2k(x + a/\sqrt{2}): & x < 0 \\ 2k(-x + a/\sqrt{2}): & x > 0 \end{cases}$$

where k is the transmittance and x the coordinate of the scan direction, so that the sine-wave response is given by

$$r \tilde{\Psi}(N) = \frac{\int_{-a/2}^{a/2} T(x) \cos \pi N x dx}{\int_{-a/2}^{a/2} T(x) dx} = \left(\frac{2\sqrt{2}}{\pi Na} \right)^2 \sin^2 \left(\frac{\pi Na}{2\sqrt{2}} \right)$$

As shown in Figure 4b, the value of n_r for this direction of scan is not unique. If "a" is the length of the side of an element, the raster constant in the region α is given by $n_r = n/\sqrt{2}$ where n is the number of plugs/inch while in the region β , $n_r = \sqrt{2}n$. In the present calculation the N_e of the target was computed by weighting each of these raster constants according to the chance the beam has of seeing that value. (It must be remembered that although the actual beam diameter may not be less than the mesh diagonal, calculations of the equivalent pass band of one element of a system always assume that the others are ideal. Therefore, in this calculation the beam spot at the target is assumed to be a point.) The weighting factor for the

region α as compared to the region β is clearly given by $\alpha/2\beta$ which for the targets in use here is $1/8$

From these relationships, one obtains

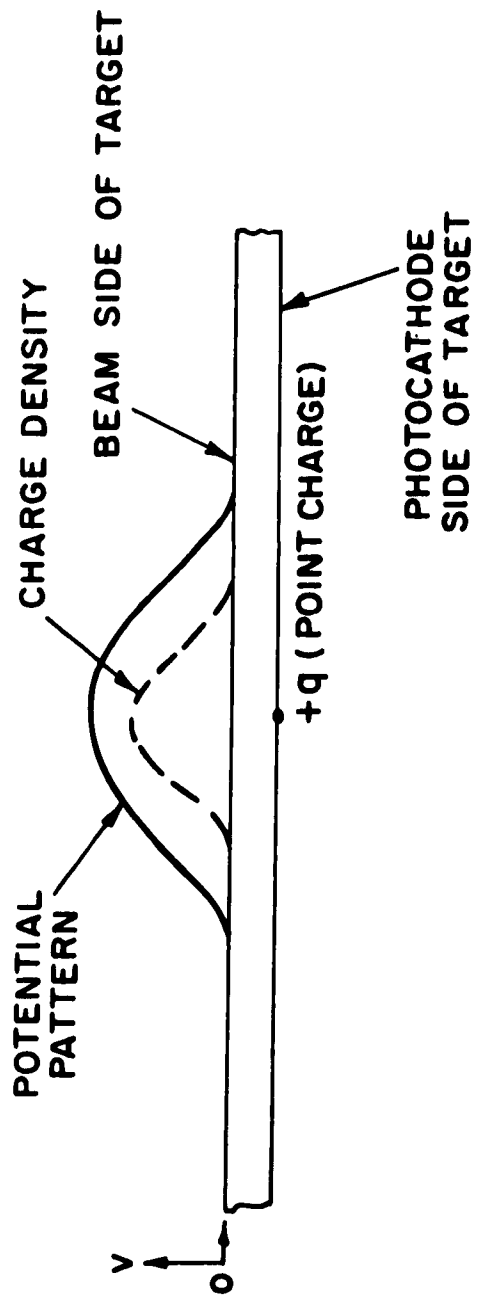
$$N_e = \frac{1}{9} \left[\int_0^n \left[r \tilde{\Psi}(N) \right]^2 dN + 8 \int_0^{\sqrt{2}\pi} \left[r \tilde{\Psi}(N) \right]^2 dN \right]$$

where $r \tilde{\Psi}(N)$ is given above. The integrals were carried out to give $N_e = 920$ TV lines/inch for plugs 0.0009 inch on a side in an $n = 1000$ line/inch mesh.

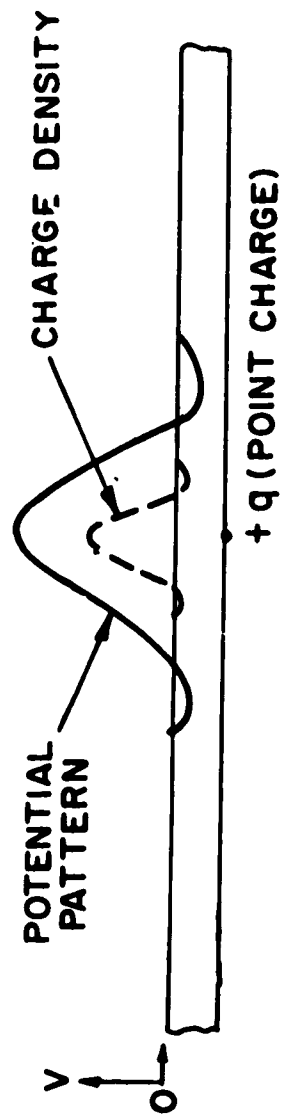
3. The Field Effect on a Glass Image Orthicon Target

The field effect is the term applied to the degradation in resolution which results because the scanning electron beam senses the potential pattern on the image orthicon target rather than the charge pattern. This effect is independent of charge spreading in the target. The charge pattern is deposited on the photocathode side of the target. The beam, however, senses the potential pattern along the surface of the beam side of the target. The area of the target which is held at a positive potential by a positive charge exceeds the charged area as shown in Figure 5a. Thus the beam deposits charge on a larger area than that imaged by the photocathode. Since the signal is determined by the modulation of the return beam this effect lowers the resolution of the tube.

In principle this effect will occur on all image orthicon targets in both the cycled and continuous mode of operation. However, an important counter-effect occurs for continuous operation of a glass target. Consider the signal derived from a positive area on the target. During the first scan the beam will deposit charge on this area and on adjacent areas which are at a positive potential due to field fringing as shown in Figure 5a. The charge deposited on the adjacent areas will tend to remain on the target because



(a) BEFORE SCANNING



(b) AFTER SEVERAL SCANS

FIG. 5 REDUCTION OF THE FIELD EFFECT AFTER SEVERAL SCANS

these areas are not discharged from the photocathode side. In subsequent scans the field effect is at least partially cancelled out by the presence of this negative charge. After many scans, balance must be maintained between the charges produced by the photoelectrons and the charge deposited by the beam. (See Figure 5b)

However, when the target surface is not highly resistive, the charge balance will be maintained in part by lateral flow of charge so that the field effect will still be operative to some degree even in continuous operation.

In a plug target the high lateral resistivity of the alumina matrix prevents the spreading of charge from one plug to the next. The field effect is further reduced by the high capacitance between the storage target and the collector mesh, as compared to the situation for conventional image orthicons.

The calculation which follows gives the field effect for a non-structured target operated in the cycled mode. The transformation of a charge pattern into a potential pattern on the surface of a dielectric can be considered an imaging process(Ref. 4). The theoretical sine-wave (Fourier) response of an aperture defined by this process may be computed from its line transmittance. In turn, the line transmittance of a storage target may be determined from the voltage distribution at its scan surface due to a point-charge at the target image surface.

If t_1 is the thickness of the image orthicon target and t_2 is the mesh-to-target spacing, then the potential at (x, y) in the target is given, approximately, by

$$V(x, y) = \frac{+q}{4\pi\epsilon(t_1^2 + x^2 + y^2)^{1/2}} + \frac{-q}{4\pi\epsilon[t_1 + 2t_2]^2 + x^2 + y^2}^{1/2}$$

where ϵ is an equivalent dielectric constant. The second term in the expression for $V(x, y)$ is the voltage at the

target scan surface due to the image charge $-q$, produced by the presence of the conducting collector mesh. The line transmittance of the storage target is then:

$$f(x) = \lim_a \int_{-a/2}^{+a/2} V(x, y) dy = \frac{q}{4\pi\epsilon} \ln \left\{ \frac{x^2 + (t_1 + 2t_2)^2}{x^2 + t_1^2} \right\}$$

The sine-wave response of an aperture is a normalized Fourier transform of its line transmittance. If $F(\omega)$ is the Fourier transform of the line transmittance, then:

$$F(\omega) = \int_{-\infty}^{+\infty} f(x) e^{-j\omega x} dx$$

For the image orthicon target:

$$F(\omega) = \frac{q}{2\epsilon} \frac{e^{j\omega t_1} - e^{j\omega(t_1 + 2t_2)}}{j\omega}$$

The variable ω is the spatial frequency corresponding to the variable x ; its dimensions are radians per unit length. If N is the television line number, defined as the number of half-cycles in a unit length, then $N = \omega/\pi$

The sine-wave amplitude is given by

$$\tilde{\psi}(N) = F(\pi N) = \frac{q}{2\pi\epsilon} \frac{e^{-\pi N t_1} - e^{-\pi N(t_1 + 2t_2)}}{N}$$

When normalized to unity at $N = 0$, this amplitude becomes the sine-wave response factor:

$$r\tilde{\psi}(N) = \frac{\tilde{\psi}(N)}{\tilde{\psi}(0)} = \frac{e^{-\pi N t_1} - e^{-\pi N(t_1 + 2t_2)}}{2\pi N t_2}$$

The area under the squared sine-wave spectrum is equal, by definition, to N_e . Because a spectrum with unity response extending to a line number N_e contains the same

total sine-wave energy, the measure N_e specifies an equivalent rectangular pass band of the aperture in the frequency domain. For the image orthicon target:

$$N_e = \int_0^\infty \left[r \tilde{\Psi}(N) \right]^2 dN$$

$$= 17 \left\{ \frac{\left[1 - \left(\frac{t_2/t}{1+t_2/t_1} \right) \right]^2 \left[1 + \left(\frac{t_2/t_1}{1+t_2/t_1} \right) \right]^{2t_2/t_1}}{2\pi t_1 (t_2/t_1)^2} \right\}$$

To verify the preceding calculation the sine-wave response of a glass target image orthicon (5820) operated in the cycled mode was measured. Photocathode illumination was initiated just before the first scan. Sine-wave responses for the first and fifth scans are plotted in Figure 6. Measured, first-field response coincided with the approximate response predicted for this target geometry ($t_1 = 0.0002$ inch and $t_2 = 0.002$ inch). The measurements were taken with the target mesh at the high potential of +10 volts, in an attempt to eliminate the aperture correction produced by redistribution.

4. Low Velocity Beam Bending

The readily identifiable aperture processes in image orthicon operation do not account for the experimental resolution figures. A further degrading factor is perturbation of the incident low velocity beam by the potential pattern on the target. The inclusion of a field mesh to reduce this effect is discussed below.

In typical operation, the image orthicon target in the dark is slightly above cutoff voltage with respect to the cathode. A very small fraction of the beam electrons are able to land on target areas which correspond to black areas in the picture. A much larger fraction of the beam is able to land on target areas which correspond to white picture areas. In typical operation, potentials at the target are expected to range from about 2 volts positive down to the neighborhood of 0 volts.

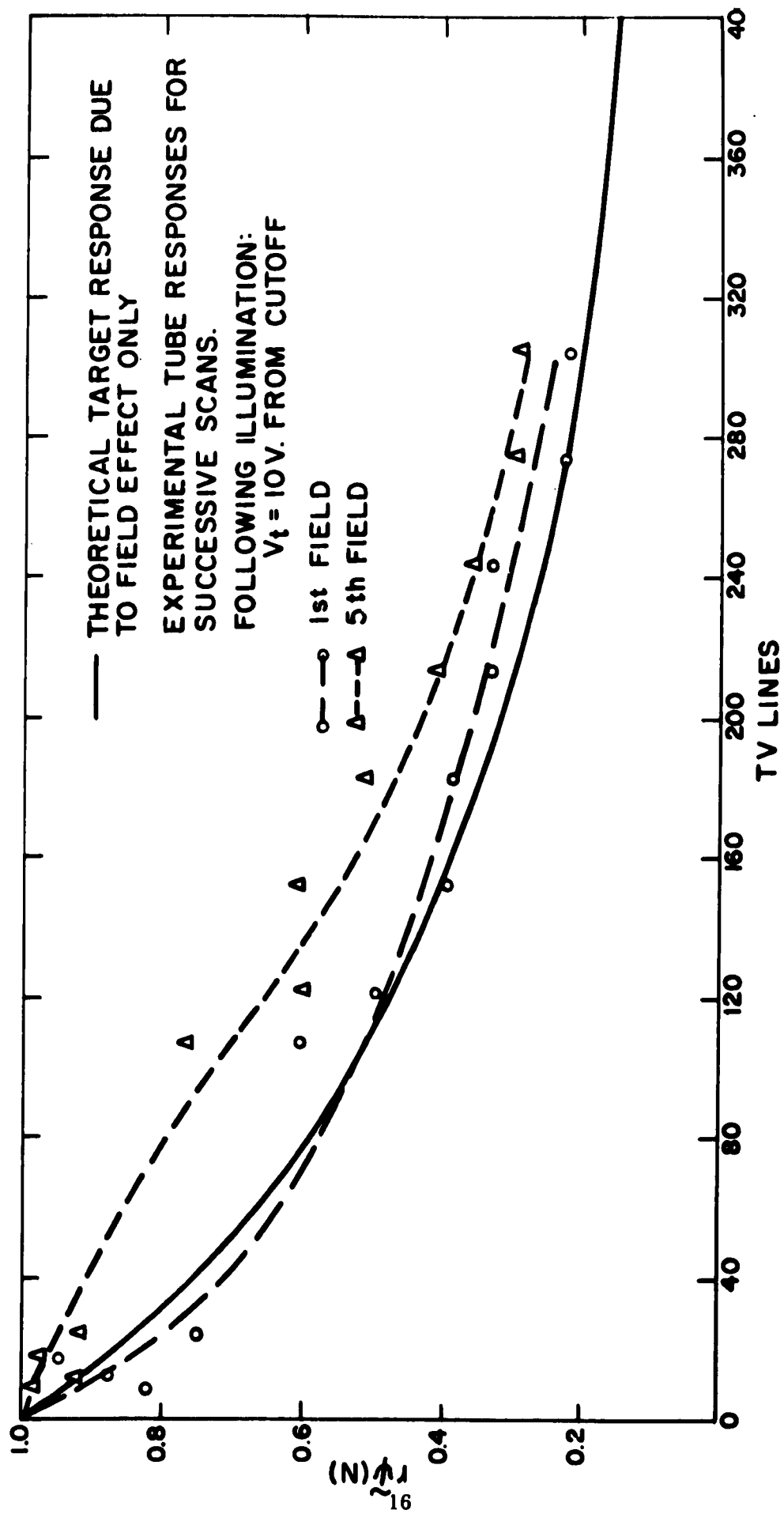


FIG. 6 SINE-WAVE RESPONSE IN 5820 GLASS TARGET IMAGE ORTHICON

The electrons which land on the target at low velocity or are turned back toward the gun, spend a relatively long time near the target surface. In the region immediately in front of the target, an electron is subject to the forces of lateral electric fields established by the stored charge pattern. Because of the long time it takes electrons near the target to reach it or be repelled from it, these lateral components of field strongly deflect the beam (beam bending), narrowing the reproduction of black areas and broadening the whites in a misinterpretation of the beam location by the system.

One method of reducing the magnitude of these effects is to insert a field mesh on the beam side of the target, so as to produce shorter electron transit time by establishing a strong decelerating field immediately in front of the target.

The mesh which provides this field should be as close as possible to the target without being in focus. The envelope of the beam has been calculated. Assuming a 1000 line/inch mesh is placed at a distance sufficient to be out of focus as determined by this calculation, the relative field strength in front of the target will be increased by a factor of 10 over that which is produced in a tube without a field mesh. This should be sufficient change to indicate whether or not beam bending is the limiting factor in the resolution obtained with integral-mesh target image orthicons.

Another effect which degrades the image and is closely related to beam bending is that of time-of-flight defocusing. Electrons which probe positive areas on the target have shorter flight times than those probing areas on the target which are near zero potential. The effect is noticeable on a monitor displaying a high contrast picture. It is observed that areas of different brightness have different optimum beam focus conditions.

Because a field mesh shortens the low velocity flight time it should reduce both these undesirable effects.

5. Analytical Value of Image Orthicon Resolution

Resolution figures obtained for the image section and the plug target can be combined with experimental values of the low velocity electron beam resolution to estimate what an image orthicon's resolution performance should be. For several apertures with Gaussian sine-wave responses in cascade the following relation holds exactly:

$$\frac{1}{N_{e_t}^2} = \sum_i \frac{1}{N_{e_i}^2} \quad \text{where } N_{e_t} \text{ is the } N_e \text{ of the}$$

system of cascaded apertures whose N_e values are the N_{e_i} . This formula will be used to determine the theoretical resolution capabilities of the image orthicon. It must be remembered that the value found will be approximate since not all the apertures to be considered are Gaussian.

The value of N_e for a nickel plug target in a 750/inch mesh was calculated for the case where the area of the plugs occupies 80 percent of the target area. For scanning diagonal to the mesh structure, the value is $N_e = 700$ TV lines/inch. The N_e of an image section for the typical single loop operating mode is approximately 1000 TV lines/inch. The nickel plug target image orthicon tested here has a standard oxide cathode. The beam from a gun with this type of cathode has a measured N_e of 1150 TV lines/inch when landing at low velocity on a monoscope target. Combining these figures in the formula above gives, for these three apertures in cascade: $N_e = 530$ TV lines/inch.

For a number of image orthicons with structured targets the experimental values of N_e are about 60 percent of this value. It is assumed that this discrepancy arises from the effect on the scanning beam of the potential pattern on the target, as described above. The experimental and predicted N_e values can be used to estimate the N_e of this aperture effect. Then $\frac{1}{(330)^2} = \frac{1}{N_e^2} + \frac{1}{(530)^2}$ where

330 TV lines/inch is a typical measured value and N_e refers to all other apertures in the image orthicon not accounted for analytically in the 530 TV lines/inch. The result is $N_e = 420$ TV lines/inch.

6. Measured Image Orthicon Resolution

Measured response curves have been taken on two groups of image orthicons. The first group consists of tubes with structured targets and standard cathodes. The second group comprises tubes with standard targets but with electron guns having standard and surface-smoothed cathodes. The resolution of tubes with smoothed cathodes or with structured targets was higher than resolution measured on image orthicons with standard cathodes and standard targets.

Results indicate that the insertion of a structured target in a standard image orthicon in place of a glass target increases the resolution capability of the tube by 60 percent.

A summary of data taken from three image orthicons with structured targets is given below.

Table 2: Resolution of Image Orthicons with Structured Targets

Tube No.	Target Structure	Mesh	Resolution-TVL/inch			
			Continuous Operation		Cycled Operation*	
			N_e	50%**	N_e	50%**
F2 (PP2206 -21)	Nickel mesh with 150Å thick alumina windows	750/inch	333	510	311	510
PF2180-6	Nickel mesh with nickel plugs	1000/inch	309	459	293	429
F196	Nickel mesh with nickel plugs	1800/inch	337	550	-	-

*1.1 second delay between expose and read.

**"50%" is the TV line number/inch for which 50 percent response is obtained.

Mesh fineness in the above tubes varies over a wide range. However, the resolution of the three tubes is nearly constant. The implication is that resolution is not presently limited by the fineness of the mesh but by some other factor.

In order to investigate the properties of the smooth cathode electron gun in complete camera tubes, several image orthicons were manufactured by the Electron Tube Division in Lancaster under standard processing procedures but with slight modifications. One tube had a smoothed cathode on active nickel, one a smoothed cathode on passive nickel, and one an "as sprayed" standard cathode on active nickel. These tubes were tested for resolution immediately after they were received and again after several days of operation. The performance characteristics for 525 line 60 fields per second interlaced scan below the knee operation are discussed below.

The image orthicon with the smoothed cathode on active metal contained a magnesium oxide target. Resolution initially measured was $N_e = 253$ TV lines/inch. Later measurements indicated that this performance had not changed.

A type 5820 image orthicon with a smoothed cathode on passive metal and one with a standard "as sprayed" cathode were evaluated concurrently. A 35 percent higher initial resolution was obtained for the smoothed cathode on passive metal as illustrated by the data below.

Smoothed Cathode: $N_e = 256$ TV lines/inch
Standard Cathode: $N_e = 192$ TV lines/inch

After two days of intermittent operation the tubes were retested with the following results:

Smoothed Cathode: $N_e = 170$ TV lines/inch
Standard Cathode: $N_e = 178$ TV lines/inch

The resolution loss suffered by the smoothed cathode tube after a short period of operation may have been caused by degradation of the cathode performance or it may have been

caused by the migration of residual free cesium to the target surface.

B. Signal-to-Noise Ratio of Image Orthicons

Meaningful measurements of the signal-to-noise ratio of an image orthicon with a structured target have been possible only on tube number F2. The target in this tube has 150Å thick alumina windows in a 750 line/inch mesh. At high light levels the peak signal-to-rms-noise voltage ratio has exceeded 100 for a 20 megacycle video bandwidth.

The structured targets of other tubes tested employed nickel plugs as the charge storage elements. These tubes have high target capacitance as demonstrated by the high light level required to reach the "knee" (Ref. 5) of the operating curve. However, it was not possible to obtain meaningful signal-to-noise data for these targets because of spurious signals from numerous plugs which were shorted or partially shorted to the mesh. The signals from these plugs had amplitudes several times larger than stored signal amplitudes.

Defects in the alumina-window target, although visible on the monitor presentation, were of low magnitude and low frequency. These defects did not interfere with the signal-to-noise measurements obtained with a line-selecting oscilloscope.

There are several reasons for the superior picture quality obtained on the alumina window targets, as compared to targets with nickel plugs. The alumina window target has better overall mechanical quality. The defects present include windows which may be thin or missing. However, in the plug target defects include not only missing plugs but also plugs which are shorted to the mesh. Shorted and partly shorted plugs cause large white spots to appear in the monitor picture which, because of beam bending, are many times larger than the actual plug size. Return beam signal from the shorted plugs, as viewed on the line-selector oscilloscope, is 3 to 4 times larger in magnitude than the stored target signal.

The alumina window target can be operated satisfactorily with a negative bias on the mesh. Good picture quality is obtained with the mesh potential at 2.5 volts below cathode potential. Operated in this manner the image orthicon tube displays very low dark current and requires far less beam current to operate at a given light level than the same tube with a positive bias on the target mesh. Open and thin alumina windows give responses which are small compared to actual target signals.

The signal-to-noise ratio measurements shown in Figure 7 were obtained with a target bias of -2.5 volts as described above. In order to demonstrate the picture quality of Tube F2, a series of photographs of the monitor was taken. Some of these are shown in Figure 8. Figure 8a shows the monitor picture when the potential on the target mesh is +2.5 volts; 8b shows the same for a target bias of -2.5 volts and 8c is an enlargement of part of 8b. It should be noted that the signal from target imperfections is decreased when the mesh potential is negative.

C. Target Signal Erasure

The most important requirements for good signal erasure are high beam current and small spread in electron energies in the beam. A detailed discussion of the theoretical aspects of signal erasure can be found in a previous report^(Ref. 6). The contract objective of not more than one percent residual signal can be achieved but beam currents far higher than optimum for resolution and good signal-to-noise ratio are required. Therefore, it is recommended that an erase scan be introduced between signal readout and exposure of the next frame. The second requirement presents no new problems; smaller energy spreads enhance resolution as well as erasure. In fact much of the work done on electron guns has had the objective of reducing the beam energy spread in order to obtain higher resolution.

Image orthicons with structured targets require extremely high beam currents to erase the target but erasure to 1 percent can be achieved at high light levels. In the case of glass

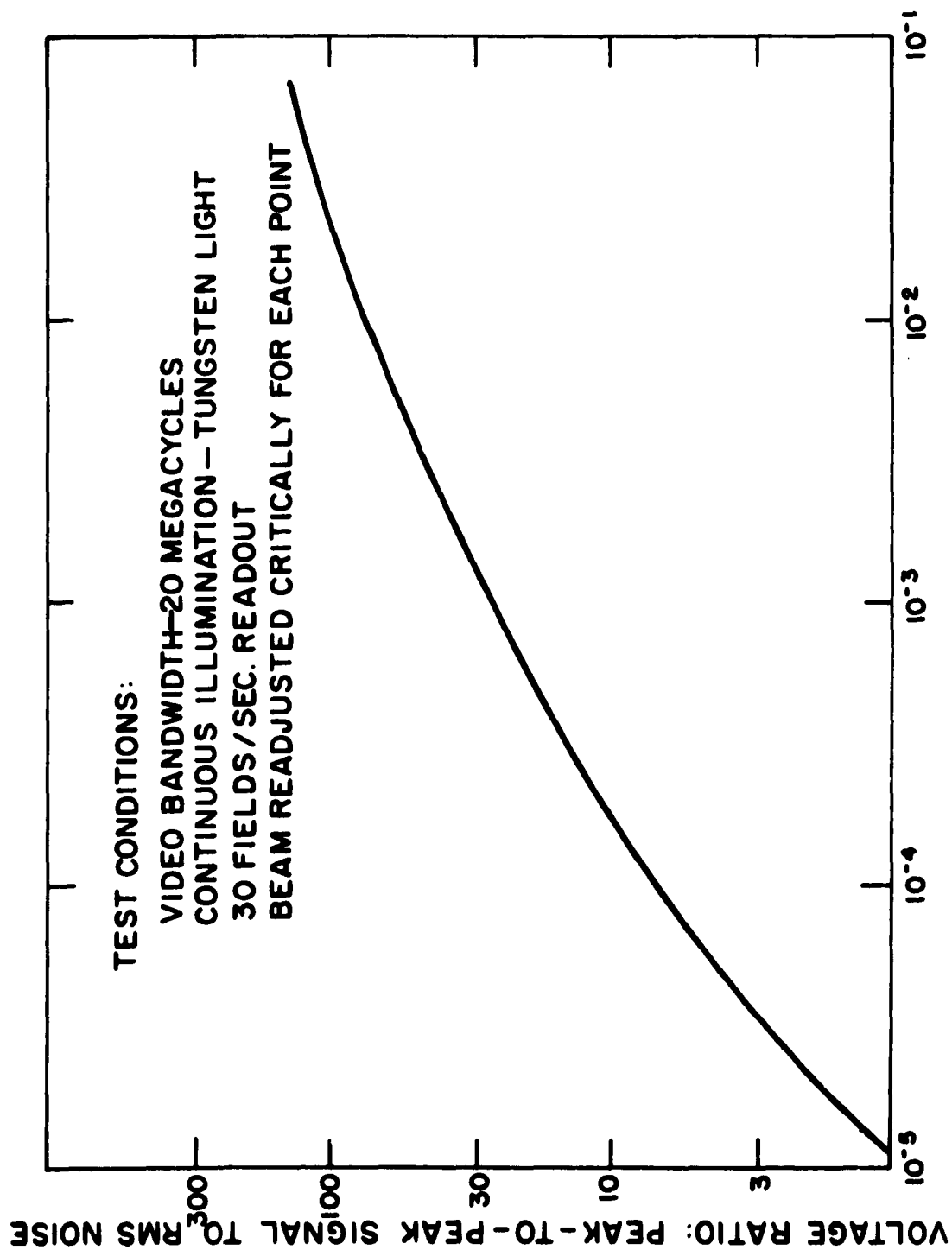


FIG. 7 SIGNAL - TO - NOISE RATIO OF F2 AS A FUNCTION OF PHOTOCATHODE ILLUMINATION

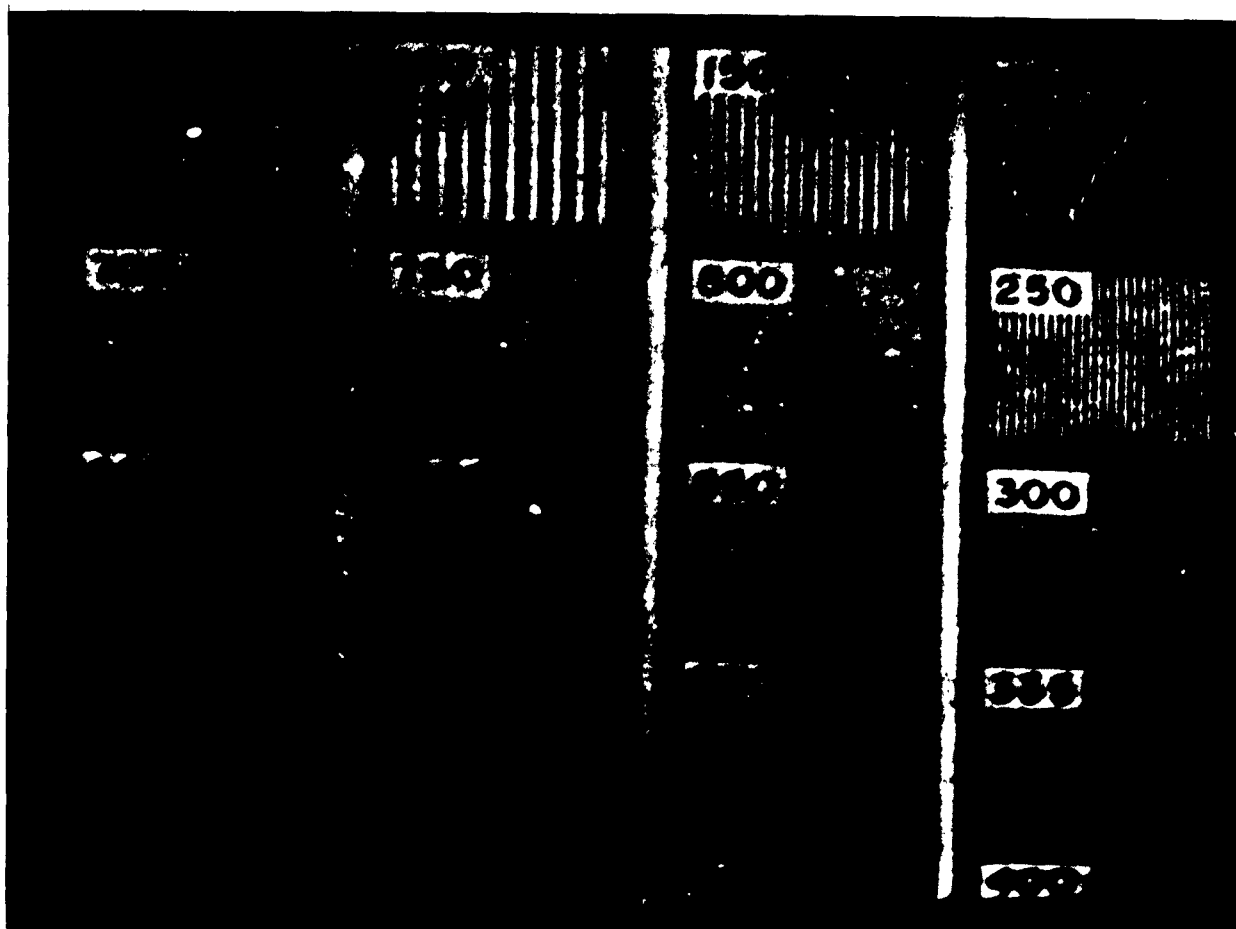


Fig. 8a Monitor Display of Image Orthicon F2 Target with
Integral Mesh Potential at +2.5 Volts

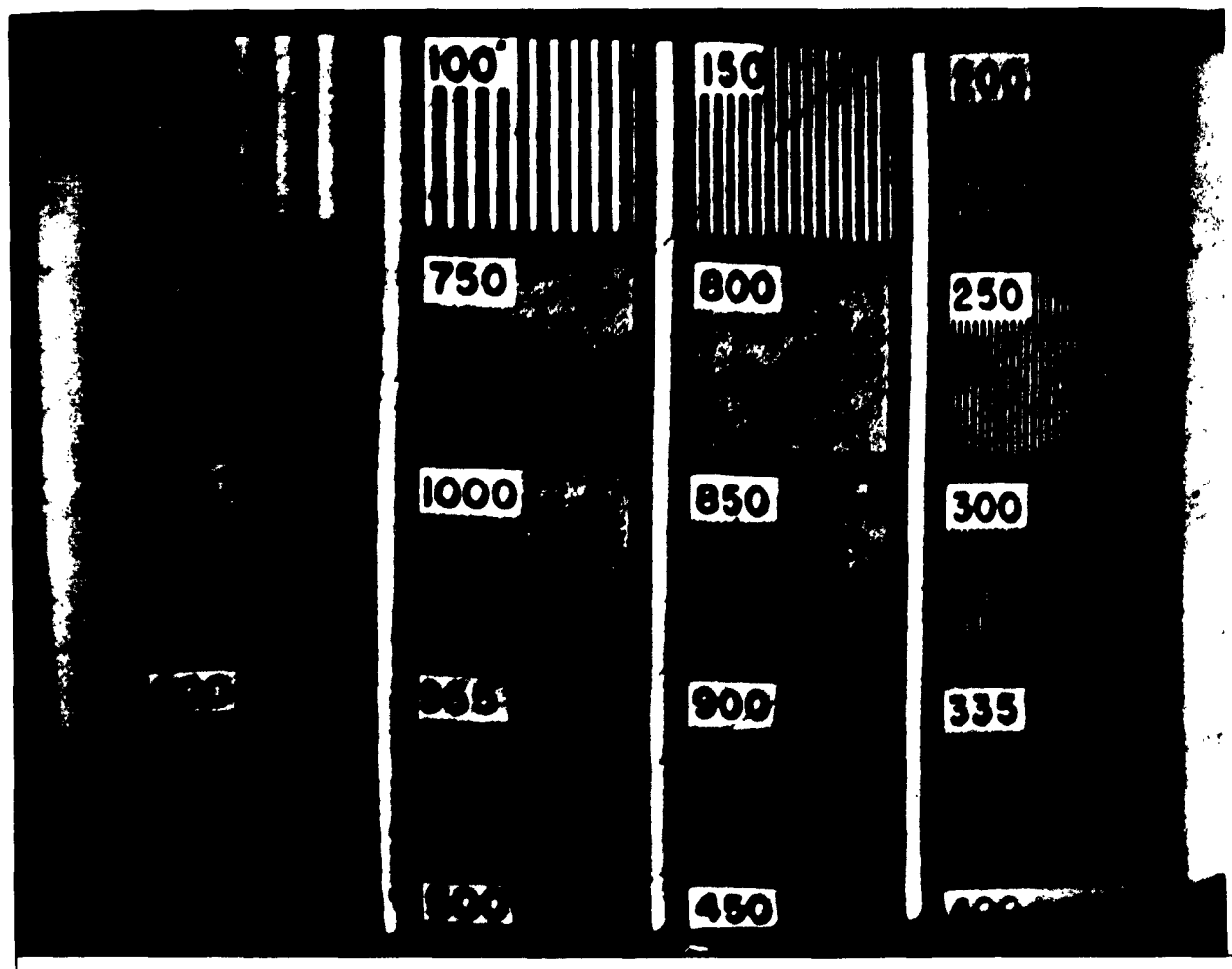


Fig. 8b Monitor Display of Image Orthicon F2 Target with
Integral Mesh Potential at -2.5 Volts

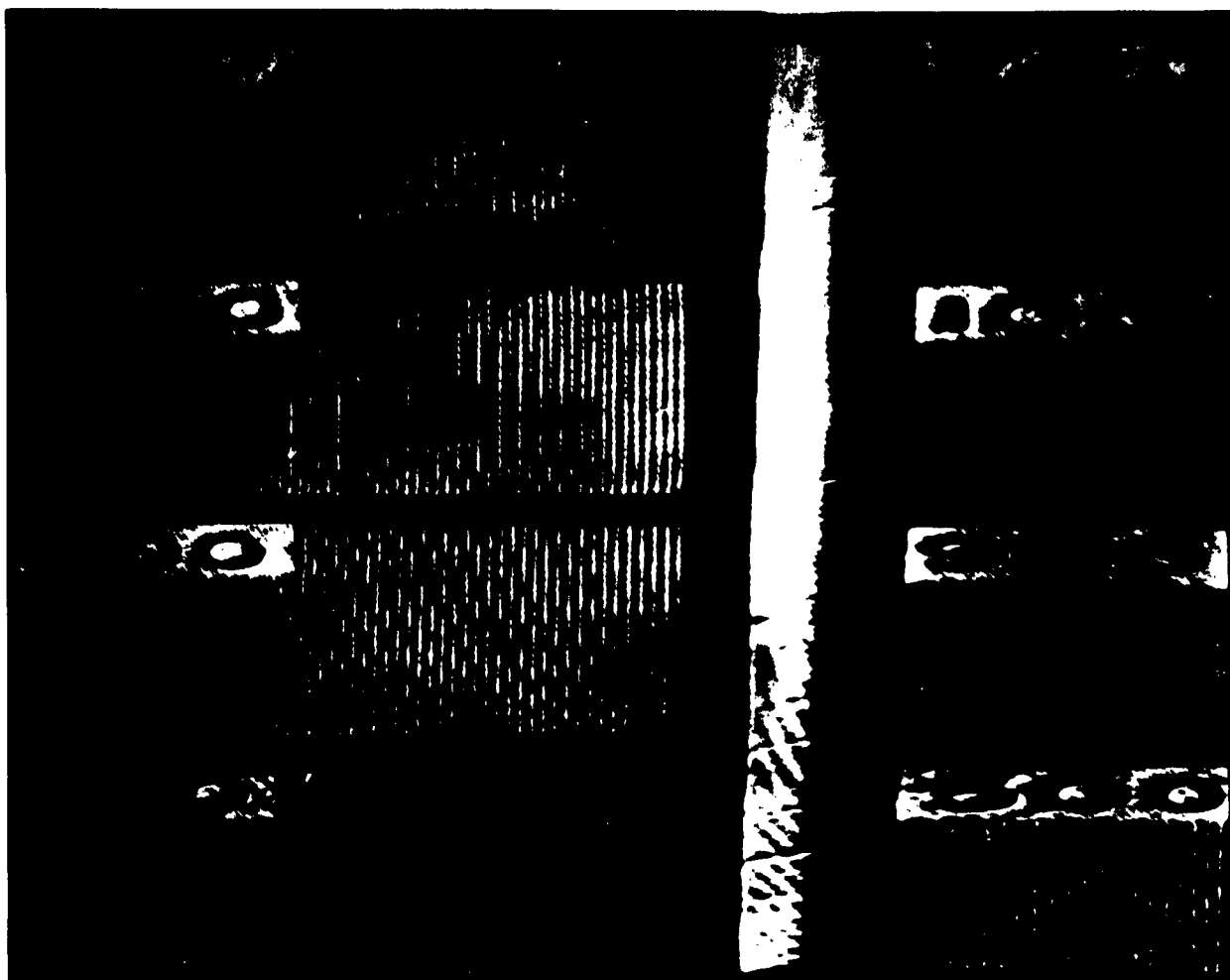


Fig. 8c Monitor Display of Underscanned Portion of
Alumina Window Target of Image Orthicon F2

targets a high degree of erasure can be achieved with currents near the optimum value for high signal-to-noise ratio operation. This difference is due to the differences in capacitance and conductivity of the two targets. The high capacitance structured target stores more charge, so that more beam current is needed to erase the signal. Also the high lateral resistivity of this target as compared to the glass target precludes any signal erasure by charge flowing across the target. It should be noted that this latter property of structured targets also prevents decay of the stored signal between the exposure and read.

The recommended cycle:

Expose

Read (Optimum Beam Current for Resolution
and Signal-to-Noise Ratio)

Erase (High Beam Current)

has been introduced so that good erasure may be achieved from a structured target image orthicon while high resolution and signal-to-noise ratio are maintained. Resolution and signal-to-noise data cited elsewhere in this report were taken at the optimum beam currents for these properties. It was assumed that the erase scan would be incorporated in the cycle.

D. Target Signal Decay

Signal decay refers to the decay time of the amplitude and resolution of a stored target signal. To decrease signal decay the lateral resistivity of the target must be increased. In homogeneous glass targets, there is a limit on lateral resistance since the resistivity of the material must be low enough to permit transverse combination of charge in a frame time. On the other hand, in structured targets one obtains low transverse resistivity while maintaining high lateral resistivity. Tests of the storage properties of structured targets indicate that the decay in resolution is

slight for storage times of a few seconds. The decay in signal amplitude for tube F2 (alumina window integral mesh target) operated in a non-interlaced scanning mode is about 7 percent of the immediate readout amplitude for delays of more than 1/2 second. The initial readout amplitude as a function of delay time is shown in Figure 9a.

Signal amplitude decay measurements have been made for a number of other tubes in an interlaced scanning mode over a range of delays between exposure and readout from immediate readout to 4.3 seconds delay. Readout signal as a function of delay in an interlaced scanning mode has been plotted for several tubes in Figure 9b. The decrease in signal for short delays and the increase to a value close to the immediate readout amplitude for long delays has not been explained. It occurs in image orthicons with high capacitance glass targets having close spaced meshes as well as in integral mesh structured targets. The signal amplitude decay of PF2180-6 was also measured in a non-interlaced scanning mode. Again one observes a decrease in amplitude for short delays with recovery to more than the immediate readout value for longer delays. Assignment of a time constant to the rate of signal decay for targets having this performance does not appear to be feasible. However, signal retention is adequate for a cycle consisting of exposure and slow scan readout.

The decrease in resolution for a delay of 1.1 seconds as compared to zero delay was measured for tube F2. The decrease amounts to about 7 percent in N_e .

III. ELECTRON GUNS AND BEAMS

During this contract period a major effort has been directed toward improving the performance of the image orthicon electron gun. The objectives have been high resolution and good life. Analytical work has been conducted in order to attain sufficient understanding of electron guns to achieve improved performance. Cathode improvements discussed below have given nearly double the beam resolution.

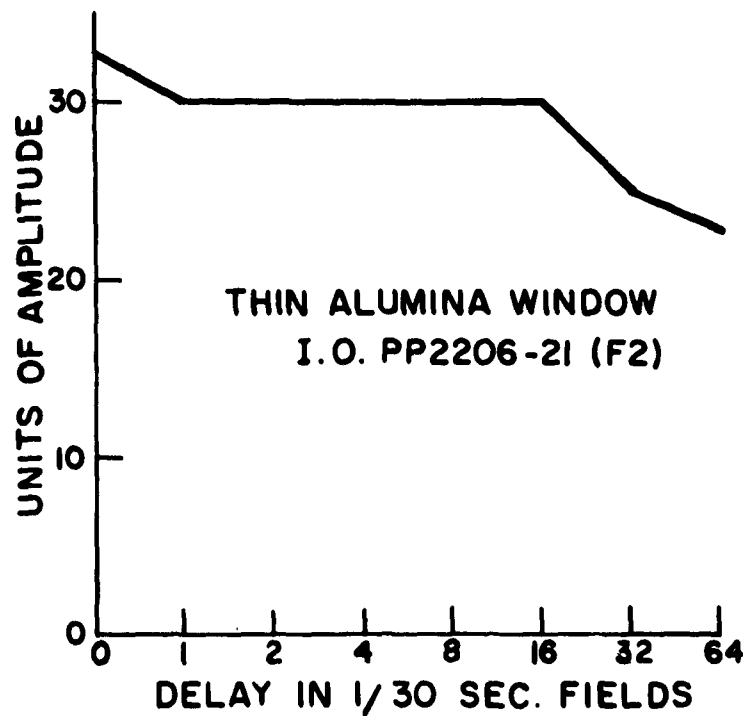
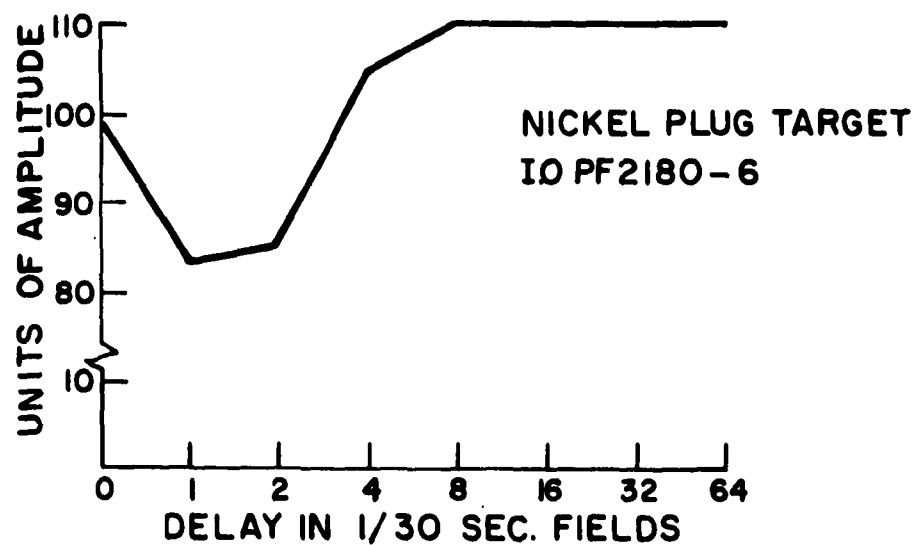


FIG. 9A AMPLITUDE OF INITIAL READOUT PULSE AS A FUNCTION OF DELAY FOR INTEGRAL MESH TARGETS

PF 2180-6 NICKEL PLUG INTEGRAL MESH
HIGH CAPACITANCE TARGET

7513 CLOSE SPACED MESH HIGH
CAPACITANCE TARGET

1939-5 NICKEL PLUG SEPARATE MESH
LOW CAPACITANCE TARGET

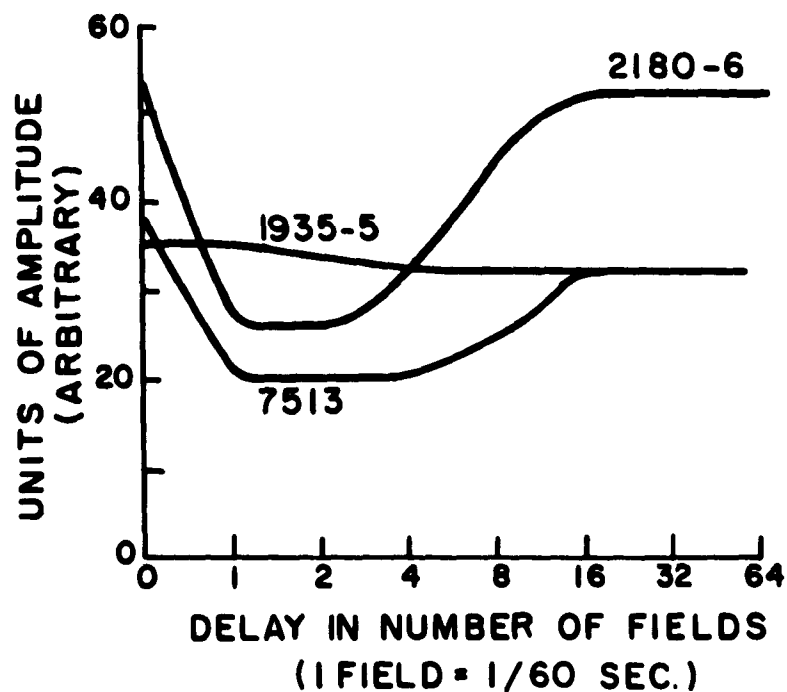


FIG. 9B AMPLITUDE OF INITIAL READOUT PULSE AS
A FUNCTION OF DELAY TIME FOR SEVERAL
IMAGE ORTHICONS

A. Effect of Energy Spreads on Resolution

The resolution of the electron gun is determined by the beam spot size at the target and the current density distribution therein. In general, smaller spot sizes and more peaked current density distributions lead to higher values of N_e , the equivalent rectangular passband^(Ref. 7). Much of the work done here on electron guns has been aimed at decreasing the beam spot size by narrowing the distribution of electron energies in the beam. Broad distributions impair both resolution and signal-to-noise ratio.

Ideally a monoenergetic electron beam would be desired; however, the best expectation for a high current density beam is one with an electron energy distribution characteristic of the temperature of the thermionic cathode. The beam is emitted from a hot cathode ($\sim 1000^\circ \text{K}$) and focused by electric lenses to form a crossover in the gun. The crossover is then focused at the target by a magnetic field so that the ultimate limitation to spot size is a diameter corresponding to the thermal energy distribution at the cathode temperature.

If it is assumed that the electron crossover in the gun being focused at the target is a point, the finite diameter of the spot (at the target) arises solely from differences in electron velocities in the beam. Electrons with initial velocities other than that characterizing the peak of the distribution will not have completed an integral number of loops in the magnetic field upon arrival at the target. Those electrons having velocities for which the magnetic field does not correspond to perfect focus will arrive at the target at a distance from true focus which is proportional to their radial velocity at the crossover. On the basis of these considerations Rose^(Ref. 8) derives $\delta = 2v_n (T - T_0)$ where δ is the spot size at the target arising from a point source at the gun, T_0 is the transit time for an electron at the peak of the distribution, T is the transit time for an electron near the tail of the distribution and v_n is the difference in radial velocities of these two

electrons. In the ideal case, where no spherical aberrations are introduced by imperfect lenses, v_n would be the thermal velocity spread. Apart from velocity considerations, the actual spot sizes will always be larger than the above expression indicates because the crossover has a finite diameter.

If the finite crossover diameter, b , is included, the formula for spot size, $S' = b + S$, is quite general. (In particular the effect of a decelerating electric field at the target can be taken into account by computing the quantities T and T_0 accordingly.)

To calculate N_e from the spot size formula, knowledge of the crossover diameter and the energy spread at the crossover is required. Then, for a Gaussian distribution, $N_e = \frac{1.6}{S + b}$. Because the energy distribution at the crossover is not known, this formula can only be used to give an upper limit to N_e by using the thermal velocity for v_n . (An approximate value of the crossover diameter has been obtained from a computer analysis of the electron trajectories in the gun.) However, the formula can be used to predict resolution at one landing velocity from an experimental value obtained at another landing velocity. In this case the spot size is found to vary directly with the decelerating distance, the distance over which the electron beam velocity is decreased from the drift velocity to the landing velocity. For a given decelerating distance and drift velocity the spot size varies inversely with the landing velocity. If the resolution is determined experimentally for a range of landing velocities, the equivalent decelerating length can be calculated. From this information the resolution at low velocity (target at 2 volts) may be calculated and compared with measured data at low velocity. The approximate calculations described here have indicated that electron energy spreads in present guns exceed thermal spreads. Therefore, better resolution could be obtained in image orthicons by improving the guns or, as discussed elsewhere in this report, by shortening the decelerating distance in front of the target.

B. Experimental Results

Most of the experimental guns were modified to narrow the radial energy distribution by smoothing the cathode surface. The geometry of the negative grid image orthicon gun causes the cathode to emit more densely at the center, and progressively less densely at larger radii. It is possible, therefore, for the center of the cathode to approach temperature-limited emission while only modest average current density is drawn. The effect of surface smoothness of a planar cathode operated with temperature-limited emission has been demonstrated by Moss^(Ref. 9) who found electrons with radial energies exceeding 10 volts from cathodes having rough surfaces. He also found that when the same cathode was operated space-charge-limited, electrons with high radial energies were not present. It is reasoned that cathode surface roughness can also cause local variations in emission density. Areas of high emission density will tend to become temperature limited while the average current density over the whole cathode surface is quite low. Thus, performance of the cathode may be seriously degraded in terms of image orthicon operation at current densities well below those normally considered acceptable for space-charge-limited operation.

1. Resolution of Electron Beams From Smoothed Oxide Cathodes

During this contract period a number of return beam monoscope tubes and a complete image orthicon were built with smoothed cathodes on active nickel bases. The measured resolution of the electron beams of return beam monoscope tubes has been nearly twice that obtained with standard sprayed cathodes and has been reproducible.

The smoothed cathode surface is obtained by first removing the sprayed carbonates from a standard 5820A image orthicon cathode cup. The standard cathode surface is shown in Figure 10a. The central portion of the cup is flattened with a coining tool (Figure 11) so that it presents a flat surface perpendicular

to the gun axis. The cathode is then resprayed so that the coating is 0.003 inches thick (this is shown in Figure 10b). It is mounted in a smoothing fixture (Figure 12) which holds the cup in position and includes a micrometer plate with a hole centered over the cathode surface. The smoothing of the cathode surface is accomplished by gradually lowering the plate while repeatedly crossing the plate and cathode surface with a sharpened tool (Figure 13) until a uniform smooth layer between 0.001 and 0.0015 inch thick is obtained. The resulting surfaces are smooth to about 0.0002 inch. The structure appears regular and fine grained as shown in Figure 10a.

The first tubes assembled with smoothed cathodes (H8643-1, 2, 3) had standard guns except for the cathode-to- G_1 spacing, which was set at 0.005 inch instead of approximately 0.008 inch^(Ref. 10).

Resolution measurements were carried out on high velocity monoscope targets; each monoscope target consisted of a line resolution pattern printed in photoresist (KPR) on a gold surface film evaporated on glass. The return beam is modulated by the difference in the secondary emission ratios of photoresist and gold.

Tubes H8643-1, 2, 3 gave an N_e of 2300 TV lines/inch with a beam current of 20 nanoamperes. The sine-wave responses are compared with the performance of a standard gun in Figure 14. The resolution decreases slowly with increasing beam current. As shown in Figure 15 the relation is approximately $N_e \sim (I_e)^{-1}$.

2. Resolution of Electron Beams From Smoothed Cathodes-Low Velocity

Later tubes with smoothed cathodes were equipped with monoscopes suitable for resolution measurements at low velocity, in order to perform evaluations under conditions more representative of image orthicon operation. These

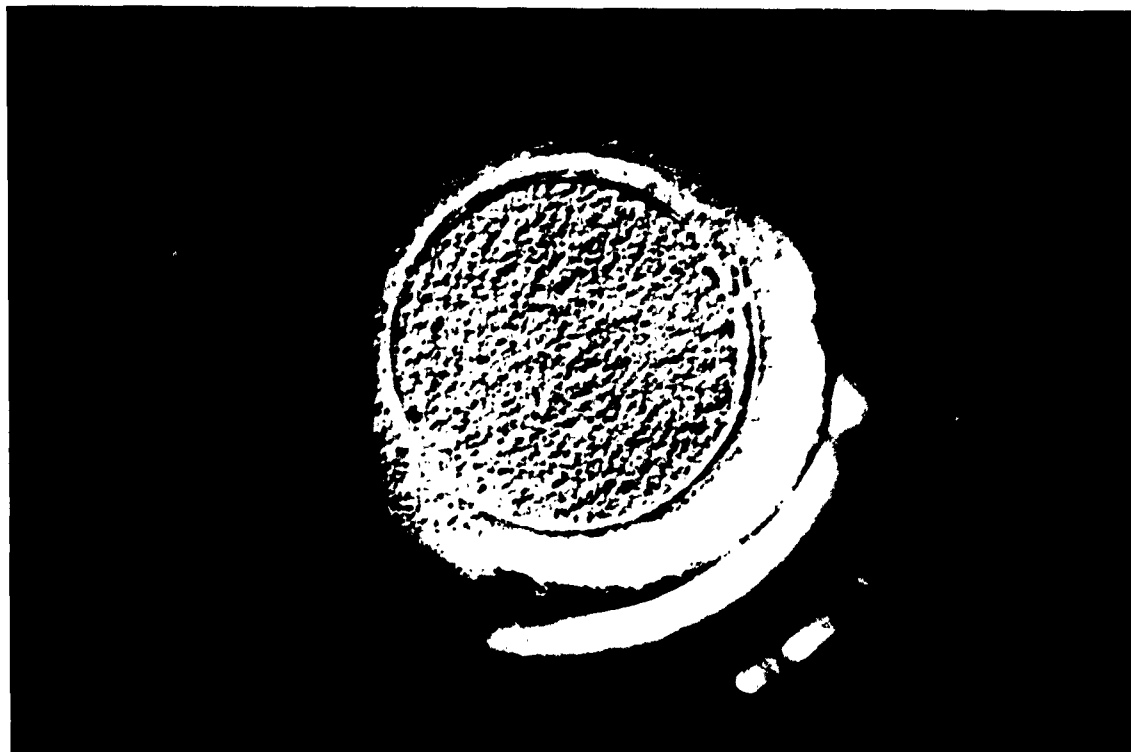


Fig. 10a Standard Cathode Surface



Fig. 10b Princeton Resprayed Cathode Surface

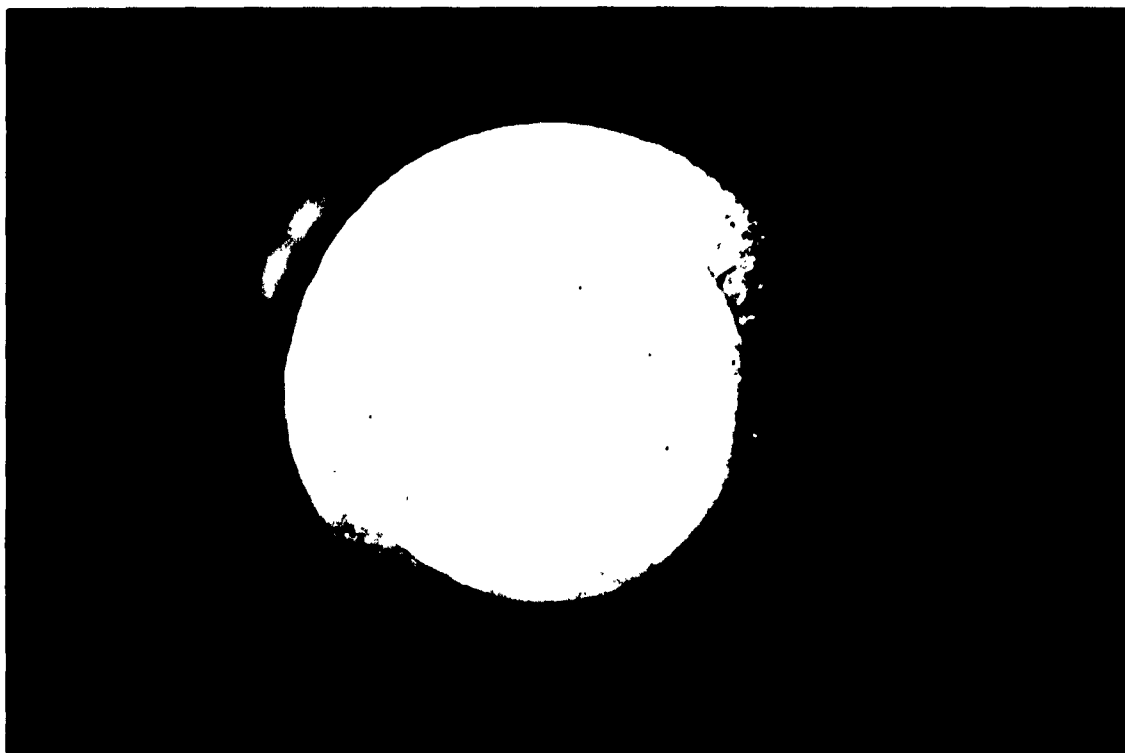


Fig. 10c Smoothed Cathode Surface

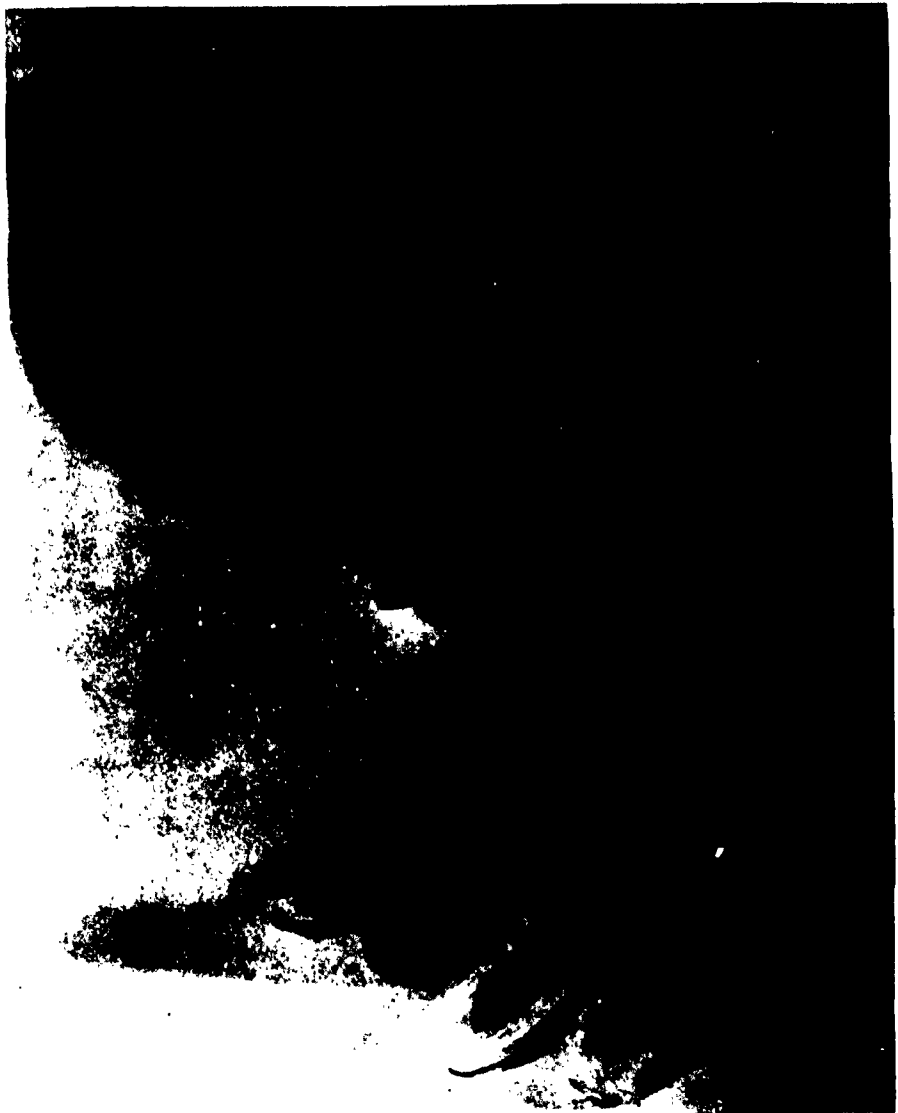


Fig. 11 Coining Operation



Fig. 12 Smoothing Tool



Fig. 13 Smoothing Operation

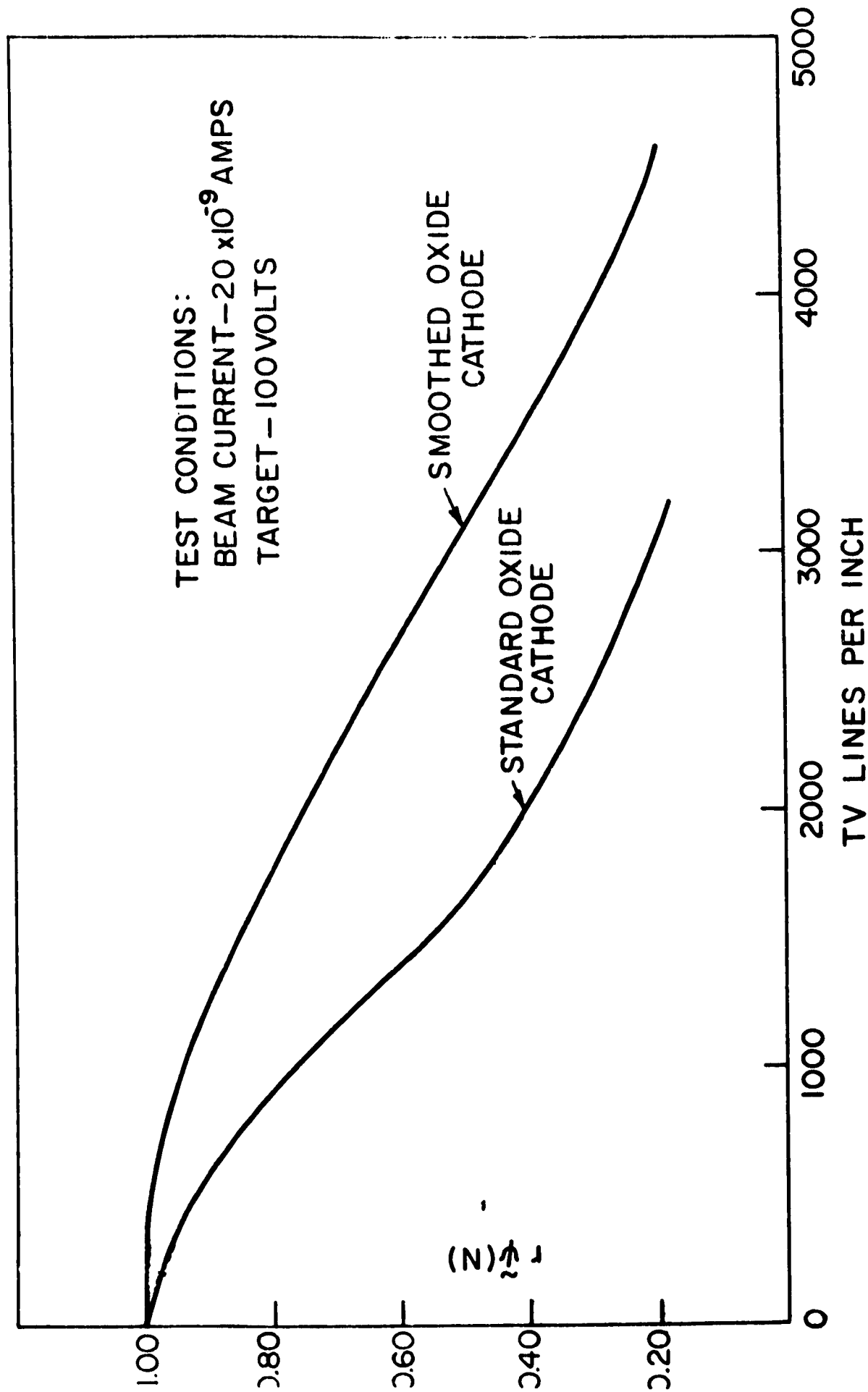


FIG.14 SINE-WAVE RESPONSE OF IMAGE ORTHICON GUNS

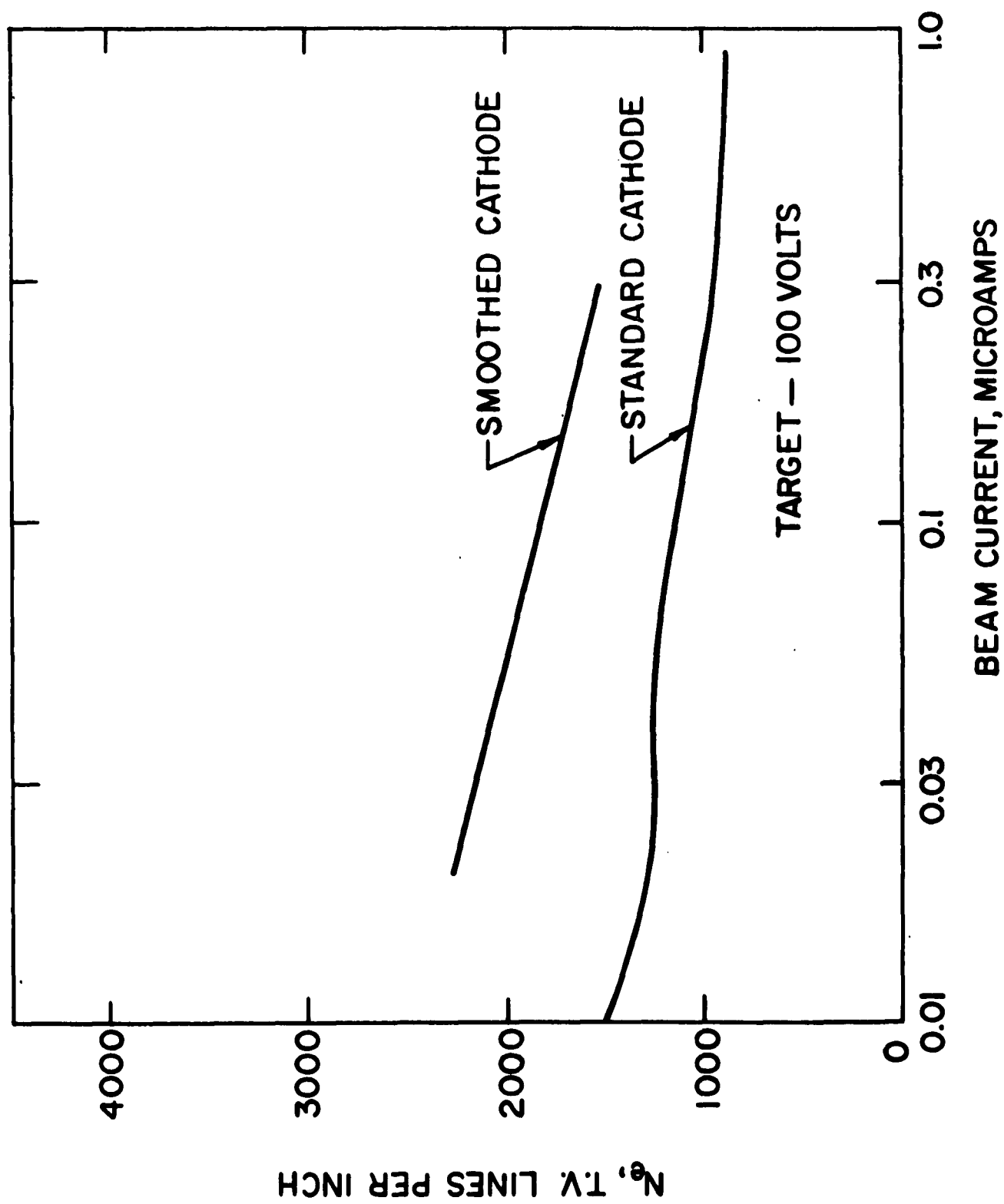


FIG.15 IMAGE ORTHICON GUN RESOLUTION AS A FUNCTION OF BEAM CURRENT.

monoscopes consisted of copper lines on a chromium base. The pattern was obtained by photo-etching the copper under carefully controlled conditions. A good pattern with resolution to 4500 lines/inch was obtained. (The photoresist targets are not suitable for low velocity evaluations because of electrical charging of the KPR insulator.)

The operation of these monoscopes at low velocity depends on differences in the work functions and accommodation coefficients of copper and chromium. The accommodation coefficient is that fraction of electrons impinging on a metal surface which is retained by the surface. This monoscope may also be operated at high velocity, in which case the return beam modulation depends on the difference in the secondary emission ratio of copper and chromium.

The purpose of resolution measurements on bi-metal monoscopes is to determine the low velocity beam performance independent of the effects of lateral electric fields near the target.

The first bi-metal monoscope tube tested (H-8643-12) gave limiting visual resolution of 4500 TV lines/inch when operated with the target 0.5 volts above beam cutoff. Because of surface irregularities the square wave response could not be measured. A later tube (H-8643-17) was equipped with a monoscope of copper on chromium and a monoscope of photoresist on gold. The resolution was measured at high and low velocity. The results, which are shown in the table below, indicate that the low velocity electron beam, unperturbed by target field effects, has not been the limiting factor in the resolution for any of the image orthicons tested thus far.

Beam Current:	0.02 microampere
Resolution - Target at 100 volts	$N_e = 1600$ TV lines/ inch
Resolution - Target at 1 volt above cutoff	$N_e = 1200$ TV lines/ inch

3. Life Tests of Smoothed Cathode Electron Guns

The life test performance of the smoothed cathode tubes has shown that although resolution degrades slightly with life, it is maintained at a higher level than the resolution of standard cathodes, as shown in Figure 16. The following table reflects the life test performance of several tubes with smoothed oxide cathodes. During life test operation the beam current was 0.05 microamperes or higher but the resolution measurements were made with $I_B = 0.02$ microamperes.

Table 3: Resolution, with Life, of Image Orthicon Guns

<u>Tube No.</u>	<u>Cathode Type</u>	<u>N_e (new)</u>	<u>N_e(200 hrs.)2300 hrs.</u>	
H8643-2	Smoothed on active metal	2300 TVL/ in.	2300 TVL/ in.	2000 TVL/ in.
H8643-3	Smoothed on active metal	2300 TVL/ in.	2300 TVL/ in.	1900 TVL/ in.
H8643-4	Standard on active metal	1200 TVL/ in.	1400 TVL/ in.	1600 TVL/ in.

4. Performance Evaluation of BN Cathodes

The use of bariated nickel (BN) cathodes was first considered because these cathodes may be polished to obtain a smoother surface with fewer loose particles than is possible with smoothed oxide cathodes. The BN cathodes are also of interest because they have displayed good life when operated under conditions adverse to oxide cathodes such as high emission density and ion bombardment of the cathode.

Thus far results of resolution measurements on tubes with BN cathodes indicate that the initial resolution is not as high as that obtained from smoothed-oxide cathodes..

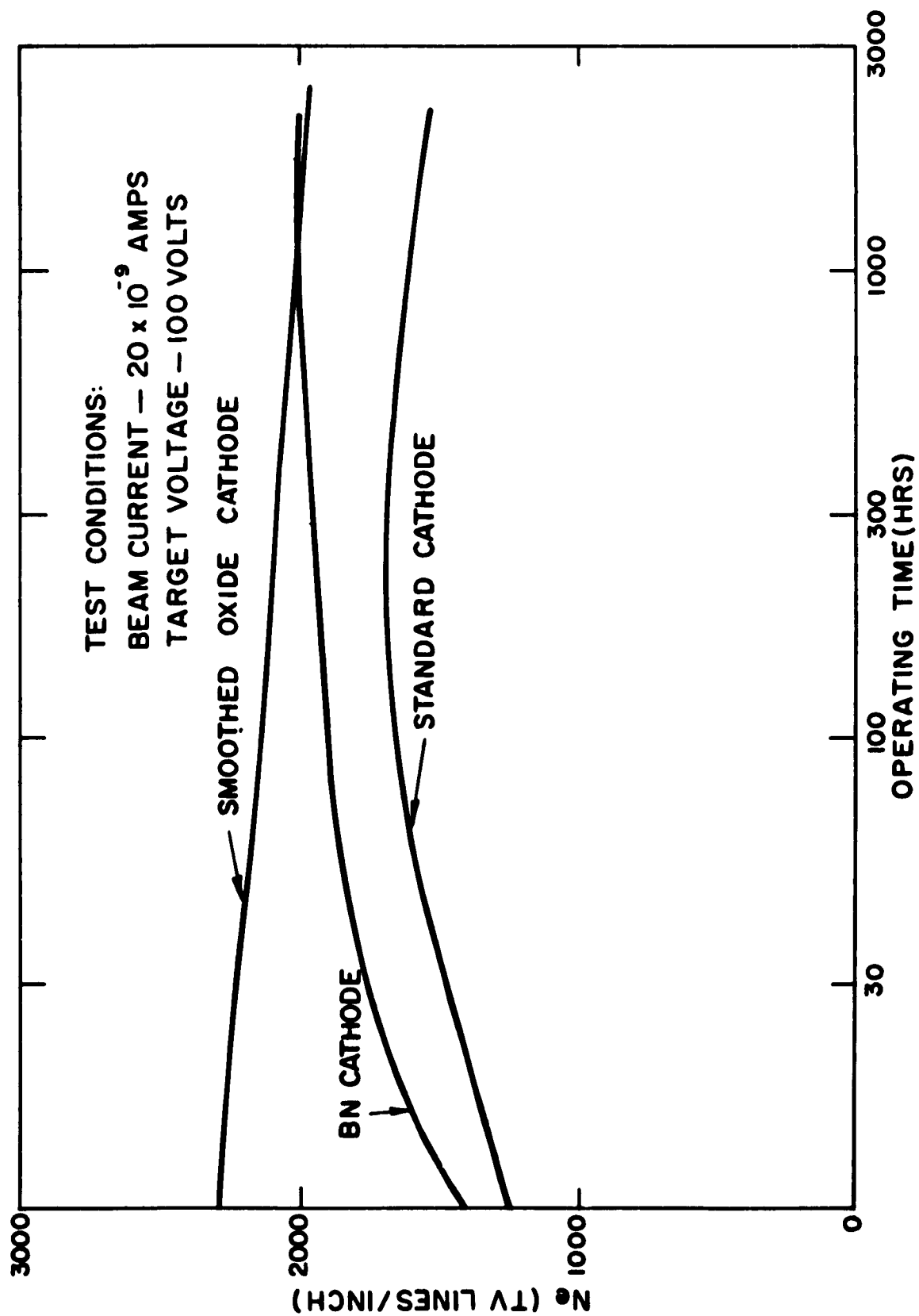


FIG.16 RESOLUTION OF IMAGE ORTHICON GUNS AS A FUNCTION OF OPERATING TIME

However, unlike the oxide cathodes, the resolution of the BN cathode guns improves with life. The graph in Figure 16 shows the life performance of two guns with BN cathodes as compared to the performance of several smoothed-oxide cathode guns.

The life test performance of the two BN cathodes indicated that the results obtained depended on the length of time the cathode had been operated. The first BN cathode tested, H-8643-7, was reported earlier to have a resolution $N_e = 1600$ TV lines/inch. This initial resolution, which is higher than the initial resolution of the two subsequent tubes, may have resulted from operating time before the resolution measurements were recorded.

5. Matrix Cathodes

The matrix cathode was investigated because it has reportedly given good life under adverse operating conditions in other types of tubes. It is manufactured by sintering a powdered nickel layer on top of a normal cathode cup. Carbonates are then introduced into and on top of the matrix. For this investigation the surface was smoothed until the sintered nickel particles were visible. One tube with such a cathode (H-8643-18) has been tested. Its resolution was $N_e = 1575$ TV lines/inch.

6. Gun Geometry Variations

Smoothed oxide cathode guns were built with several different cathode-to- G_1 spacings and limiting aperture diameters. None of these gave resolution figures as high as those reported above for tubes H-8643-1, -2, -3 with 0.005 inch cathode to G_1 spacing and 0.0016 inch aperture diameter.

Tube H-8643-6 was made with a cathode-to- G_1 spacing of 0.010 inch and H-8643-5 with 0.0025 inch. The data obtained from these tubes indicate that the close spacing

is definitely detrimental to resolution but the more distant spacing causes only a small loss in resolution. The fact that resolution is a slowly varying function of grid-to-cathode spacing between the distances of 0.005 inch and 0.010 inch is useful for determining fabrication tolerance of future tubes.

The standard aperture used in tubes is 0.0016 inch in diameter. Return beam monoscopes made for several resolution tests had aperture diameters of 0.0003 inch and 0.008 inch. The first aperture was obtained from the Electron Tube Division and the second was made at RCA Laboratories by piercing a standard aperture. Neither of these tubes had performance equal to that of previous monoscope tubes with the standard aperture. With the small aperture, limiting visual response as observed on the monitor was almost as high as that obtained with the smooth cathode and standard aperture with 100 volts at the monoscope target. However, maximum beam current was limited to 20×10^{-9} amperes and the signal-to-noise ratio was low. The large-aperture-tube square-wave response was much lower than was obtained with the standard aperture.

C. Electron Trajectory Studies

To predict and improve the resolution of an electron gun requires detailed knowledge of the fields and electron trajectories in the gun. In principle, the fields and trajectories can be determined, at least in the space-charge-free approximation, by solving Laplace's equation in the gun region. The initial conditions for the trajectories are given by the thermal velocity distribution appropriate to the cathode temperature. An analytical solution is not feasible because of the complicated electrode structure. However, such a problem can be solved on a digital computer by replacing Laplace's differential equation with an equivalent difference equation and solving by an iterative technique.

Digital computer studies of the image orthicon gun have been made in this manner. Results obtained here related gun

geometry to beam current and crossover diameter in negative grid guns. (Since the crossover is imaged on the target its diameter is of prime importance in determining resolution.) Estimates of the fraction of cathode current used in the beam have also been obtained. Significant results are reported below.

Experimental results have indicated that resolution will increase, for a given value of beam current, if the ratio I_{G_2}/I_B increases. (See Figure 17; note that, for fixed beam current, only one point on the graph can be obtained from any one gun.) The results of computer studies of a standard image orthicon gun indicate that this effect arises because as the ratio of currents increases the crossover moves back toward the cathode. The electrons which may then enter the beam are those having trajectories which make the smallest angles with the axis. However, as the crossover moves back, the effective cathode area, i.e., the area which contributes to the beam, decreases. This is due to the linearity of the relation $r_A = 1.3 r_K$ where r_K is the radius of departure from the cathode and r_A is the radius of arrival at the plane of the limiting aperture. This relation appears to hold for all radii of arrival less than about twice the limiting aperture radius. (See Figure 18.) In the figure the sets of data points with the same r_K correspond to different emission energies.

However, the size of the effective cathode area is somewhat inexact. The electrons leave the cathode with random radial velocities. If the cathode is perfectly smooth these velocities are thermal only; if the cathode is rough these radial velocities increase in proportion to the roughness (Ref. 11). A definite radius can be assigned to the cathode area only in the ideal case of a perfectly smooth cathode which emits monoenergetically. In all other cases the value of r_A will be affected by the initial velocity of the electron as well as its position. Therefore, the relation $r_A = 1.3 r_K$ holds more accurately for smooth cathodes and less accurately for rough cathodes.

In an effort to learn, within the bounds of the errors discussed above, how to obtain the maximum effective cathode area while maintaining good resolution two guns were designed and then

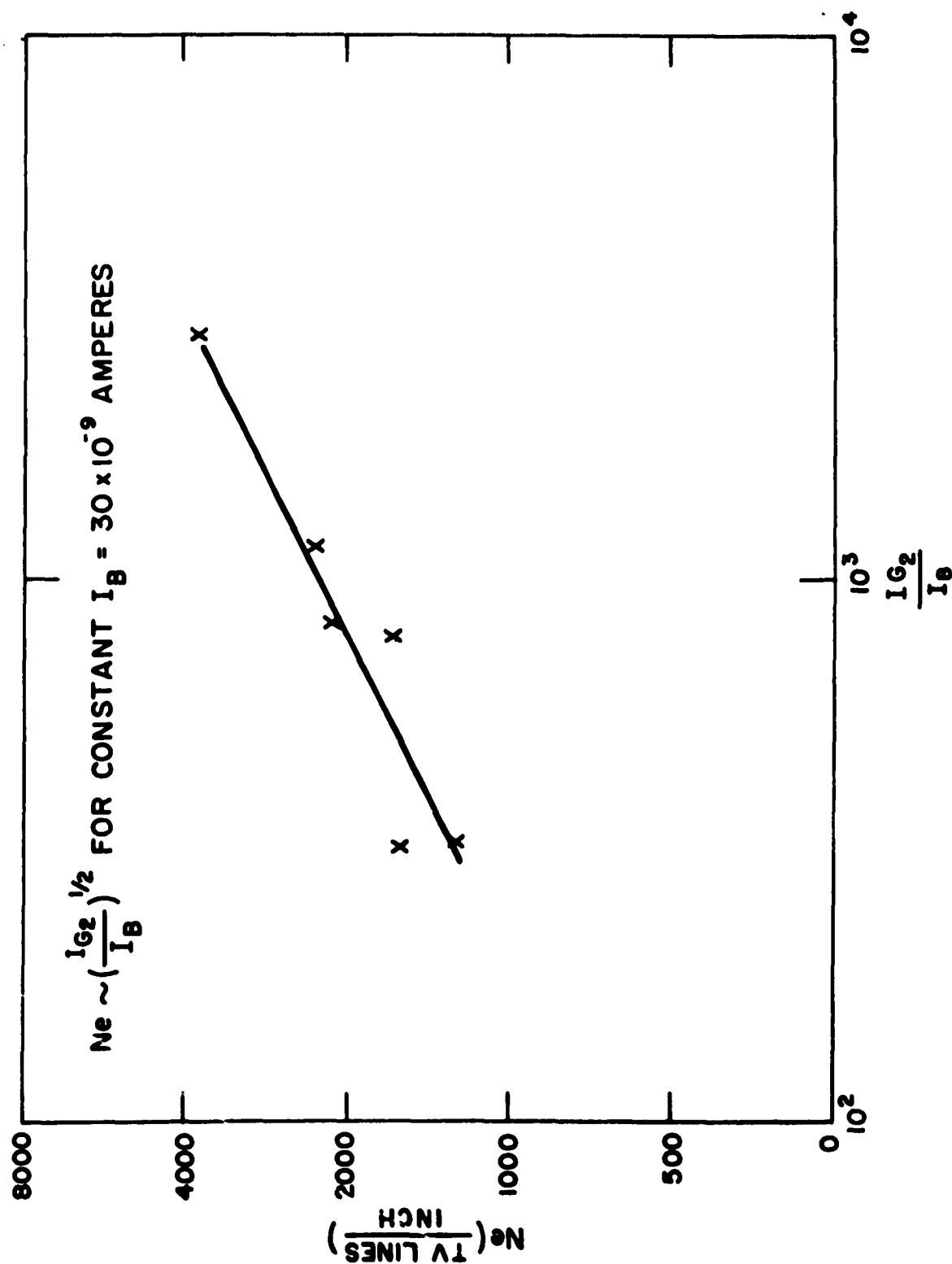


FIG.17 RELATION BETWEEN Ne AND IG_2/I_B

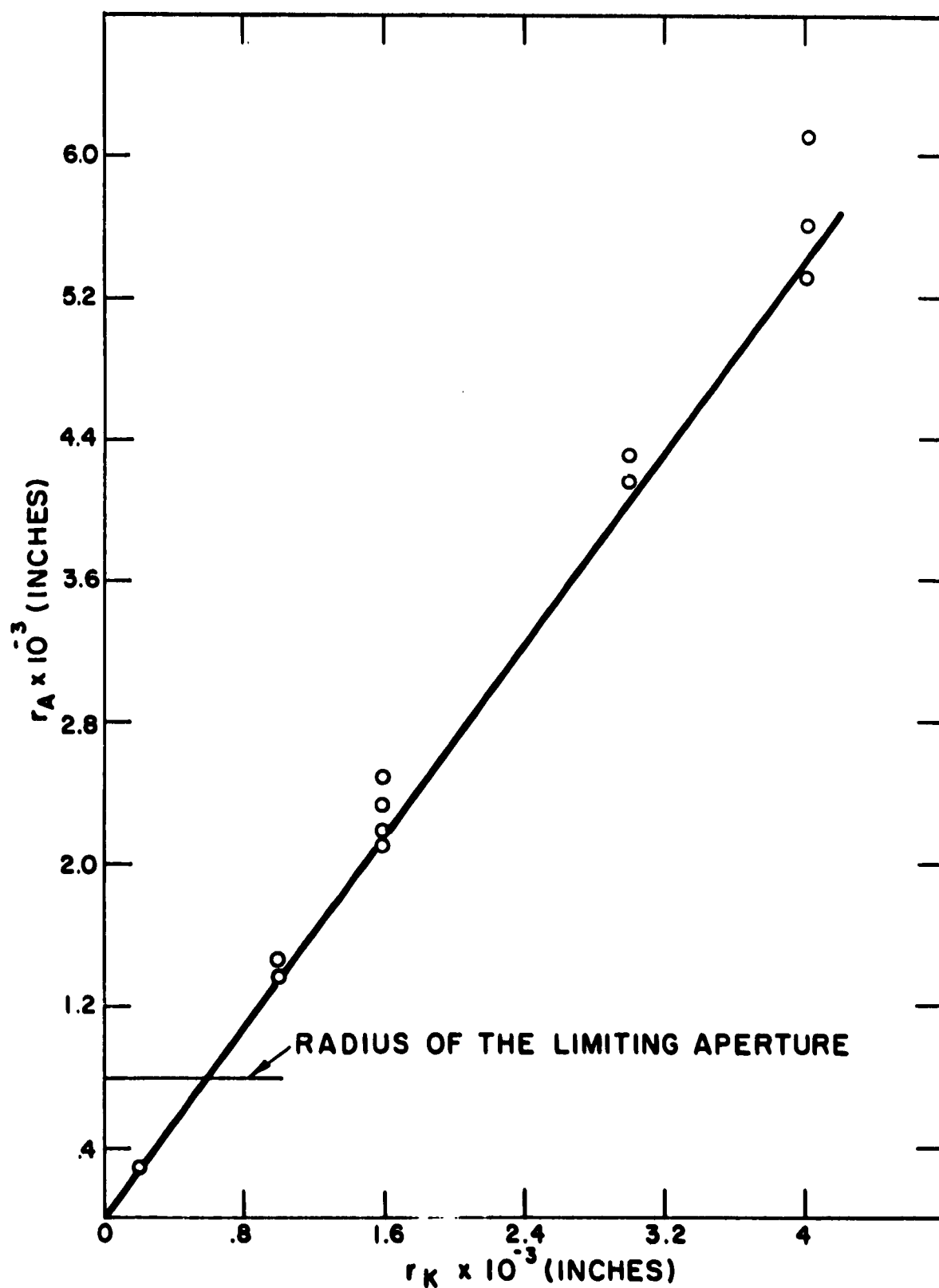


FIG.18 RADIUS OF ARRIVAL AT LIMITING APERTURE (r_A) AS A FUNCTION OF STARTING RADIUS (r_K)

analyzed on the computer. The results were compared with results obtained for the standard gun (Figure 19). One of the experimental guns (Figure 20c) was designed to give high I_B/I_{G_2} and the other (Figure 20b) low I_B/I_{G_2} . The computer diagrams are shown in Figure 20 along with the standard gun diagram (Figure 20a). The "long" gun which is shown in Figure 20b has a G_1 -to- G_2 spacing of 0.060 inch while the "short" gun (Figure 20c) has a G_1 -to- G_2 spacing of 0.028 inch.

The computer results obtained for the standard gun structure indicated that there is a diverging electric field near the axis near the cathode side of G_2 . This results from the penetration of the negative G_1 potential into the G_2 region and causes the crossover to move toward the limiting aperture. Since the electron trajectories after the crossover are rectilinear, the displacement of the crossover toward the limiting aperture results in higher beam current. Another result of this crossover displacement is an increase in the angle subtended by the beam at the limiting aperture and a consequent loss in resolution. It is then concluded that, if other variables (particularly the G_2 -to-limiting aperture distance) are held constant, an increase in the distance between G_1 and G_2 will increase resolution while a decrease in this distance will increase the beam current at the expense of resolution.

The trajectories in the three electron guns shown in Figure 20 were obtained by a computer calculation. A comparison of the results supports the conclusions discussed in the paragraph above. The beam predicted for the short gun does not show a definite crossover and the ratio of beam current to cathode current appears high. On the other hand the trajectories computed for the long gun form a narrow crossover close to the cathode. The part of the beam which gets through the limiting aperture has a small diameter which indicates good resolution. However the effective cathode area is quite small. These results support the significance of the relation $N_e \propto \left[\frac{I_{G_2}}{I_B} \right]^{1/2}$ which had been found empirically.

To parallel this computer study a gun was built which is a more extreme example of the structure shown in Figure 20c. This gun has a 0.015 inch G_1 -to- G_2 spacing. The experimental results

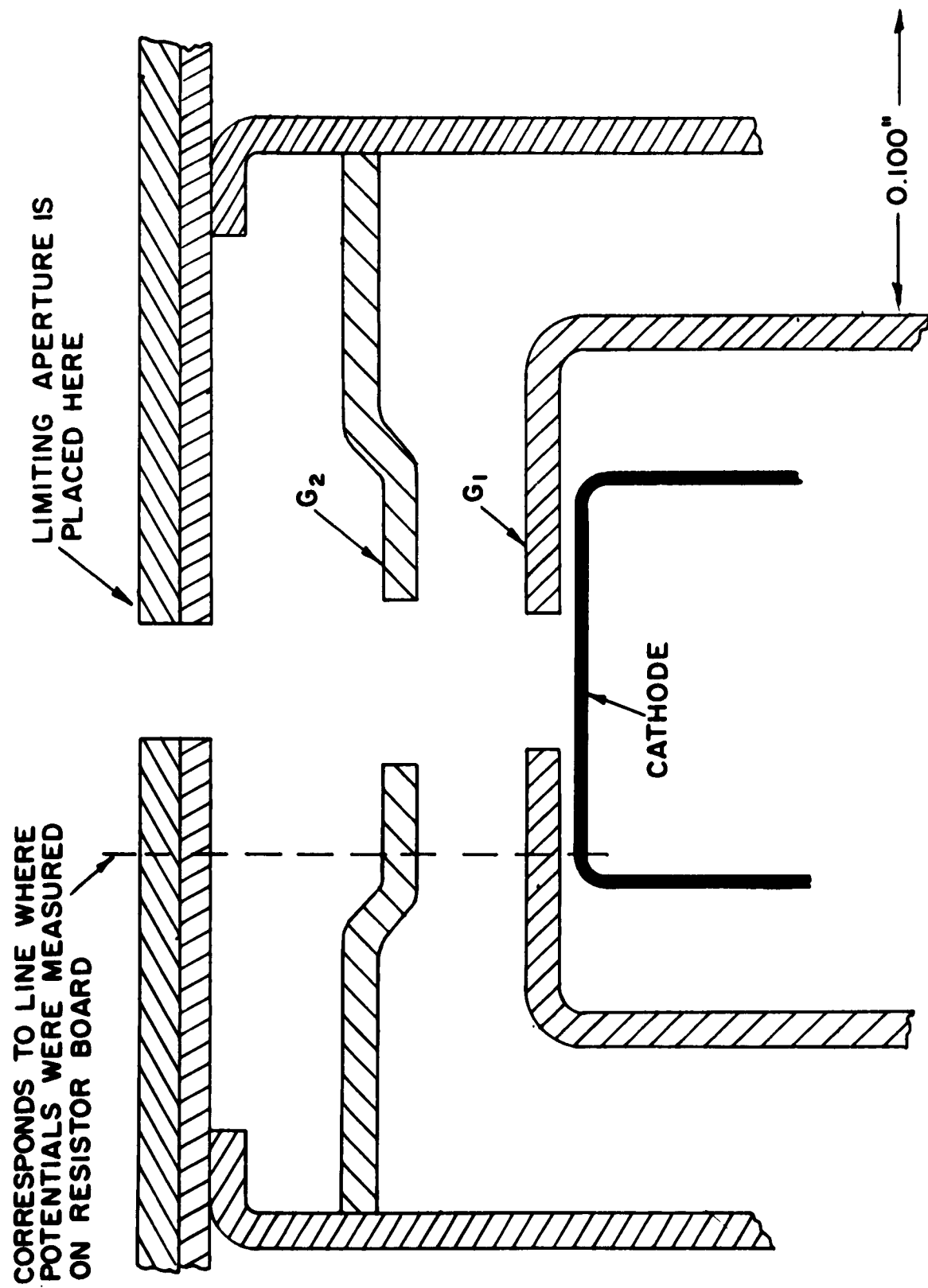
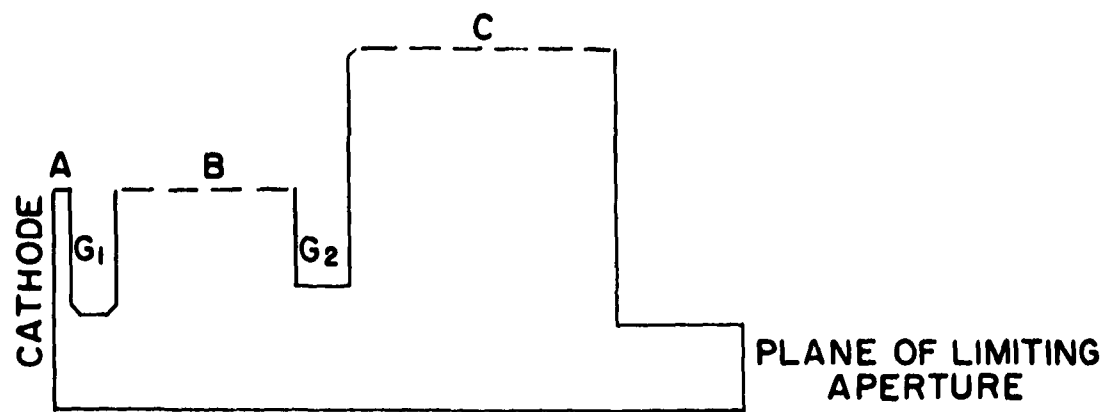
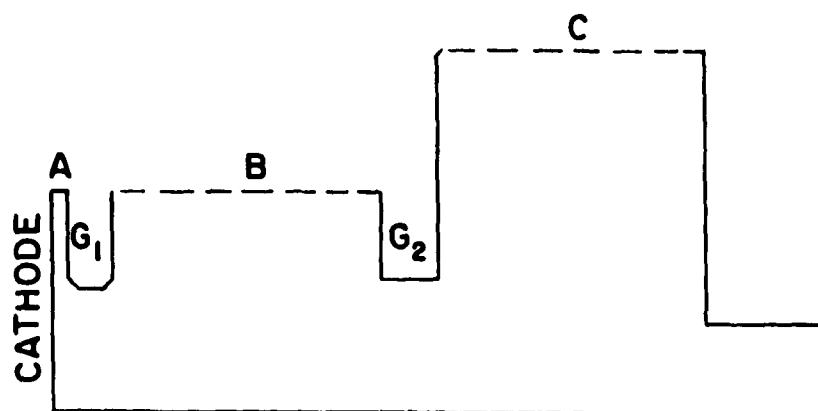


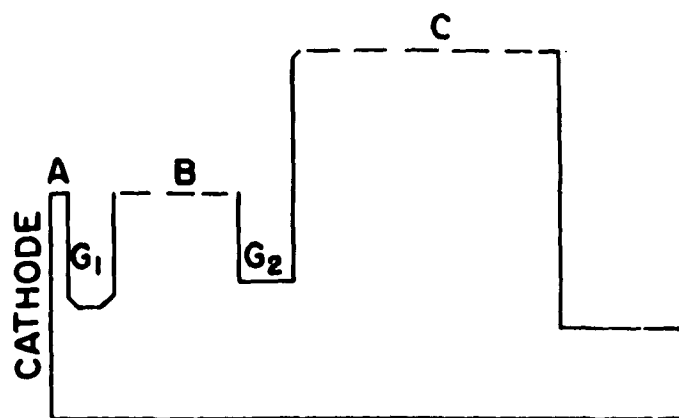
FIG. 19 5820A ELECTRON GUN



(a) STANDARD GUN



(b) LONG GUN



(c) SHORT GUN

SCALE: 0.040 INCH

A, B, C — FOR THESE LINES
POTENTIALS WERE
MEASURED ON
RESISTOR BOARD

FIG.20 GUN DIAGRAMS FOR COMPUTER INPUT

indicate that there is no decrease in resolution as predicted above. However, this result must be considered inconclusive since the G_2 -to-limiting aperture distance was also lengthened.

D. Digital Computer Program for Plotting Electron Trajectories

The computer program which was used in these trajectory determinations was written for an IBM 7090 digital computer by the Computation Section of RCA Laboratories. The program solves Laplace's equation by a relaxation technique on a mesh. The mesh dimensions are selected so that the potential field in the gun may be found to any desired degree of accuracy. The unknown boundary potentials were measured on a resistor board along the dashed line shown in Figure 19. The program also can be used to compute the trajectories of electrons emitted from the cathode with given radial and axial energy. Thus the thermionic nature of the emission is taken into account. However, the effects of space charge are not included in the program. The trajectories may then be plotted automatically from the output cards on an Electronic Associates Data Plotter. Typical results for a standard image orthicon gun are shown in Figure 21 where the trajectory (a) had initial radial and axial energies of 0.09 eV while (b) had zero emission energy.

To estimate whether the omission of space-charge effects from the computer program leads to serious errors, one can calculate the value of the axial potential minimum required to turn back to the cathode that number of electrons which equals the difference between computer-predicted beam current and actual beam currents obtained under the same operating conditions. Since the beam is composed of electrons whose trajectories are never far from the axis, the depression of the axial potential below the value found on the computer is a good measure of space charge effects. Because electrons are lost to the beam through other mechanisms (such as scattering off the walls of the limiting aperture) the value found here for the axial potential depression due to space charge will be (in absolute value) an upper limit to the actual depression.

For a cathode current density of 0.5 amperes/cm² the beam current predicted by the computer for the standard gun structure shown in Figure 20a is $I_i = 3.7$ microamperes. Data obtained from

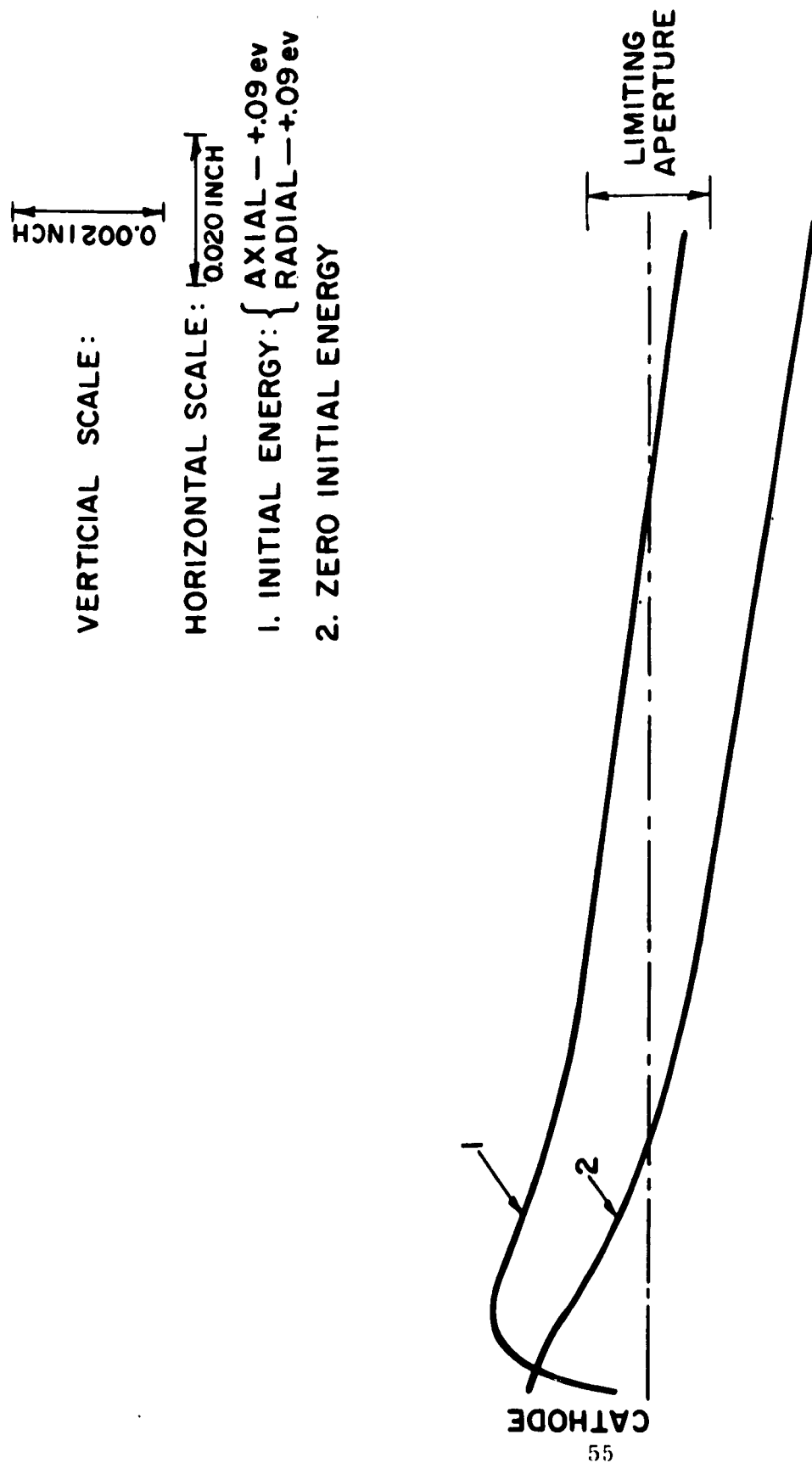


FIG. 21 ELECTRON PATHS COMPUTED IN
 THE STANDARD GUN

1

tube H-8643-3 indicate that 80 percent of this current does not appear in the beam. Assuming that this 80 percent is lost because of space charge depression of the axial potential an upper limit to the potential minimum is $|V| = 0.08$ volts.

The earliest computer results indicated that the axial potential varies rapidly with the cathode to G_1 spacing. Since the spacing under operating conditions is not known the cold spacing was used as input data in the first run. In subsequent runs a correction for thermal expansion was introduced, but the precision of this correction is not known.

E. Positive Grid Guns

In designing new electron guns for use in image orthicons the principal objective has been to produce an electron beam of high current density and small diameter while providing good depth of focus, that is, a gun in which resolution is not sensitive to small changes in deflection and focus fields. The depth of focus will improve if the angular width of the beam at the exit aperture is decreased while good resolution will be maintained at higher current densities if the energy distribution in the beam is narrowed. The time of flight defocusing mentioned above will be a less serious problem in a gun with improved depth of focus.

A positive grid gun provides increased depth of focus because the absence of a crossover in the gun leads to electron trajectories in the beam which are nearly parallel to the axis. It was also thought that such a gun would give a narrow energy distribution because of the uniform starting potential seen by electrons emitted from all parts of the cathode. However, in view of the small effective cathode area found in computer studies of negative grid guns this is probably not an important consideration. (Because there is no crossover, the effective cathode area in a positive grid gun is not larger than that in a negative grid gun.)

Several positive grid guns were built both with and without magnetic shields. In general it was found that, in the non-shielded guns,

the current density at the limiting aperture increased while the depth of focus decreased. The reason for the better depth of focus of the magnetically shielded gun is probably that the elimination of high radial velocity electrons by the aperture plates in the gun is unhampered by the confining effects of a magnetic field.

Because the beam current densities in the above guns were only a small fraction of the cathode current densities, a tube was built with a low voltage drift space between the cathode and the anode. The purpose of this long tube was to permit magnetic focusing of the cathode in the plane of the limiting aperture. The cathode current density would then be achieved at the limiting aperture. Some of the expected focusing action of the drift tube was observed if the tube was positioned further into the focusing field than normal. However, the magnetic field at the electron multiplier was then too large for proper functioning of this component.

Two other positive-grid gun monoscope tubes (H8545-5, 6) were built. Both of these have smoothed cathodes. In the first of these the positive grid was placed closer to the cathode than in former tubes. This configuration permitted the use of a lower positive grid voltage for the same electric field, so that poisoning of the cathode by electron bombardment of the first grid was reduced. The spacing between the positive grid and the anode in this gun is 0.120 inch and 50 percent square-wave response is measured at 1125 TV lines/inch. This resolution figure is substantially independent of beam current for $0.08 \mu\text{amp} < I_B < 0.8 \mu\text{amp}$.

Tube H-8545-6 is similar to H-8545-5 but the spacing between the positive grid and the anode is 0.600 inch. One would expect lower beam currents, better depth of focus, and possibly higher resolution from this tube. This was found to be the case; maximum usable beam current decreased to 0.05 microamperes but 50 percent square-wave response occurred at 2500 TV lines/inch.

The depth of focus of tubes H-8643-5, 6 was compared to that of a negative grid tube by measuring the range of wall voltage over

in spot size due to these changes in the electron velocity distribution in the converging, as opposed to the uniform, field.

The work on positive grid guns was not emphasized during most of the year because both predicted and measured resolution figures were far higher for negative grid guns. However, recent tests on image orthicons with structured targets and negative grid guns have indicated that the deep focus properties of positive grid guns may be required in spite of their lower on-focus beam resolution. (See earlier section on Beam Bending.)

F. Experimental Guns

A number of exploratory gun designs were investigated to determine feasibility for image orthicon use. These are described in the section which follows.

1. Smoothed Cathode on Passive Nickel Base

Experimental use of a smoothed cathode has led to improved beam resolution. The mechanism involved is the narrowing of the radial energy spread. Further increase in resolution can be obtained by decreasing the axial electron energy spread. A decrease in axial energy distribution was sought by substituting a less active cathode material for the standard material, so as to reduce the potential drop in the cathode interface. Spatial variation of the electron starting potential which is due to variations in interface resistance would broaden the axial energy distribution.

Tube H-8643-9 was made with a smoothed cathode on a passive nickel cathode cup. This alloy (RCA N81) has a low impurity content and should give very low interface resistance. This tube showed a large increase in resolution over that obtained from smoothed cathodes on normal nickel bases.

the current density at the limiting aperture increased while the depth of focus decreased. The reason for the better depth of focus of the magnetically shielded gun is probably that the elimination of high radial velocity electrons by the aperture plates in the gun is unhampered by the confining effects of a magnetic field.

Because the beam current densities in the above guns were only a small fraction of the cathode current densities, a tube was built with a low voltage drift space between the cathode and the anode. The purpose of this long tube was to permit magnetic focusing of the cathode in the plane of the limiting aperture. The cathode current density would then be achieved at the limiting aperture. Some of the expected focusing action of the drift tube was observed if the tube was positioned further into the focusing field than normal. However, the magnetic field at the electron multiplier was then too large for proper functioning of this component.

Two other positive-grid gun monoscope tubes (H8545-5, 6) were built. Both of these have smoothed cathodes. In the first of these the positive grid was placed closer to the cathode than in former tubes. This configuration permitted the use of a lower positive grid voltage for the same electric field, so that poisoning of the cathode by electron bombardment of the first grid was reduced. The spacing between the positive grid and the anode in this gun is 0.120 inch and 50 percent square-wave response is measured at 1125 TV lines/inch. This resolution figure is substantially independent of beam current for $0.08 \mu\text{amp} < I_B < 0.8 \mu\text{amp}$.

Tube H-8545-6 is similar to H-8545-5 but the spacing between the positive grid and the anode is 0.600 inch. One would expect lower beam currents, better depth of focus, and possibly higher resolution from this tube. This was found to be the case; maximum usable beam current decreased to 0.05 microamperes but 50 percent square-wave response occurred at 2500 TV lines/inch.

The depth of focus of tubes H-8643-5, 6 was compared to that of a negative grid tube by measuring the range of wall voltage over

which 100 percent square-wave response is maintained at a given line number. The results, shown in Table 4 below, demonstrate the superior depth of focus of the positive grid guns.

Table 4. Depth of Focus Measurements

Tube No.	Description	Δw (volts*)	
		1000 $\frac{\text{TVL}}{\text{inch}}$	500 $\frac{\text{TVL}}{\text{inch}}$
H-8643-2	Neg. Grid Gun	$\pm 0.5 \text{ V}$	$\pm 3.0 \text{ V}$
H-8545-5	Positive Grid G_1 - $G_2 = .120''$	$\pm 1.0 \text{ V}$	$\pm 2.5 \text{ V}$
H-8545-6	Positive Grid G_1 - $G_2 = .600''$	$\pm 1.5 \text{ V}$	$\pm 5.0 \text{ V}$

*Range of wall voltage over which 100 percent square-wave modulation is maintained at the given line number.

The maintenance of resolution over a larger range of wall voltage is equivalent to maintaining resolution over a larger range of target voltage. Therefore, the use of positive guns in image orthicons should reduce the problem of time-of-flight defocusing which arises because of voltage variations on the target.

Since no crossover occurs in the positive grid gun the minimum attainable beam diameter in the absence of magnetic effects is the diameter of the limiting aperture, b . The maximum value of N_e is then given approximately by $1.6/b$ for a wide range of physically probable current density distributions in the beam. The fact that values of N_e higher than this have been obtained should be attributed to the magnetic demagnification of the beam which occurs because the magnetic field at the monoscope target is larger than that at the gun.

In the ideal positive grid gun, the electrons would emerge from the gun parallel to the axis and the flow would be laminar. Therefore, the electrons, travelling under the influence of a magnetic field, do not come to a series of foci. Thus, if the magnetic field is constant, the diameter of the beam does not vary appreciably along the axis. In the case of laminar flow in an increasing magnetic field the electrons, to the first order, tend to follow the field lines. (More precisely, by crossing the converging magnetic field lines, the electrons assume a cyclotron motion which tends to converge them to the axis) If the magnetic field at the target is larger than at the limiting aperture, in this approximation, the Larmor radius at the target will be smaller than at the limiting aperture by a factor $(B_0/B_T)^{1/2}$ where B_T is the value of the magnetic field at the target and B_0 is the value at the limiting aperture. Experimental data for positive grid guns indicate that the flow is not laminar, and that a series of loops is executed. However, values of N_e are found which are larger than that corresponding to a Gaussian beam whose diameter is the same as the limiting aperture diameter. Therefore, one concludes that magnetic demagnification is effective in producing smaller spot size. It should be noted that in a typical case where $B_T/B_0 \sim 4$ the predicted N_e in the case of complete magnetic demagnification does not exceed the values obtained experimentally on smoothed cathode negative grid guns. Because focusing in the negative grid gun depends on the imaging of a crossover, the spot size depends on the product of the radial velocity spread in the beam and the difference in transit times for two electrons one of which is at the peak of the velocity distribution and the other at the edge. In this gun the flow is even more non-laminar so that target spot size is not directly related to Larmor radius. In an increasing magnetic field the axial spread in speed decreases according to $(1 - \frac{B_T}{B_0} \sin 2\theta_0)^{1/2}$ (Ref. 12) where θ_0 is the angle subtended by the beam at the limiting aperture.

The radial spread in speed increases according to $(B_T/B_0)^{1/2}$ (Ref. 12). Preliminary calculations indicate that for the magnetic fields in use here there will be no detectable change

in spot size due to these changes in the electron velocity distribution in the converging, as opposed to the uniform, field.

The work on positive grid guns was not emphasized during most of the year because both predicted and measured resolution figures were far higher for negative grid guns. However, recent tests on image orthicons with structured targets and negative grid guns have indicated that the deep focus properties of positive grid guns may be required in spite of their lower on-focus beam resolution. (See earlier section on Beam Bending.)

F. Experimental Guns

A number of exploratory gun designs were investigated to determine feasibility for image orthicon use. These are described in the section which follows.

1. Smoothed Cathode on Passive Nickel Base

Experimental use of a smoothed cathode has led to improved beam resolution. The mechanism involved is the narrowing of the radial energy spread. Further increase in resolution can be obtained by decreasing the axial electron energy spread. A decrease in axial energy distribution was sought by substituting a less active cathode material for the standard material, so as to reduce the potential drop in the cathode interface. Spatial variation of the electron starting potential which is due to variations in interface resistance would broaden the axial energy distribution.

Tube H-8643-9 was made with a smoothed cathode on a passive nickel cathode cup. This alloy (RCA N81) has a low impurity content and should give very low interface resistance. This tube showed a large increase in resolution over that obtained from smoothed cathodes on normal nickel bases.

An equivalent passband, N_e , of 4000 TV lines/inch was obtained with a beam current of 20 nanoamperes.

The initial resolution was not maintained during life testing as shown by the table below.

Table 5: Resolution of Tube H-8643-9,
Smooth Cathode on Passive Nickel
Base

<u>Beam Current</u>	<u>N_e Before Life Test</u>	<u>N_e After 1000 Hr. Life Test</u>
0.02 μ a	4000 TV lines/inch	2500 TV lines/inch
0.03 μ a	3750 TV lines/inch	2250 TV lines/inch
0.05 μ a	2750 TV lines/inch	1940 TV lines/inch
0.10 μ a	2500 TV lines/inch	1800 TV lines/inch
0.50 μ a	-	850 TV lines/inch

The N_e of this tube decreased rapidly with life as compared to other oxide cathode tubes being life tested. However, the resolution of tube H-8643-9 remains measurably better than the resolution of smoothed-oxide cathode tubes with active nickel bases.

The excellent results obtained with this tube have not been reproduced. Of the other monoscope tubes built with smoothed cathodes on passive bases several were too noisy to obtain square-wave response data. Measurements of resolution on tube H-8643-16 gave an initial N_e of 1875 TV lines/inch with a beam current of 0.02 microamperes.

Tube H-8643-21 was built with a smoothed cathode on N-130 alloy. This metal is not actually passive (with

respect to activation speed) but it does form a low resistance interface with the oxide coating. This tube was equipped with high and low velocity monoscopes. The initial N_e values, measured with beam current of 0.02 microamperes, were 1600 TV lines/inch at high velocity and 1140 TV lines/inch at low velocity. These results are comparable to values obtained with standard oxide cathodes.

It must be concluded that low cathode interface resistance, by itself, does not account for the higher initial resolution observed on tube H-8643-9.

2. Cesium-Plasma Hollow-Cathode Image Orthicon Gun

The cesium-plasma hollow-cathode was investigated because it has several unique features which may be useful for a low-noise, high-resolution image orthicon gun. A practical cesium-plasma cathode has been developed at the RCA Princeton Laboratories by A. Eichenbaum. Tests of a gun with a cesium cathode in a low-noise traveling-wave tube had shown low-noise performance approaching the best low noise results obtained with oxide cathodes.

Although electrons actually originate from the inner walls of the hollow cathode cup of the cesium cathode, they are effectively emitted from the plasma cloud surrounding the exit hole. Space-charge neutralization of the electrons within the cup allows high emission densities at the hole while maintaining low densities of emission from the walls. The practical limit of this increase in effective emission density is not known for the present cathode design. The important difference between the oxide cathode and the cesium plasma cathode, however, is its indestructibility in the usual sense. Unlike the oxide cathode, the emitting "surface" cannot be permanently destroyed by overload or by ion bombardment. Thus whatever resolution is initially observed with such a cathode should be observed throughout the life of the cathode.

Since the requirements for a high resolution image orthicon gun are quite different from those for a low-noise traveling-wave tube gun, an experimental investigation of the cesium-plasma hollow cathode was begun to determine its resolution properties. A limiting visual resolution of 5000 TV lines/inch was observed on tube H-8643-14. The operation of the cesium source heater and cathode heater were satisfactory and no free cesium was observed outside of the gun during or after approximately 20 hours of operation. However, emission current was observed from G_1 . It was felt that an extensive development program would be required before this type of gun would become competitive with oxide-cathode guns.

3. Point Cathode Image Orthicon Gun

A study was made of the feasibility of using a "point" source of electrons. In this design the active cathode surface would be very small and would be imaged directly, eliminating the need for a small defining aperture. Therefore, the current density available from the cathode could be substantially realized in the beam and the beam would be space-charge current limited. The absence of the small defining aperture would minimize the parition noise in the beam, allowing effective space-charge suppression of noise.

Computer studies have indicated that in standard guns the cathode area which contributes to the beam has a diameter of 0.0013 inches. Therefore, in order for a point cathode to be effective, the spot of active material would have to be less than 0.0013 inches in diameter. One method of obtaining a point source is the application of a small dot of the usual oxide cathode material on a nickel surface. An experimental gun was fabricated with an 0.003 inch diameter spot of triple carbonate cathode mixture in the center of a standard cathode cup. A small additional amount of carbonate was deposited along the perimeter of the

cup to help create the proper atmosphere for activation of the central spot. Tests of this oxide point cathode indicated that active cathode material was not limited to the areas on which it was applied but spread to cover most of the metal surface during activation.

Another approach to a point cathode is the cesium plasma hollow cathode gun described above. However, spurious emission from the grid and the sides of the hole preclude the use of this structure as a point cathode. Two other possibilities are the fabrication of a bariated nickel cathode of the required small dimensions or the mounting of a small single crystal emitter on a non-emitting surface.

The latter course was followed in a preliminary investigation to determine if a satisfactory point cathode could be made using lanthanum hexaboride (LaB_6). A small crystal can be embedded in colloidal graphite on the end of a hairpin heater. The graphite surrounding the crystal is not an effective electron emitter so that a very small source of electrons from the crystal should result and the need for a small aperture diameter would be eliminated. The emission properties of LaB_6 have been known for sometime, but life data for LaB_6 mounted on various materials is not well established. It is anticipated that metallurgical as well as physical handling technology may have to be developed before this material would be of practical use in a rugged cathode structure.

Another practical problem is the high operating temperature required to obtain useful emission densities from this material. This high temperature, combined with the effects of a larger aperture diameter, would cause a thousandfold increase in the light falling on the photocathode from the gun region. Such an increase is thought to be above tolerable limits.

4. Hydrogen Activation of Image Orthicon Cathodes

It has been demonstrated at RCA Laboratories and elsewhere that a passive-metal oxide-cathode activated in a hydrogen atmosphere has higher initial activity and higher activity during life than a vacuum-activated cathode. Because resolution has been found to depend strongly on cathode condition, several attempts were made to convert image orthicon cathodes in a hydrogen atmosphere. Results of two tests indicated that these cathodes cannot be hydrogen activated in their present design. Cathodes which have been successfully activated in hydrogen have had open geometry with maximum ventilation, so that hydrogen could circulate freely around the cathode during activation. The image orthicon cathode is highly confined in order to minimize light leakage to the photocathode and electron leakage to the multiplier. For successful hydrogen activation a major redesign of the gun would be necessary. Effort on hydrogen activation was therefore discontinued.

G. High Beam Current Life Tests

In order to meet contract objectives, beam currents an order of magnitude larger than those used by ordinary image orthicons are required. Smoothed cathode guns have been life tested at high beam currents over long periods to determine whether they are suitable for this type of service. The results of life tests indicate that they will be satisfactory.

The use of high beam currents decreases the resolution of negative grid electron guns. The relation $N_e \sim I_B^{-x}$ where x is between 0.1 and 0.2 holds approximately for negative grid guns tested here. In positive grid guns the resolution varies more slowly with beam current but resolution is lower even at high currents. (There is some decrease as the beam current is increased.)

Another difficulty encountered in high current operation is the possibility of shorter life. There can be deterioration of cathode activity and of resolution if tubes are operated with large beam currents for long periods of time. Life tests were made to evaluate the performance of smoothed cathode guns. A number of tubes have been operated for more than 2500 hours with beam currents up to 0.5 microamperes. Periodic tests of resolution have been made. The results, shown in Figure 16, indicate that the resolution of smoothed cathode guns decreases slightly during life but remains substantially higher than that of standard cathode guns.

IV. TEST EQUIPMENT

Two major pieces of equipment were built during this year to satisfy testing requirements of the program. A life rack was built to demonstrate the properties of the smoothed-oxide cathodes developed early in the year. Cycling equipment was constructed to be used, in combination with the high resolution test set, to evaluate resolution, signal decay, erasure, field effect and signal-to-noise ratio under cycled operating conditions.

A. Life Test Rack and Power Supply

In order to have a systematic record of the continuing performance of return beam monoscope tubes, a life test rack was built and put into operation. The rack holds up to ten tubes and maintains normal cathode operation. Voltages are supplied to the heater, cathode, G_1 and G_2 . The beam current of each tube can be set independently by adjusting the G_1 voltage. The tubes are removed periodically to test resolution, noise level, and cathode activity. At present six tubes have been on life test for times in excess of 2500 hours while a number of others have been tested for shorter periods.

B. Cycled Operation Equipment

Cycled operation separates the functions of target exposure, readout, and erasure of the stored target signal by the beam. The image section is operated as an electronic shutter. The

shutter may be opened by applying a voltage to the photocathode (i. e. , exposure on) for 0.0005 sec (0.03 fields) to 0.017 seconds (1.0 field). The "shutter" is then closed by driving the photocathode voltage and the stored target signal is read out after a predetermined delay time which may vary from zero to 4.55 minutes. Readout and erasure may be repeated from 1 to 128 fields.

The equipment has been used to measure the decay and erasure properties of targets and to verify the existence of the field effect in target resolution. In decay measurements the amplitude of the initial readout pulse and the square-wave response may be measured as a function of delay between exposure and readout. To expose, a light pattern is projected continuously on the photocathode. The photocathode voltage is gated on for the required exposure time. The photocathode is then turned off and readout of the stored potential pattern on the target by the electron beam commences after a delay interval. The delay interval may be binarily selected to a maximum of 16,384 fields or 4.55 minutes. The beam is off during both the exposure and delay times.

In signal erasure measurements, the same exposure and delay parts of the cycle are used. After a specified delay time, the stored target signal amplitude is recorded for a number of successive scans without re-exposing the photocathode. In the ideal case of 100 percent erasure there would be no residual signal after the first scan. In actual tests the erasure is not complete. The rate of erasure has been observed as a function of beam current.

To detect the field effect, a different test cycle is required. The target is first erased completely. The photocathode is then exposed and remains on while the square-wave response is measured for several successive scans. As discussed earlier theoretical considerations predict that the square-wave response will increase after the first scan. Experimental measurements confirmed this prediction.

The cycled test set has also been used to measure the signal-to-noise ratio of image orthicons. Signal-to-noise ratio may be measured as a function of light level in either the continuous or the cycled mode.

Recent improvements in this equipment provide greater flexibility and stability of operation. The test set may now be operated in a 525 line non-interlaced, 30 fields per second scanning mode. Formerly the test set scanned a 525 line interlaced raster at the rate of 60 fields per second. This change was made in order to allow more direct interpretation of the data. It had been noted that, on glass targets, despite the use of interlaced scan, the signal remaining after one scan was low. If the beam spot were naturally small and undistorted by the potential field on the target, the second field amplitude in the interlaced scanning mode should be nearly equal to first field amplitude.

The test set performance has been made more consistent by stabilizing the voltages applied to the target, the "sync" generator and the image producing light source. The reset time which in initial construction existed between cycles of operation has been removed to permit uninterrupted sequencing. It was noted earlier that the finite reset time affected the reproducibility of data.

A block diagram of the cycled operation equipment is shown in Figure 22. Basic operation of the equipment may be traced on this diagram. A more detailed functional block diagram is shown in Figure 23. This diagram displays the pulse and digital circuitry only. The individual units of the test set are discussed below; each is referenced to a circuit diagram. The pulse and digital circuitry is described in the first six paragraphs followed by descriptions of the other chassis.

1. Functional Block Diagram (D1681064), Figure 23

This block diagram shows the functional layout of the cycled digital equipment. All the stages that are primarily

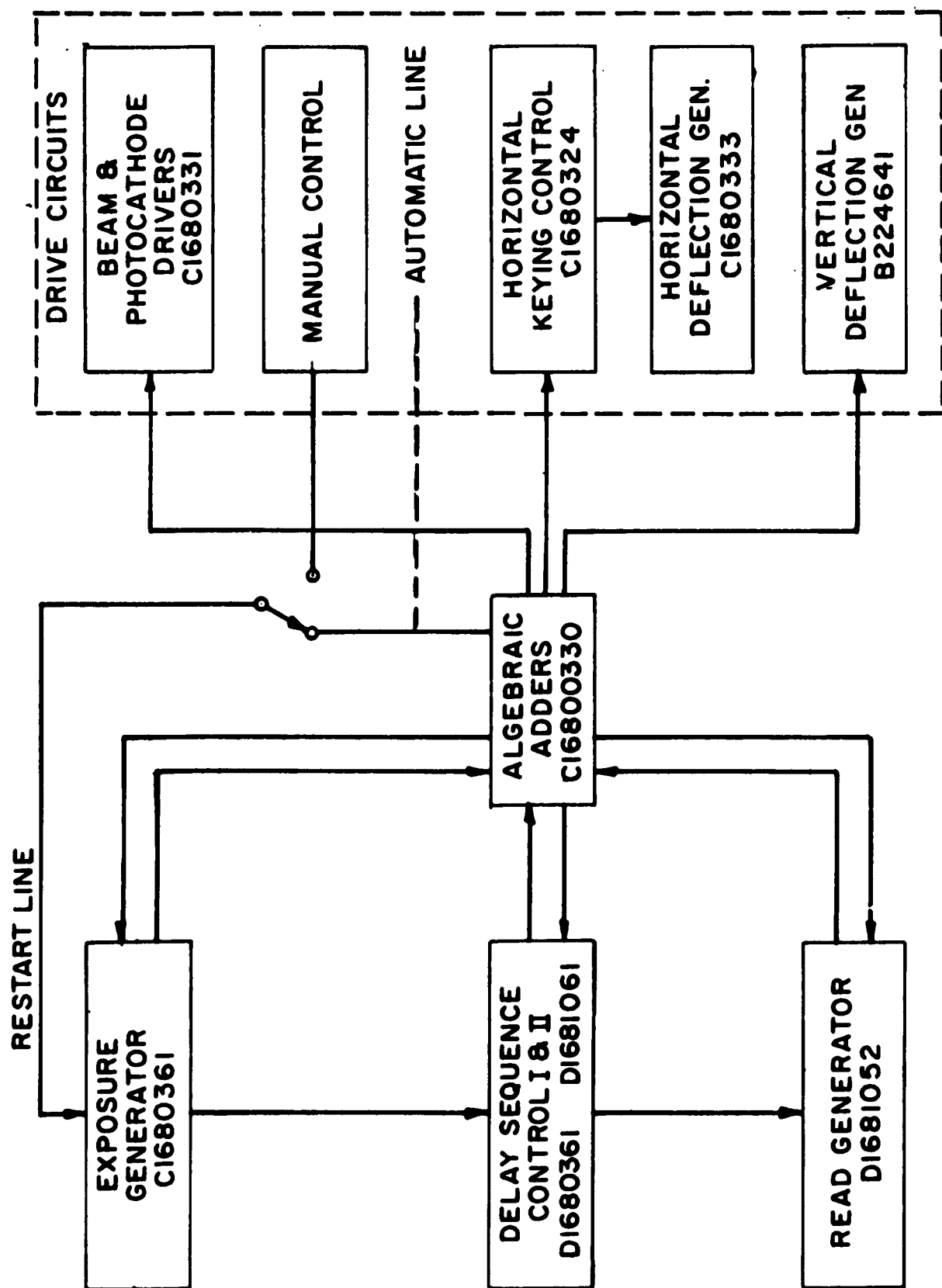


FIG. 22 CYCLED IMAGE ORTHICON EQUIPMENT BLOCK DIAGRAM

concerned with establishing the timing sequence and control are included within this diagram.

The Q subscripts are the transistor stage number and chassis location, i.e. Q₉₁₀ is transistor 9, location chassis #10, Q₆₃ is transistor 6, location chassis #3. The T number is the terminal and the subscript is the chassis location. (Signal flow is in direction of arrow.)

2. Exposure Generator (C1680361), Figure 24

This circuitry is capable of producing three independent exposure pulses, one of exactly one field duration, a second with variable front edge with the back edge synchronized to the vertical drive, and a third with both the back and front edge variable.

3. Delay and Sequence Controls I and II, (D1681050 & D1681061), Figures 25a and 25b.

These networks allow the operator to select a delay interval between exposing and reading. The delay can be binarily selected to a maximum of 16,384 fields. In addition, these circuits can also eliminate the delay time entirely and synchronize the beginning of the reading interval to the trailing edge of exposure.

4. Read Generator (D1681052), Figure 26

The Read Generator binarily selects any read interval from 1 to 128 fields. The reading begins on the trailing edge of exposure or delay. The mode of reading is preselected by the operator.

5. Algebraic Adders (C1680330), Figure 27

The Algebraic Adders synchronize the entire operation of exposing, delaying, and reading.

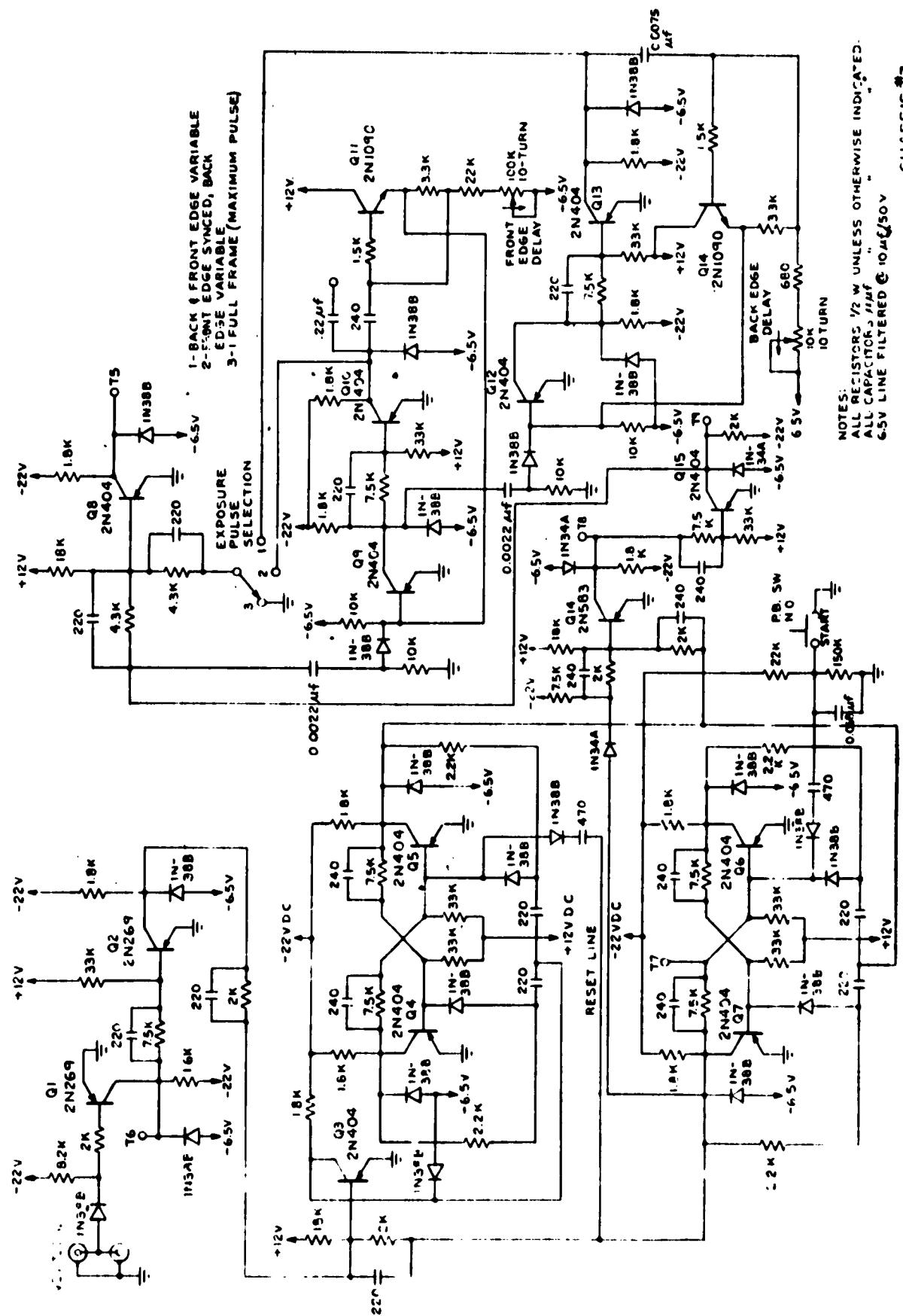


Fig. 24 Exposure Generator

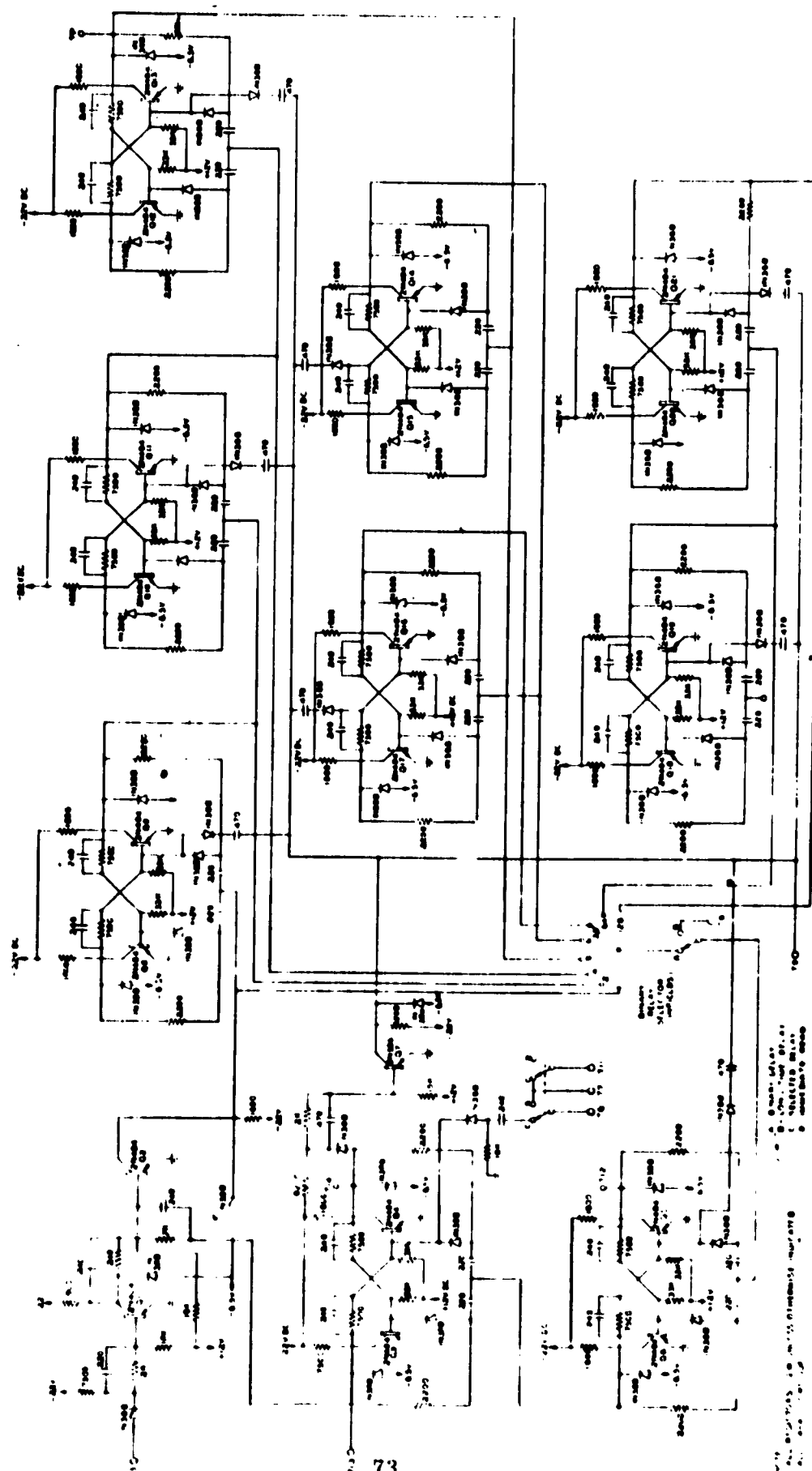


Fig. 25a Delay and Sequence Controls I

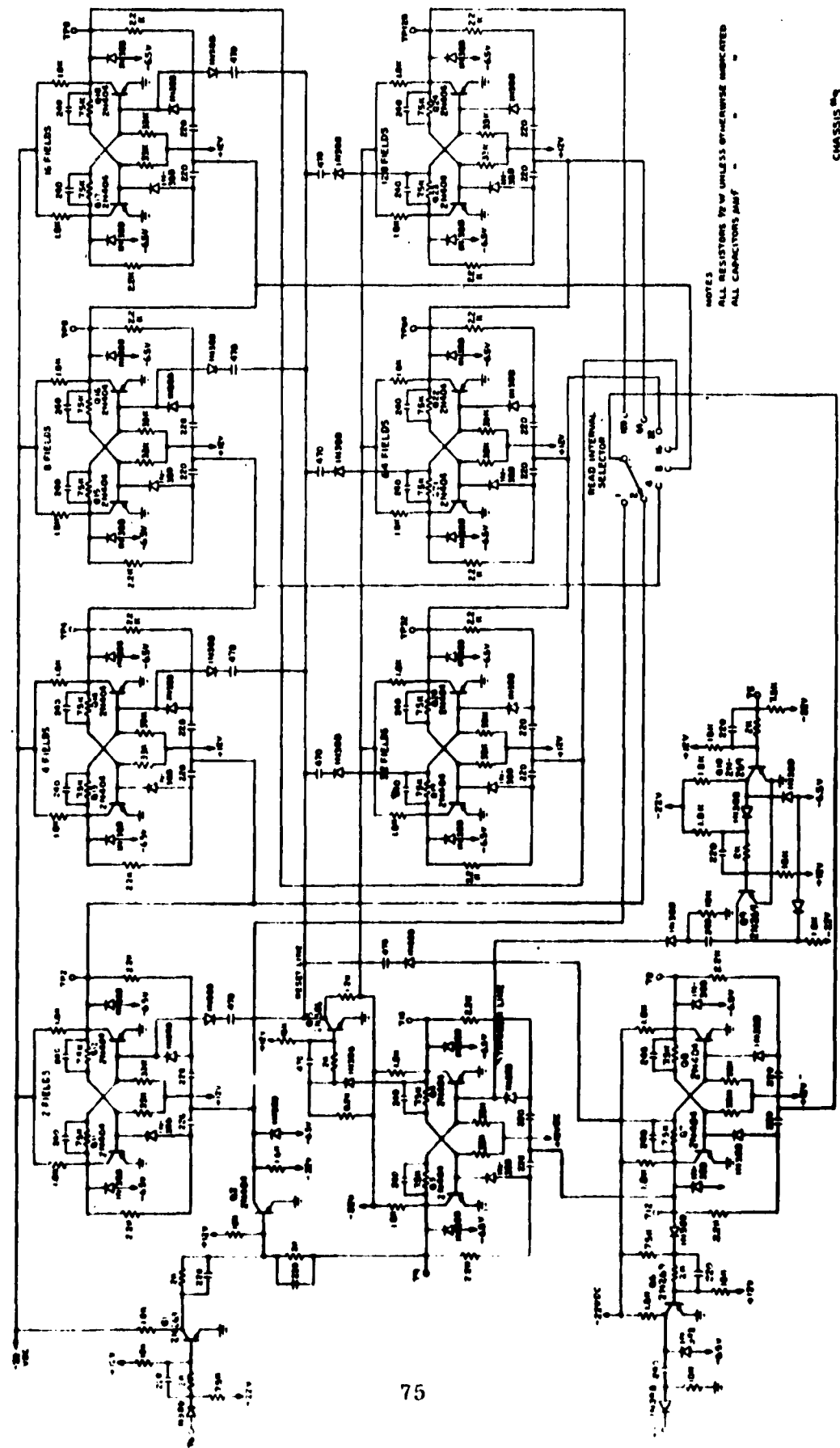


Fig. 26 Read Pulse Generator

Pulses are fed to the networks from all other chassis in the cycling equipment. Here the incoming pulses are algebraically added, placed in proper sequence, synchronized to vertical drive, and channeled to power amplifiers, deflection generators, and other equipment as required. If the pulsing mode is accidentally interrupted the networks sort out the incoming signals and resynchronize all equipment. Recycling is also handled by these circuits. By sampling all function intervals, i. e. exposure, delaying, and reading, an algebraic adder determines the longest interval and "holds" all the other circuitry until the resetting of the binary counters is completed. It then automatically restarts the entire program. (Automatic recycling can be halted and the equipment placed in manual operating mode. This does not interrupt the important duties of the Algebraic Adders.)

In addition, the Algebraic Adders prevent an accidental double exposure, double delay, or double read by taking command of the entire mode of operation once the "start" is initiated. Also provided on this particular chassis are line drivers for all function intervals. These line drivers are capable of driving 100 feet of terminated (75 ohms) coaxial cable.

6. Horizontal Keying Control (C1680324), Figure 28

The Horizontal Keying Control turns "off" the Horizontal Deflection Generator C1680333 during the exposure time. The circuit is essentially a shorting network for the horizontal sawtooth voltage. (Horizontal deflection recovers in less than one horizontal line.) Incorporated into this circuit is a balancing control that regulates the amount of attenuation of the horizontal deflection. The keying control drives only the horizontal deflection generator and is synchronized to the exposure pulse.

7. Beam and Photocathode Drivers (C1680331 and A220174), Figures 29a and 29b

The main function of this network is to switch the beam

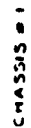


Fig. 29a Beam and Photocathode Drivers (C1680331)

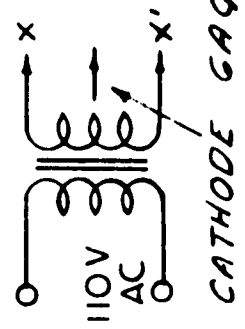
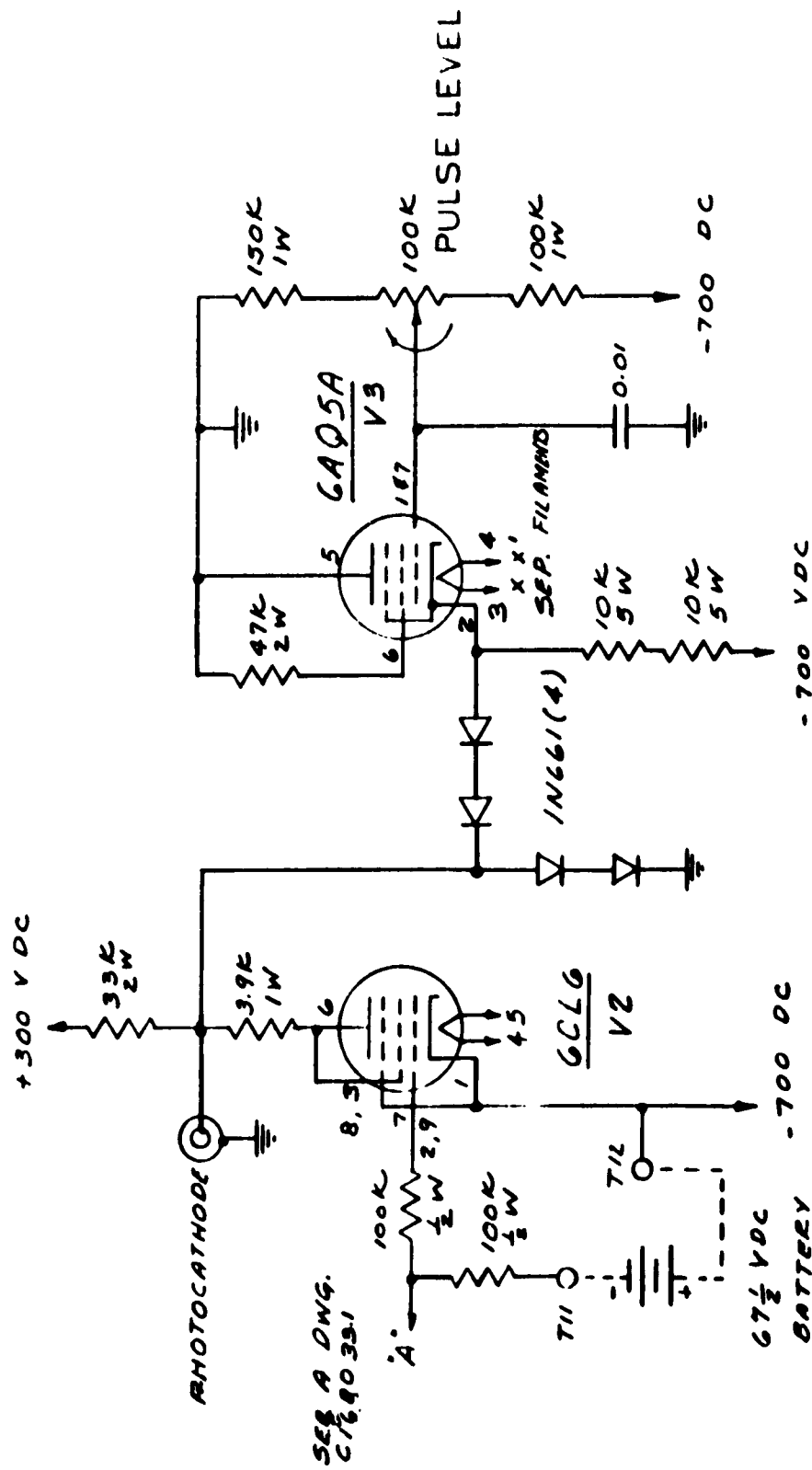


Fig. 29b Beam and Photocathode Drivers (A220174)

"off" and photocathode "on" for exposure. This chassis receives its signals directly from the algebraic adders. The circuits mainly consist of vacuum tube power amplifiers to regulate the beam bias and photocathode pulse amplitude.

The beam may be switched "on" and will remain in the "on" position regardless of the exposing interval.

8. Vertical Deflection Generator (B224641 and A220173), Figures 30a and 30b

The Vertical Deflection Generator provides deflection current for the image orthicon. Vertical drive and "off" keying is received from the Algebraic Adders.

The Vertical Deflection Generator has an input voltage isolation amplifier (A220173) to limit the input drive signal. This eliminates the possibility of over-driving the circuit and losing complete control of the vertical deflection.

The amplifier allows variations of up to 100 percent (as in unterminated coaxial lines) in the input drive signal without disrupting normal circuit operation.

9. Horizontal Deflection Generator (C1680333), Figure 31

The Horizontal Deflection Generator provides deflection current for the image orthicon. Horizontal drive is received from the master sync generator directly while "off" keying is received from the Horizontal Keying Control.

10. Voltage Adapter and Beam Signal Control (B224657), Figure 32

During the cycled operation the vertical deflection amplifier is sensitive to changes of input DC level.

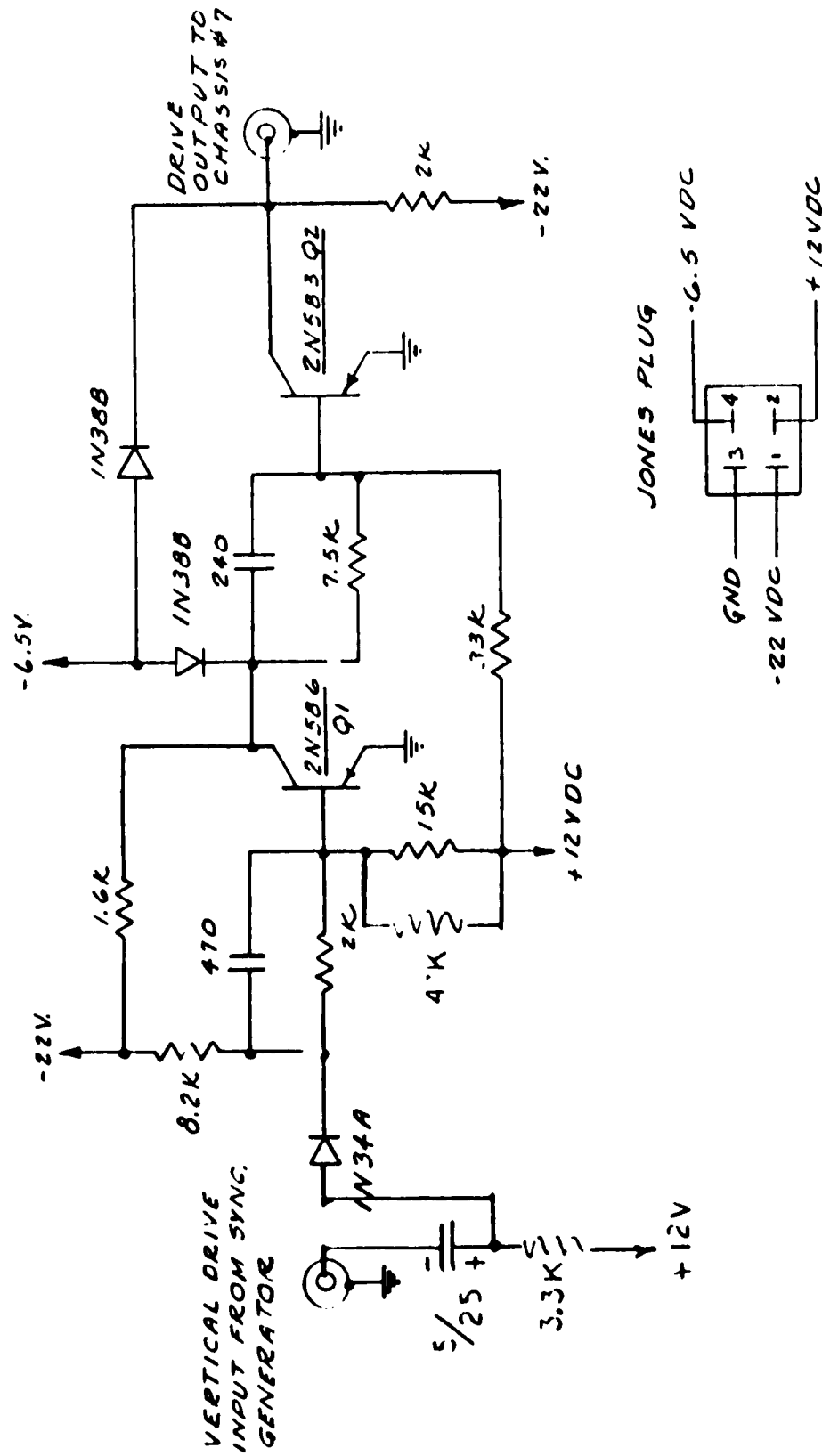


Fig. 30b Vertical Deflection Generator (A220173)

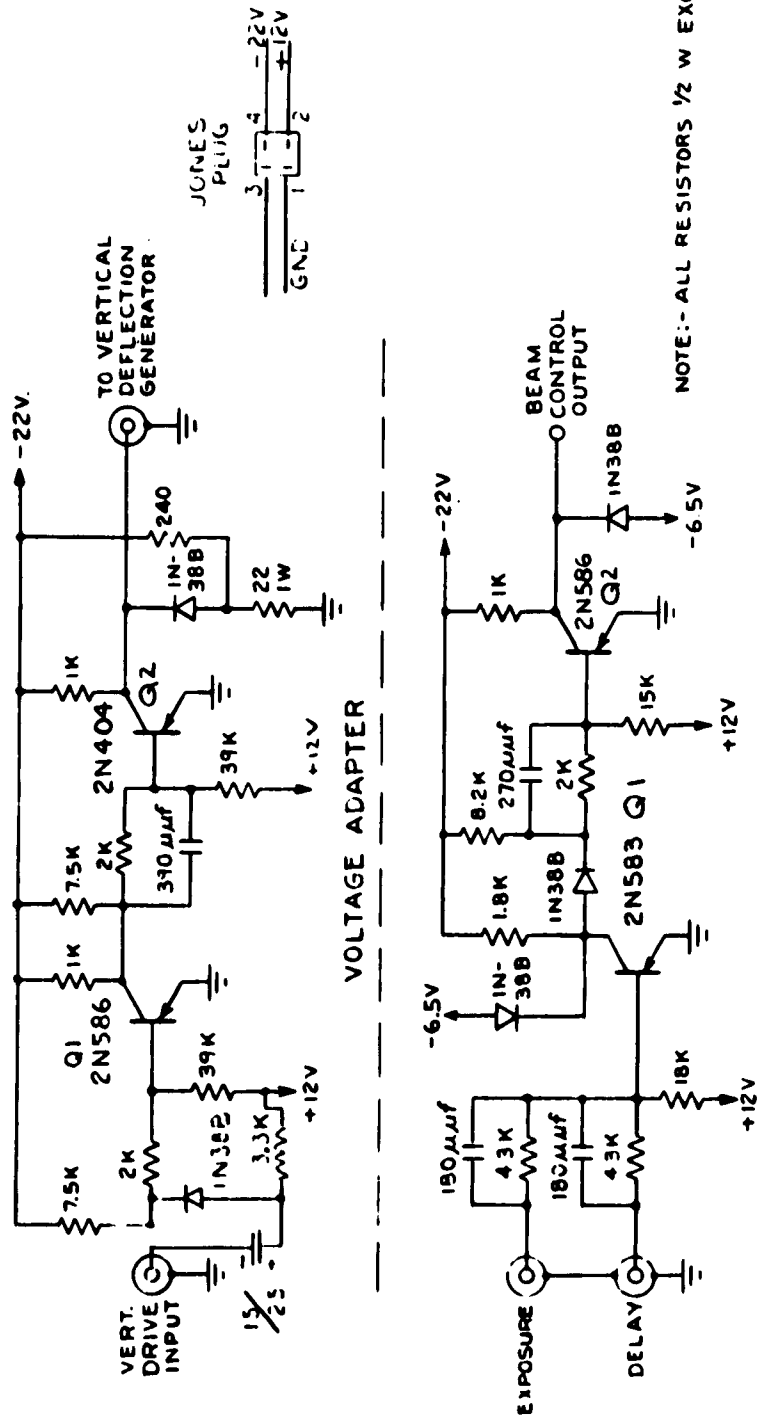


Fig. 32 Voltage Adapter and Beam Signal Control

and drive amplitude. The Voltage Adapter, was designed primarily to eliminate input drive fluctuations and produce reliable vertical deflection for all operating modes.

The Beam Signal Control sums the delay and exposure interval, amplifies the summation, and sends its output signal to the Algebraic Adders. The Algebraic Adders cross reference the generated beam signal and the delay-expose interval resulting in exact control and synchronization of the beam during the read interval.

11. Power Supplies (C1680342), Figure 33

Four low voltage, high current power supplies are mounted on this chassis. These adjustable power supplies provide biasing and DC control for all pulse and digital circuitry involved in the cycled image orthicon operation.

The low level clamp voltage relay controls all the DC outputs from this chassis. This control prevents transistor collector-emitter breakdown in the event the clamping voltage fails.

12. Power Supply (B224527), Figure 34

Large vertical deflection current is needed if over-scanning is required during cycled operation. Therefore, this power supply was developed specifically to provide currents for either the underscan or overscan mode of operation.

V. DISCHARGE DEPOSITION OF INCLUSION-FREE ALUMINUM TARGET BLANKS

This study was conducted to evaluate the feasibility of discharge deposition of high-purity inclusion-free layers of aluminum for possible use as structured target blanks. A variety of deposits was obtained but none

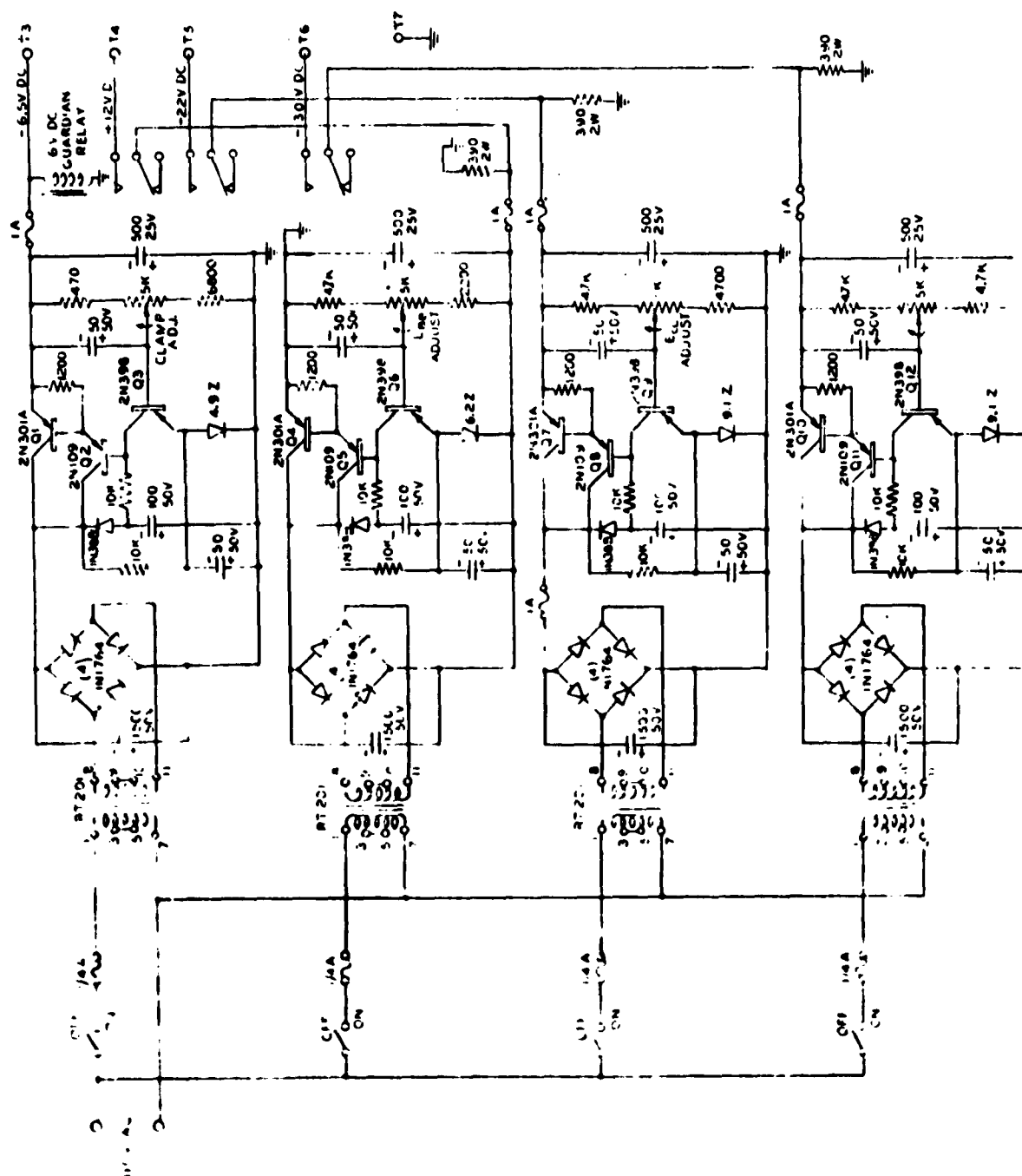


Fig. 33 Low Voltage Power Supplies

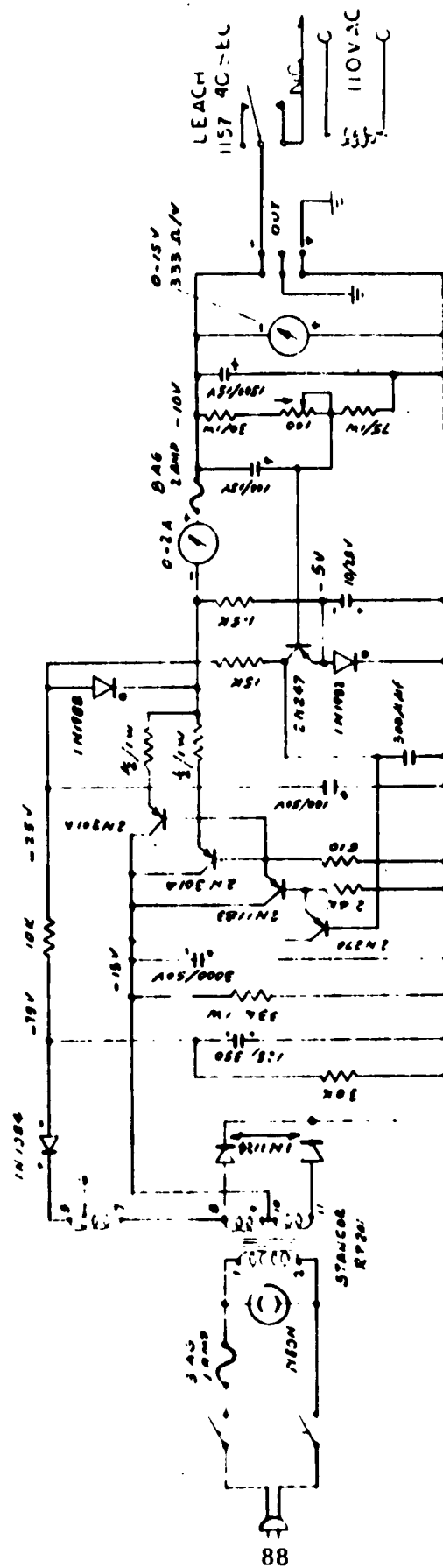


Fig. 34 Power Supply

of them contained observable quantities of aluminum.

The glow discharge studied took place in an atmosphere of tri-isobutyl-aluminum vapor between a nichrome electrode and a TIC coated glass slide electrode. The metallo-organic compound used is known to decompose into aluminum, isobutylene and other gases at 250°C. RCA-AED performed this work with existing apparatus and facilities, and with prior experience in discharge deposition of other materials.

In order to maintain sufficient vapor pressure to operate the glow discharge, the entire apparatus and source were maintained at 50°C. Discharge deposits were then obtained for pressures in a range from 0.2 mm of mercury to 1.0 mm of mercury with discharge currents ranging between 0.5 ma and 2.5 ma.

The nature of the deposits obtained varied from clear, moisture-sensitive, soft films to dark brown, moisture-resistant, hard films.

No films resembling aluminum were obtained. A sample was made for infrared analysis by replacing the TIC coated glass slide with a metal mesh and positioning a rock salt sample plate behind it. The deposit for this geometry was a soft film even though the discharge conditions would have given a dark hard film on a slide. Analysis of the sample showed the presence of poly-isobutylene and water-of-hydration. No further observations have been made on the dark hard film deposits other than to note that they are too hard to be scratched by steel wool. The color and lack of reflectivity rule out the possibility that significant quantities of aluminum are present.

SECTION II: ELECTRON TUBE DIVISION, LANCASTER, PA. CONTRIBUTION

This portion of work covers the work effort performed from
1 December 1961 to 1 December 1962.

I. INTEGRAL MESH PLUG TYPE TARGETS

At the beginning of 1962 the most satisfactory starting material for targets was 99.999% pure aluminum sheets made in Switzerland. These sheets contained about 1.5 ppm Si, 2.5 ppm Fe and 2.5 ppm Cu maximum with no detectable Tr., Mg and Zn. The dimensions of these sheets are 0.010 inch by 6 inches by 8 inches. Even though these sheets were received in a nearly mirror finish rolled condition they still contained roll marks and occluded elongated bubbles.

A. Processing of Targets Using Old Procedure

Targets made with the Swiss aluminum were processed according to the procedure outlined below:

1. Preparation of Sheet Aluminum

- (a). Buff with a canvass wheel 5 inches wide and cream wax stick abrasive.
- (b). Wash in blakasolv and then in acetone to remove all the wax.
- (c). Anodize in 12% H_2SO_4 holding for 30 minutes at 6.5 amperes per square foot at room temperature.
- (d). The resulting Al_2O_3 surface is stripped off in a solution of 21 g $\text{K}_2\text{Cr}_2\text{O}_7$ plus 35 ml per liter concentrated phosphoric acid at 70°C . This requires 20 to 30 minutes.
- (e). A bright dip consisting of 1880 ml concentrated phosphoric acid plus 125 ml of HNO_3 is used to smooth the aluminum surface. The sheet is immersed for two minutes in the bright dip bath which is held at 70°C .
- (f). Wash for 10 minutes in deionized water.
- (g). Dry with N_2 .

2. Anodizing

The procedure outlined below is used to anodize aluminum sheets:

- (a). Anodize for 40 minutes in a bath consisting of 130 g per liter of CrO_3 at 41°C using 40 volts and 0.23 amperes.
- (b). Rinse for 10 minutes in deionized H_2O .
- (c). Anodize in the H_2SO_4 bath of A4 for a half a minute at 1.9 amperes and 22 volts.
- (d). Rinse for 10 minutes in deionized H_2O .
- (e). Dry with N_2 .

3. Generation of Collector Mesh and Al_2O_3 Mesh

The procedure used for the generation of collector mesh and Al_2O_3 mesh is as follows:

- (a). Nickel is evaporated onto the anodized sheet in a circle 3 inches in diameter to a thickness that will give 20 ohms per square inch at a pressure of 2×10^{-6} mm hydrogen.
- (b). The sheet is cut into squares $3\text{-}1/4$ by $3\text{-}1/4$ inches and the edges are filed to remove burrs.
- (c). The aluminum squares are coated with Kodak Photo Resist (KPR) by pouring an excess of the KPR onto the squares and spinning off the surplus. (The KPR was previously filtered through a medium glass filter, under vacuum.) The squares are spun for 2 minutes at 78 rpm. They are then placed under an infrared lamp and spun for 5 minutes at 78 rpm. After this drying operation, the Al squares are inspected for bubbles and occluded dust particles.
- (d). Place a drop of immersion oil on the aluminum square and 1000 line master, place in contact in a vacuum frame and expose for 6 minutes in the standard color light house.

- (e). Remove from frame and place in KPR developer for 5 minutes.
- (f). Rinse in acetone and dry in N_2 .
- (g). Bake for 5 minutes at $200^{\circ}C$.
- (h). Place platers tape on the back of the plate.
- (i). Etch the Ni away with $FeCl_3$ solution heated to $35^{\circ}C$. This operation takes only a few seconds and must be stopped immediately, by washing, so that the Ni is not dissolved out from under the resist mesh.
- (j). Wash in deionized H_2O for 10 minutes and dry in N_2 .
- (k). Etch in 15% NaOH (held at $40^{\circ}C$) for about three minutes until the Al_2O_3 is removed to the bare aluminum. Care must be taken, during this operation, to etch only long enough so as not to remove the mesh. The etching is stopped by removing the aluminum square and immersing it in methanol.
- (l). Wash for 10 minutes in deionized H_2O and dry in N_2 .

4. Plating of Ni Plugs

The operations required to plate Ni plugs are as follows:

- (a). Use a solution composed of 1012.6 g $NiSO_4 \cdot 6H_2O$ + 343.8 g $NiCl_2 \cdot 6H_2O$ + 112.5 g H_3BO_3 diluted to 5 liters with distilled H_2O . Bring the solution to a pH of 5.0 with NH_4OH . The solution is heated to $40^{\circ}C$. Plate according to the following schedule:

1.5 minutes at 1.0 amperes			
2.5	"	"	.7 "
7.0	"	"	.5 "
4.0	"	"	.3 "

- (b). Wash for 10 minutes in deionized water and dry with N_2 .

5. Preparation for Mounting

The operations required to prepare targets for mounting are:

- (a). Remove the Mylar tape from the back of the aluminum sheet by dissolving in blakasolv, rinsing in acetone and drying in N_2 .
- (b). Flood microstop onto the target surface of the sheet, drain off excess and dry under infrared lamp.
- (c). Attack the sheet to the spinner with the back-up so that the center coincides with center of spinner. Paint a circle 2-1/4 inches in diameter with microstop and let it dry. Then fill in the edges with microstop. This leaves a 2-1/4 inches diameter area of Al_2O_3 exposed.
- (d). Remove the Al_2O_3 with 40% NaOH and wash off with deionized H_2O .
- (e). Suspend the sheet in a solution of 35% HCl + .5 of $NiCl_2 \cdot 6H_2O$ until the Al metal backing is entirely removed. This generally takes about 10 minutes.
- (f). Carefully pull the target from the solution and lower it into a beaker of deionized water.
- (g). Remove the target from the water and lower it into a beaker of acetone in order to dissolve away the microstop and then dip into fresh acetone. Allow the target to dry when it is removed from the second acetone bath.

6. Mounting

The targets are mounted in accordance with the steps listed below:

- (a). Coat one face of the ceramoseal ring with a suspension of 5 g of #4360-2 DuPont

colloidal alumina in 100 ml deionized water.

- (b). Lower the target carefully onto the ring and allow to air dry.
- (c). Cut the aluminum frame and excess target away by running a hypodermic needle around the outer edge of the ceramoseal ring.

7. Firing

The operations required to fire targets are:

- (a). Place the target, which is mounted on a ceramoseal ring, on a porcelain boat and insert into a tube furnace.
- (b). Fire to 400°C at the rate of 3°C per minute in O₂. At 400°C change to N₂ and then to H₂ and hold for one-half hour in order to convert the oxidized Ni collector mesh back to metallic Ni. Cool in H₂ until room temperature is attained at the rate of 1.5°C per minute.
- (c). Mount the fired target in the metallic cup device and insert into the tube mount.

The procedure explained above (Section A - 1 thru 7) produced targets that had a few obvious defects. Microscopic examination showed that most of the targets produced were not fit to put into tubes. The defects detected were (1) fringes of nickel growing out from the collector-mesh during plating shorted to the nickel plug, and (2) nickel plugs were either over filled or under filled.

The complicated procedure outlined above was also responsible for targets being lost during handling and tube processing because the Al₂O₃ mesh is very fragile. Because of these reasons, most of the work performed during 1962 was devoted to finding new methods for the handling and processing of targets in order to eliminate fringing, produce solid, flat nickel plugs and eliminate breakage during firing.

Late in 1962, the Swiss manufacturer of high purity aluminum sheet decided to stop manufacturing it. Since the Swiss aluminum sheet was not entirely satisfactory, new sources of this type aluminum sheet were under constant evaluation. The most satisfactory, and purest aluminum sheet evaluated was manufactured by the United Mineral and Chemical Corp. It was satisfactory for purity but was not useable because of surface defects.

The idea of using a sheet generated by pyrolytic decomposition of aluminum from tri-isobutylaluminum onto glass and peeling it off was advanced during 1962. This was discussed with J. J. Crosby^(Ref. 13) of the Materials Central, ASD. He saw no inherent difficulty with the new procedure. Samples are being prepared by the General Technologies Corp., Alexandria, Virginia.

B. Processing of Targets Using the Revised Procedure

Towards the end of 1962, the procedure for processing targets was revised. The revisions resulted from the gradual evolution of testing and methods procedures. The revised procedure for processing targets is contained below:

1. Preparation of Sheet Aluminum

- (a). The process of buffing the surface of the sheet was eliminated because it was found that minor scratches and roll marks on the Al sheet, prior to anodizing, did not show up during tube operation. Before this conclusion was reached, many samples of aluminum sheet were sent to commercial metal polishers to have the scratches and roll marks removed. The only company that made any significant improvement over the process used by RCA was the Penn

Optical Company. They produced a few sheets, by rolling and electropolishing, which produced good targets.

Scratches and imperfections placed on the final anodized layer show up as imperfections in the picture when the tube is in operation.

- (b). Wash the aluminum sheet in blakasolv and acetone to remove dirt and grease which may have accumulated during processing.

Another step was added to this operation because it was observed that the organic solvents did not entirely clean the surface. The step added was to wash the sheet in concentrated HNO_3 for 30 minutes, using tray agitation. A special motorized device was made to work the tray six times a minute. The sheet is then washed in deionized water for 10 minutes and dried in N_2 .

- (c). Anodize in 12% H_2SO_4 holding for 30 minutes at 6.5 amperes per square foot at room temperature.

This step is used to round off small elevations and depressions on the surface of the sheet which might cause points at which the target could rupture during handling.

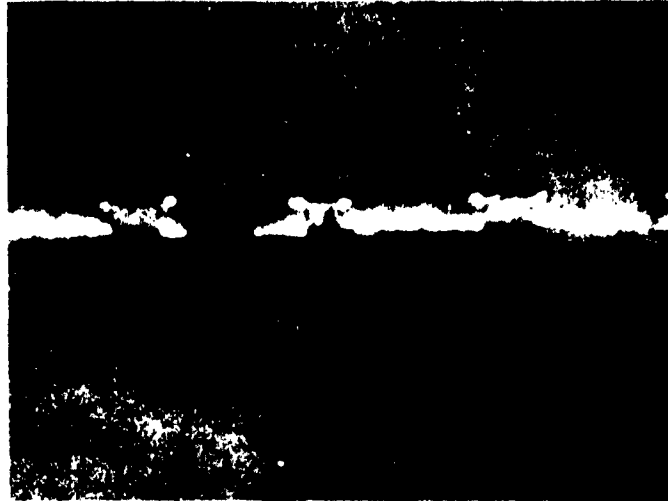
- (d). The resulting Al_2O_3 surface is stripped off in a solution of 21 g $\text{K}_2\text{Cr}_2\text{O}_7$ plus 35 ml per liter concentrated phosphoric acid at 70°C . This requires 20 to 30 minutes.
- (e). The bright dip operation was eliminated because it tends to expose the grain structure. This produces a very rough sheet making it difficult to electroplate when the nickel plugs are generated.
- (f) Wash for 10 minutes in deionized water.
- (g). Dry with N_2 .

2. Anodizing

- (a). The method used to anodize is virtually the same as explained in Section IA-2 except that the anodizing time was increased from 40 minutes to 60 minutes. Increasing the anodizing time increased the thickness of the oxide layer from 0.00017 inch to 0.00022 inch. Heavier oxide layers were tried and abandoned because they were difficult to etch in the NaOH solution. Figure 35a and 35b are cross-section photographs of the 1000 line per inch target made from aluminum anodized 40 minutes and 120 minutes respectively.

Evaluation showed that a much stronger anodized layer is developed when the voltage is increased to at least 47 volts by decreasing the bath temperature to $36 \pm 0.1^{\circ}\text{C}$. In this case, strength was judged by the ability of the target to withstand strains introduced by the firing operation. It was also observed that the introduction of lead as 0.5% Pb Cr O₄ in the chromic acid (final) anodizing bath tends to increase the ease of etching of the anodized layer with NaOH.

- (b). Rinse for 10 minutes in deionized water.
- (c). Anodize in the H₂SO₄ bath for three minutes. The time was increased from one-half a minute to three minutes because it breaks up the barrier layer made by CrO₃ anodizing and produces Al₂O₃ which is more easily removed from the bottoms of the holes during the NaOH etching of the mesh.
- (d). Rinse for 10 minutes in deionized water.
- (e). Dry with N₂.



(a)



(b)

0.001"

**Fig. 35 (a) Cross-section of a 1000 Line per Inch Target
Made from 40 Minute Chromic Anodized Layer
(b) Made from Two Hour Chromic Anodized Layer**

3. Generation of Collector Mesh and Al_2O_3 Mesh

- (a). Same as procedure explained in Section IA-3(a) except that a thicker layer of nickel was found more desirable because it was observed that the firing operation, in some cases, was removing the nickel mesh. The amount of nickel now being used is 2 ohms per square.

At first it was thought that when nickel evaporated normal to the target surface it could enter the pores as metal fingers extending down into the anodized structure. Then during etching some of these fingers would be exposed along the side walls of the holes which could cause a short between the collector mesh and the nickel plug. In order to verify this assumption, the nickel surface was made by evaporating the nickel at a sharp angle to the surface so that the nickel would not enter the pores. This did not eliminate the shorting problem.

- (b). This operation was changed to allow cutting of sheets without danger of breaking the fragile Al_2O_3 layer. The sheets are now cut with a straight edge razor blade. It was observed that when the Al_2O_3 layer is broken, the nickel plated plugs are quite porous. Apparently electrical shorting must take place between the collector mesh and the aluminum backplate so that plating occurs at the edges of the mesh rather than on the aluminum. This condition also results in fringing.
- (c). Same as explained in Section IA-3(c).
- (d). The exposure is done in the same way as explained in Section IA-3(d) except that a metal ring, slightly smaller than the evaporated Ni circle is placed on the master.

This stops light from exposing the KPR and in the subsequent developing process, the evaporated Ni is exposed in the form of a continuous ring around the mesh area. It was found that it was impossible to obtain well plated rings unless this ring was used.

- (e). It was found that during the development process the immersion oil used in the printing frame of the preceding step interfered with development. Because of this it was necessary to develop three successive changes of developer which progressively dissolved the oil and allowed the exposed KPR to develop out uniformly.
- (f). Same as Section IA-3(f).
- (g). Same as Section IA-3(g).
- (h). Same as Section IA-3(h).
- (i). Same as Section IA-3(i).
- (j). Same as Section IA-3(j).
- (k). It was found that using methanol as a short stop interfered with the plating step. Apparently methanol combines with the freshly etched aluminum surface so that during Ni plating, the Ni deposits only in isolated spots. The corrective measure taken was to wash the plate with a rapidly flowing stream of deionized water. It was also observed that the side walls of the holes being etched into the anodized aluminum were much straighter and more perfect when etched in steps. This is done by placing the sheet in the NaOH solution for several seconds then washing it with a rapid stream of water and drying it in N₂. This is repeated until the aluminum is entirely exposed at the bottom of each hole, as observed with a microscope. This technique produces the best preferential

etching along the pores perpendicular to the aluminum surface without etching too much in a lateral direction.

If the products of the etching are removed periodically by washing the penetration of the etching solution is much faster than the lateral etch.

(1). Same as Section IA-3(1).

4. Plating of Ni Plugs

(a). The solution used to plate nickel plugs is composed of the same mixture explained in Section IA-4(a) but it was found that under similar temperature and amperage conditions, the grain size of the deposited Ni is very coarse. This resulted in porous plugs, which were not uniform in thickness and which randomly contact the collector mesh. This problem was overcome by holding the plating bath at $10 \pm 2^{\circ}\text{C}$ and using less amperage. The schedule presently being used is:

1.0 minute at 1.0 ampere
4.0 minutes at 0.5 ampere

It was theorized that the fringing which formed on the edges of the collector-mesh could be caused by a field generated in the collector-mesh during the plating. Tests were made to eliminate this by placing full anode potential on the mesh by attacking a third terminal to the collector-mesh. During plating, the collector-mesh was held at the same potential as the aluminum plate. This produced the most satisfactory means of eliminating the fringing.

(b). Same as Section IA-4(b).

5. Preparation for Mounting

- (a). Same as Section IA-5(a).
- (b). " " " " (b).
- (c). " " " " (c).
- (d). " " " " (d).
- (e). " " " " (e).
- (f). " " " " (f).
- (g). " " " " (g).
- (h). The anodized layer is composed of a complex hydrated aluminum oxide which is very fine grained. Since the material can be classified as a colloid, it is reasonable to assume that various cations and anions would be absorbed onto the colloidal particles. According to the Hofmeister series, these ions will be replaced by others to the right, thus

H > Ca > Mg > Sr > Ba > Li > Na > K > Rb > Cs
OH > F > SO₄ > Cl > tartrate > Br > I > CNS.
(The symbol > means "is replaced by".)

In order to make the series progress to the left, it is necessary to apply an electrical field across the colloidal material suspended in H₂O. This is an electrophoretic cell which was constructed using platinum gauze electrodes. A target was run in the cell in order to remove ions (this is shown in Fig. 36). Magnesium ions were added to the target by putting a few grams of magnesium acetate into the cell after the current was turned off. The magnesium replaced the H-ions attached to the colloids.

A target treated in the manner mentioned above was placed in an image orthicon (IO) tube and showed excessive sticking. The electrophoretic treatment without Mg additions produced targets which were much less susceptible to breakage during firing.

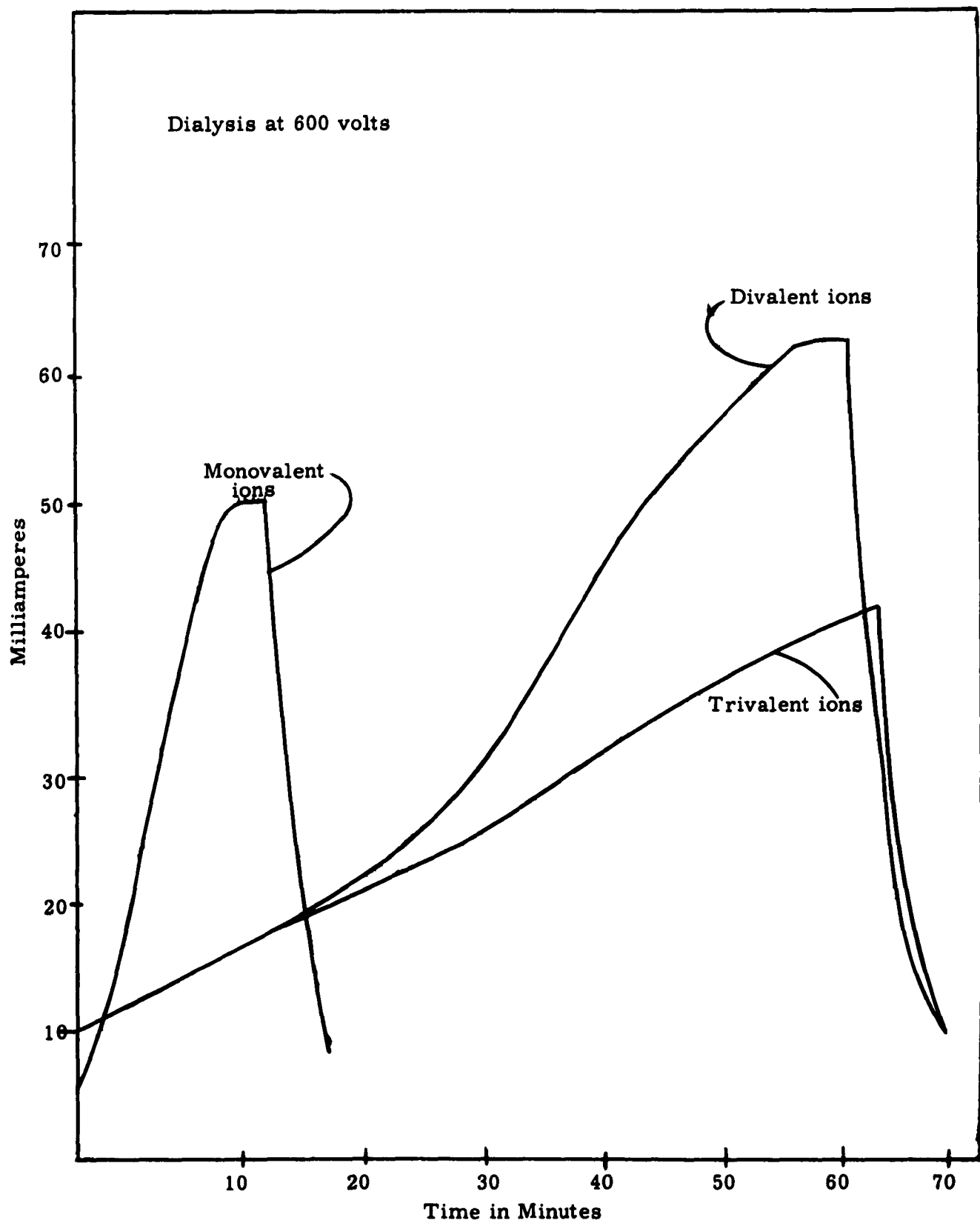


Fig. 36 Electrodialysis of an Alumina Target

6. Mounting

- (a). Same as Section IA-6(a).
- (b). Same as Section IA-6(b).
- (c). Same as Section IA-6(c).

7. Firing

- (a). Because frequent breakage was experienced during the firing operation, a close evaluation of the actual firing schedule was made. It was found that variations in temperature, from the desired schedule, were as great as $\pm 16^{\circ}$ and that the rate of temperature increase was as great as 38°C per minute during some of the on-off cycles. Due to the fact that an on-off method of temperature control was detrimental to targets, a new furnace and controls were designed and built. The furnace was made from a Vycor tube 90 mm in diameter so that targets large enough for the 4-1/2 inch IO could be processed. A sighting port was also constructed on the furnace in order to observe targets during firing. The furnace control consisted of a variable transformer driven by a continuously variable drive making it possible to select any desired rate of temperature increase. It was theorized that a continuously uniform temperature change was more important than the specified rate of 3°C per minute. (This proved to be correct.)

The present firing schedule is: fire for one hour to 400°C in O_2 and hold 15 minutes, then change to a N_2 flush for 15 minutes and finally to forming gas when the temperature is slowly reduced.

This operation requires four hours to come back down to room temperature. All rates of gas flow are 0.8 cubic foot per hour.

Another method that was used to relieve strain in the target, during firing, was to cut a 0.030 inch wide gap in the cerama-seal ring before mounting the target. During firing, as the differential shrinkage and expansion of the Al_2O_3 and metal ring is encountered, the gap is squeezed together or opened up. This was very satisfactory but the resulting target was difficult to handle because the ring was easily deformed by slight pressure, thereby, causing the target to crack.

During firing tests, it became apparent that it was difficult to properly oxidize the KPR without removing the nickel collector mesh. Three commercial KPR strippers were tried without success. When the stripper was strong enough to remove the baked KPR it also removed the nickel mesh.

The procedure of firing the target between two ceramic rings, after it had been cut away from the aluminum frame and before mounting, was tried. It was found that the target wrinkles during firing and that there is no way of stretching it during mounting. Because of these reasons, the procedure was dropped.

- (b). It was found that it was necessary to have a good electrical contact to the nickel collector-mesh. At first this was done by placing an indium-coated kovar ring in contact. This proved to be unsatisfactory because during tube processing, the indium spread over the surface of the target causing shorting between the collector-mesh and the plugs. This was remedied by using Au plated kovar rings.

II. SUMMARY OF PROCESSING

During 1962 the major processing problems confronted were:

1. Production of perfect nickel plated plugs by elimination of fringing and generation of smooth, bright, fine-grained plugs.
2. Improving target production by better control of the firing operation.
3. Improving the handling operation.
4. Finding a new source for high purity aluminum.

Success was attained in elimination of the fringing problem and the firing problem was overcome by building a new furnace and establishing a new firing schedule. Partial success was experienced in plating as evidenced by the fact that a few good targets were made. The handling operation was generally improved and a start was made to obtain pure aluminum from pyrolytic deposition of tri-isobutylaluminum.

Most of the useable targets made during 1962 were tested in the three inch (3") IO tube. A four and one-half inch (4-1/2") IO tube was designed for testing larger targets with S-2D photocathodes. The design included a short-single-loop-of-focus image section in order to give maximum image section resolution. Several of the 4-1/2 inch IO tubes, using the usual glass target, were made and tested. It was found that the image was free of distortion thereby, confirming the fact that the electron optical design of the new tube was satisfactory. In order to test the new tubes under optimum conditions, an old laboratory 4-1/2 inch IO test set was overhauled and a new deflection amplifier built.

The various three inch (3") tubes fabricated revealed that the major problems to be solved are dark current in the target and elimination of shorted plugs. The best tube built, during the latter part of 1962, had only 0.2% shorted plugs but still produced a very poor picture because 0.2% of approximately one million plugs per square inch of target surface is a substantial figure. Figure 37 gives an idea of the number of shorts on such a target.



1" = .026"

**Fig. 37 Expanded Monitor Picture of Target Made From 60 Minute
Chromic Acid Anodized Film Operated in an Image Orthicon**

**(Large white spot and white bar is film nonuniformity.)
(Small white spots are individually shorted plugs.)**

Limiting resolution in the better targets is practically 1000 TV lines in areas where the dark current is a minimum.

III. ENLARGED PORE TARGETS

Processing of the enlarged pore targets was performed in accordance to the procedure outlined below:

1. Use 2S type aluminum sheet three inches wide by 0.005 inch thick.
2. Mount in stainless steel jig with Teflon gaskets between the stainless steel and aluminum.
3. Just before anodizing, strip the sheet in a solution of 21 g $K_2Cr_2O_7$ plus 35 ml per liter concentrated phosphoric acid at $70^{\circ}C$. This removes the oxide film down to the bare aluminum.
4. Anodize for 50 minutes in a bath consisting of 130 g per liter of CrO_3 at $34^{\circ}C$ using 105 volts and 0.23 amperes.
5. Wash in deionized water.
6. The pores are enlarged by placing the frame and anodized sheet in a beaker of distilled water and holding in the ultrasonic bath for 5 minutes. Continue for three changes of water until the solution becomes colorless. The residual CrO_3 causes an enlargement of the pores but must be removed so that the pores do not become progressively enlarged.
7. Coat the face of the target and around the back edges with Kodak Photo Lacquer (KPL) in order to keep the etching solution from seeping under the jig.
8. Use 40% NaOH to clean the back of Al_2O_3 .

9. Dip into solution of 35% HCl + .5 of $\text{NiCl}_2 \cdot 6\text{H}_2\text{O}$ to remove the aluminum back.
10. Soak in 3% NaOH at 37°C for 3.25 minutes to reduce the thickness of the barrier layer to approximately 200 A. U.
11. Wash in H_2O and acetone and dry with IR bulb.
12. Mount target on zirconia body ceramic ring using a suspension of 5 g of #4360-2 DuPont Colloidal Alumina in 100 ml deionized water.
13. Fire in O_2 using 5 ml/sec. flow and $5^\circ\text{C}/\text{minute}$ rise to 425°C . Hold one hour and cool at $3^\circ\text{C}/\text{minute}$.
14. Evaporate Mg from a 30% Mg and 70% Al alloy to give 250 to 300 A. U. thickness coating.
15. Fire in O_2 using 5 ml/sec. flow and $5^\circ\text{C}/\text{minute}$ rise to 525°C . Hold one-half hour and cool at $3^\circ\text{C}/\text{minute}$. This is done to oxidize the Mg. Target must be kept absolutely dry, if it isn't, the Mg will hydrate, expand and disrupt the target.
16. Evaporate nickel at a 20° to 25° angle.
17. Mount target in tube using a dry box.

Most of the tubes made, using the enlarged pore target, had a negative picture polarity. This was attributed to either very low secondary emission, probably caused by insufficient oxide, or the nickel collector-mesh being excessively thick. In order to correct the negative picture polarity, various amounts of Mg was deposited on targets and evaluated.

Also evaluated were collector-meshes made with smaller amounts of Ni, Ag, Cu and Au. It was found that targets made with copper collector-mesh had a positive picture polarity but in most cases the mesh opened up with any of the metals used with the exception of nickel. When nickel

was used as the collector, it produced, in addition to negative picture polarity, high dark currents and low resolution.

Work on the enlarged pore targets was dropped, in spite of its desirable features, because it appeared that targets with correct parameters could not be made in this way. It is calculated that to have the required capacitance, the mesh-to-storage surface spacing (depth of pores) should be between 2 to 5 microns. The material pore diameter was of the order of 0.3 microns making the ratio between pore depth to diameter very great. It appeared unlikely that secondary electrons, emitted in all directions, could be collected through such narrow diameters without striking the side walls. The typical negative signal obtained from tubes built with these targets was evidence that only the negative charge of the primary electron deposited is useful in producing signals. This evidence supports the deep-pore picture. Most of the tubes which gave positive signals had no collector mesh and appeared very fast at low signal levels. This indicated that the signal was based only on stray capacitance to other tube parts rather than the desired mode.

Other reasons why the enlarged pore target was dropped were (1) negative polarity picture, (2) low resolution, and (3) dark current. The negative polarity picture problem was corrected but difficulties with low resolution and dark current were too severe to continue work in this area.

This portion of work covers the work effort performed from 1 December 1962 to 31 March 1963.

I. INTEGRAL MESH PLUG TYPE TARGETS MADE WITH POSITOP RESIST

Toward the end of 1962 an integral mesh plug type target was fired in O₂ for three hours. The tube made with this target showed a considerable reduction in dark current which lead to the conclusion that the KPR on the target was not being entirely oxidized during firing and that the remaining KPR was present as semi-conductive carbon.

During this time, a new photo resist was obtained which is soluble in acetone, after processing. This resist is known as Positop, and is

manufactured by the Azoplate Corporation. Positop photo resist is a positive type because the portion of the resist exposed to light is developed and removed chemically. The previous resist used (KPR) is a negative type which means that light exposure causes the resist to become inactive towards the developer. The unexposed portions of the resist are then removed by solution when immersed in the developer,

In order to use the Positop resist it was necessary to make new printing masters. The old printing masters used with KPR had transparent lines and opaque squares. The new printing masters were made with opaque lines and transparent squares. The reason for reversing the procedure is explained in the preceding paragraph,

A target made with the Positop resist had 750 TV lines per inch structure. The plugs used in the target were thin Al_2O_3 , 150 A. U. thick. When this target was placed in a tube, very little dark current was observed and shorts from the collector-mesh to the plugs were eliminated.

A. Processing of Targets Using Positop Resist

1. Preparation of Sheet Aluminum

Same as Section IB-1.

2. Anodizing

Same as Section IB-2.

3. Generation of Collector Mesh and Al_2O_3 Mesh

(a). Same as Section IB-3.

(b). " " " " "

(c). Apply Positop onto the anodized sheet by pouring. The excess is drained off and the sheet is spun for one minute at 78 RPM. A heat lamp is then used for two minutes to dry the resist followed by one minute oven heating at 100°C .

- (d). Place the dry sheet in a vacuum frame and place the master in contact. (It was found that oil or other liquids is not necessary between the two surfaces.) The vacuum line is then connected to the pump and a metal ring is taped to the surface of the master (described in Section IB-3). This assembly is placed 24 inches away from a Bausch and Lomb laboratory electric arc light source and a 10 minute exposure made.
- (e). Develop the sheet in the proprietary developer for the Positop resist. It is necessary to rub the surface of the sheet with a cotton swab during development so as to remove the reaction products formed by combining the resist with the developer.
- (f). Rinse in deionized water and dry in N₂.
- (g). Bake at 100°C for 10 minutes.
- (h). Rinse in deionized water and dry in N₂.
- (i). Etch the nickel away with FeCl₃ solution heated to 35°C. This takes only a few seconds and must be stopped immediately by washing so that the nickel is not dissolved out from under the resist mesh.
- (j). Wash in deionized water for 10 minutes and dry in N₂.
- (k). Paint microstop on the back of the sheet in order to keep the anodized layer from being removed in the NaOH etch. This is necessary because the microstop used in step IA-3(k) to mask the back does not stick to bare aluminum.
- (l). Same as Section IB-3(k).

4. Production of Dense Al₂O₃ Plugs

- (a). Place the sheet (from step (l) above) immediately in a bath of 3% ammonium

citrate, at room temperature. The anode is a bare aluminum sheet 6 inches by 8 inches (6" x 8") and the cathode is the processed sheet. A current of 30 milliamperes is applied and the voltage is gradually increased as the thickness of the dense Al_2O_3 increases on the bare areas of the sheet. The Al_2O_3 thickness is 13.7 A. U. per volt making it necessary to allow the voltage to increase to 11 volts in order to obtain a 150 A. U. thick layer in the holes of the Al_2O_3 mesh.

- (b). Remove the sheet from the anodizing bath and wash in deionized water for 10 minutes.
- (c). Dry the sheet with N_2 .
- (d). Remove the microstop from the back of the sheet and Positop from the face of the sheet by soaking in two changes of acetone for 10 minutes each, wash with deionized water and dry in N_2 .

5. Preparation for Mounting

- (a). Same as Section IA-5(b).
- (b). " " " " (c).
- (c). " " " " (d).
- (d). " " " " (e).
- (e). " " " " (f).
- (f). " " " " (g).

6. Mounting

Same as Section IA-6 except use a zirconia ceramic ring.

7. Firing

Same as Section IB-7.

Subsequent to the use of Positop resist, a new source of aluminum sheet was found. The Reynolds Aluminum Co. offered to supply a continuous roll of 99.993% purity aluminum with as good a surface as the Swiss aluminum. This aluminum contained 25 ppm of Cu and less than 1 ppm Fe + Si. The Swiss aluminum contained 2.2 ppm of Cu, 1 ppm Fe and 1 ppm Si. The reflectivity of the Reynolds aluminum is not as good as the Swiss aluminum, which contained some very deep scratches, because the surface contains many very shallow scratches. After preliminary anodizing in H_2SO_4 and stripping, the scratches on the Reynolds aluminum disappeared completely whereas the deep scratches on the Swiss aluminum remained.

The grain size of the Reynolds aluminum is much finer than the Swiss aluminum, thereby, making the anodized layer more fragile. However, using this type aluminum should make the target surface more cleaner during actual operation of the tube. It was also found that the Reynolds aluminum accepts nickel plating much more readily than the Swiss aluminum. This is probably due to the fine grain size of the individual aluminum crystals in the sheet.

It remains to be seen whether the additional copper in the Reynolds aluminum will cause additional dark current in target operation. Experience is also necessary to determine whether the extra fragility of the anodized layer can be handled.

References

- 1 ASD Technical Report "Supporting Research and Development Program for Advanced Camera Tubes" by O. Choi, S. Gray, R. R. Handel, Contract No. AF33(616)6682, December 1961, pp 99-119.
- 2 O. Schade, "Image Gradation, Graininess and Sharpness in Television and Motion Picture Systems," Journal of the SMPTE, (1955). N_e is the equivalent rectangular passband of the aperture. It is equal, by definition, to the area under the squared sine-wave spectrum.

See also, "Field Effect on Glass Image Orthicon Target" section in this report.
- 3 O. Schade, Private Communication.
- 4 O. Schade, Loc cit.
- 5 Image orthicons with structured targets do not have a well defined knee as found with other close-spaced image orthicons.
- 6 Loc. Cit. pp 172-177.
- 7 O. Schade, Loc. Cit.
- 8 "Electron Optics of Cylindrical Electric and Magnetic Fields," Rose, A., Proc. IRE, 28, 30 (1940).
- 9 H. Moss, "A Note on Anomalous Radial Velocity Spectra from Rough Thermionic Emitters," Jour. Elect. and Cont. 11, 289 (1962).
- 10 Guns fabricated in Princeton had the cathode-to- G_1 measured and set to 0.005 inches by using an optical depth gauge on the finished smoothed cathode. Guns fabricated at the Electron Tube Division have this distance set mechanically to 0.010 inch before the cathode coating is applied. Final spacing depends on coating thickness.
- 11 H. Moss, loc. cit.
- 12 Jackson, Classical Electrodynamics, p 420. These relations are derived, for slowly varying magnetic fields, from the adiabatic invariance condition: $P_{\perp}^2 / B = \text{a constant}$ where P_{\perp} is the momentum perpendicular to B.
- 13 Jesse J. Crosby, "Vapor Plating of Aluminum on Steel" ASD-TDR 62-907

DISTRIBUTION:

ACTIVITIES AT WPAFB

~~AS~~NXRR (Library)

ASNXR (3)

ASRNR-31 (2)

ASRNE-42 (15)

AFIT (Library)

ASEP

OTHER DEPT OF DEFENSE ACT.

Air Force

RADC(RCSGA)

Attn: Mr. Kesselman

Griffiss AFB, NY

AFSWC (SWOI)

Kirtland AFB, NMex

AFMTC

Attn: Technical Library (MU-135)

Patrick AFB, Fla

RADC (RCSSL-1)

Attn: Documents Library

Griffiss AFB, NY

APGC (PGTRI)

Eglin AFB, Fla

BSD (WDTG)

AF Unit Post Office

Los Angeles 45, Calif.

AFMDC (MDGRT-1)

Holloman AFB, NMex

ESD

LG Hanscom Fld

Bedford, Mass

SSD

AF Unit Post Office

Los Angeles 45, Calif.

Navy

Chief, BuShips

Attn: Mrs. F. R. Darne

Code 691A

Wash 25, DC

Chief, NRL

Bldg 33, Rm 105

Wash 25, DC

Naval Ordnance Test Sta

Attn: Mr. J. Rughe

1207 Michelson Lab.

China Lake, Calif.

Naval Ordnance Lab.

Attn: Mr. Nordseth

Corona, Calif

Army

Commanding General

USAERDL (WARfare Vision Br)

Attn: Mr. C. Freeman)

Ft. Belvoir, Va

Commanding Officer

USASRDL (SIGRM/EL-PRG)

Ft. Monmouth, NJ

Commanding Officer

USAEPG

Attn: Combat Area Surveillance

Department

Ft. Huachuca, Ariz

Commanding General

Frankford Arsenal

Attn: Dr. M. L. Chwalow, 1130

Philadelphia 37, Pa

DISTRIBUTION: (CONT'D.)

OTHER U. S. GOV'T. AGENCIES

DDC (TIPCR) (30)

Cameron Station
Alexandria, Va

Advisory Group on Elect. Devices (4)

Attn: Secy, Working Group on
Special Devices

346 Broadway, 8th Floor
New York 13, NY

Office of Technical Services (10)

1200 S. Eads St.
Arlington, Va

NON-GOV'T. INDIVIDUALS & ORGS.

The Rand Corp

Attn: Librarian
1700 Main St
Santa Monica, Calif

Westinghouse Electric Corp (3)

Attn: Mr. John Basista
32 N. Main St
Dayton 2, Ohio

General Electric Co

Pickup Tube Operation

Power Tube Dept

Attn: Dr. H. Hannam
Bldg 6, Electronics Park
Syracuse, NY

Univ. of Minnesota
Institute of Technology
Dept of Electrical Engr
Attn: Dr. W. G. Shepherd
Minneapolis, Minn

Mass. Inst of Tech
Lincoln Lab.
Attn: Library
P. O. Box 73
Lexington 73, Mass

ITT Federal Labs.
Attn: Reports Librarian
3301 Wayne Trave
Ft. Wayne 1, Ind

Hallamore Electronics Div
Attn: R. VanWechel
714 N. Brookhurst St
Anaheim, Calif.

DISTRIBUTION: (CONT'D.)

OChoi
CWBizal
DWEpstein
PGHerold
SGray, Princeton
REHoffman
HFHafker, Chicago
FFMarinaro
BHVine
PMurray, Princeton
ARotow
HJohnson, Princeton
FAJordano
MEMarkell, Newark
FDMarschka
RENelson/GRivers
KCHarding, Los Angeles
PKWeimer, Princeton
WAZalesak, Princeton
RWEngstrom
MPetrisek

<p>1. Camera Tube 2. Electron Gun 3. Electron Beam 4. Storage Target, Aluminum Oxide 5. Film</p> <p>1. AFSC Project 4156, Task 415605 II. Contract AF33(65)76-59 III. Radio Corporation of America, Lancaster, Pennsylvania IV. Gray, S. et al V. In D.D.C. Collection</p>	<p>Aeronautical Systems Division, AF Armistice Laboratory, Electronic Technology Division, Wright-Patterson AFB, Ohio. Rpt. No. ASD-TN 63-433, APPLIED RESEARCH ON HIGH RESOLUTION CAMERA TUBES Technical Documentary Report, March 1963, 115 pages including illustrations, tables, references.</p> <p>Unclassified Report</p> <p>Image cathodes with structured targets were tested using a new cycled test set which separates the functions of exposure and read-out by a selected time interval. Resolution of image cathodes, when cycled in a manner corresponding to film scan read-out, has exceeded 50 percent line-pairs per mm at 500 TV lines/inch. Possible means of increasing resolution toward the contrast objective of 1500 TV lines/inch are discussed.</p> <p>Electron gun resolution, measured at high velocity, was nearly doubled during the year. Improvement was achieved by annealing the mixed ceramic cathode coating.</p> <p>The procedure used to increase targets is explained in detail.</p> <p>Toward the end of 1962 the procedure used to process targets was revised. These revisions resulted from the gradual evaluation of testing and methods procedures. The revised procedure is explained in detail.</p> <p>The processing procedure for "charged pore targets" is explained in detail.</p> <p>Images fabricated with integral non-plug type targets made with Penitop resist showed a considerable reduction in dark current. The processing procedure of targets made with Penitop resist is explained in detail.</p>	<p>1. Camera Tube 2. Electron Gun 3. Electron Beam 4. Storage Target, Aluminum Oxide 5. Film</p> <p>1. AFSC Project 4156, Task 415605 II. Contract AF33(65)76-59 III. Radio Corporation of America, Lancaster, Pennsylvania IV. Gray, S. et al V. In D.D.C. Collection</p>	<p>Aeronautical Systems Division, AF Armistice Laboratory, Electronic Technology Division, Wright-Patterson AFB, Ohio. Rpt. No. ASD-TN 63-433, APPLIED RESEARCH ON HIGH RESOLUTION CAMERA TUBES Technical Documentary Report, March 1963, 115 pages including illustrations, tables, references.</p> <p>Unclassified Report</p> <p>Image cathodes with structured targets were tested using a new cycled test set which separates the functions of exposure and read-out by a selected time interval. Resolution of image cathodes, when cycled in a manner corresponding to film scan read-out, has exceeded 50 percent line-pairs per mm at 500 TV lines/inch. Possible means of increasing resolution toward the contrast objective of 1500 TV lines/inch are discussed.</p> <p>Electron gun resolution, measured at high velocity, was nearly doubled during the year. Improvement was achieved by annealing the mixed ceramic cathode coating.</p> <p>The procedure used to increase targets is explained in detail.</p> <p>Toward the end of 1962 the procedure used to process targets was revised. These revisions resulted from the gradual evaluation of testing and methods procedures. The revised procedure is explained in detail.</p> <p>The processing procedure for "charged pore targets" is explained in detail.</p> <p>Images fabricated with integral non-plug type targets made with Penitop resist showed a considerable reduction in dark current. The processing procedure of targets made with Penitop resist is explained in detail.</p>	<p>1. Camera Tube 2. Electron Gun 3. Electron Beam 4. Storage Target, Aluminum Oxide 5. Film</p> <p>1. AFSC Project 4156, Task 415605 II. Contract AF33(65)76-59 III. Radio Corporation of America, Lancaster, Pennsylvania IV. Gray, S. et al V. In D.D.C. Collection</p>	<p>Aeronautical Systems Division, AF Armistice Laboratory, Electronic Technology Division, Wright-Patterson AFB, Ohio. Rpt. No. ASD-TN 63-433, APPLIED RESEARCH ON HIGH RESOLUTION CAMERA TUBES Technical Documentary Report, March 1963, 115 pages including illustrations, tables, references.</p> <p>Unclassified Report</p> <p>Image cathodes with structured targets were tested using a new cycled test set which separates the functions of exposure and read-out by a selected time interval. Resolution of image cathodes, when cycled in a manner corresponding to film scan read-out, has exceeded 50 percent line-pairs per mm at 500 TV lines/inch. Possible means of increasing resolution toward the contrast objective of 1500 TV lines/inch are discussed.</p> <p>Electron gun resolution, measured at high velocity, was nearly doubled during the year. Improvement was achieved by annealing the mixed ceramic cathode coating.</p> <p>The procedure used to increase targets is explained in detail.</p> <p>Toward the end of 1962 the procedure used to process targets was revised. These revisions resulted from the gradual evaluation of testing and methods procedures. The revised procedure is explained in detail.</p> <p>The processing procedure for "charged pore targets" is explained in detail.</p> <p>Images fabricated with integral non-plug type targets made with Penitop resist showed a considerable reduction in dark current. The processing procedure of targets made with Penitop resist is explained in detail.</p>	<p>1. Camera Tube 2. Electron Gun 3. Electron Beam 4. Storage Target, Aluminum Oxide 5. Film</p> <p>1. AFSC Project 4156, Task 415605 II. Contract AF33(65)76-59 III. Radio Corporation of America, Lancaster, Pennsylvania IV. Gray, S. et al V. In D.D.C. Collection</p>
--	---	--	---	--	---	--

<p>Aeronautical Systems Division, AF Avionics Laboratory, Electronic Technology Division, Wright-Patterson AFB, Ohio. Rpt. No. ASD-TDR 63-433, APPLIED RESEARCH ON HIGH RESOLUTION CAMERA TUBES Technical Documentary Report, March 1963, 115 pages including illustrations, tables, references.</p> <p>Unclassified Report</p> <p>Image cathodes with structured targets were tested using a new cyclot test set which separates the functions of exposure and read-out by a selected time interval. Resolution of image cathodes, when cycled in a manner corresponding to slow scan read-out, has exceeded 50 percent diameter response at 500 TV lines/inch. Possible means of increasing resolution toward the contract objective of 1500 TV lines/inch are discussed.</p> <p>Electron gun resolution, measured at high velocity, was nearly doubled during the year. Improvement was achieved by modifying the shield current cathode coating.</p> <p>The procedure used to process targets is explained in detail.</p> <p>Toward the end of 1962 the procedure used to process targets was revised. These revisions resulted from the gradual evaluation of testing and methods procedures. The revised procedure is explained in detail.</p> <p>The processing procedure for "unlabeled pure targets" is explained in detail.</p> <p>Image fabricated with internal non plug type targets made with Philips resist showed a considerable reduction in dark current. The processing procedure of targets made with Philips resist is explained in detail.</p>	<p>1. Camera Tube 2. Electron Gun 3. Electron Beam 4. Storage Target, Aluminum Oxide Film</p> <p>I. AFSC Project A156, Task A156C II. Contract AF33(65)76-59 III. Radio Corporation of America, Lancaster, Pennsylvania IV. Gray, S. et al V. In D.D.C. Collection</p>	<p>Aeronautical Systems Division, AF Avionics Laboratory, Electronic Technology Division, Wright-Patterson AFB, Ohio. Rpt. No. ASD-TDR 63-433, APPLIED RESEARCH ON HIGH RESOLUTION CAMERA TUBES Technical Documentary Report, March 1963, 115 pages including illustrations, tables, references.</p> <p>Unclassified Report</p> <p>Image cathodes with structured targets were tested using a new cyclot test set which separates the functions of exposure and read-out by a selected time interval. Resolution of image cathodes, when cycled in a manner corresponding to slow scan read-out, has exceeded 50 percent diameter response at 500 TV lines/inch. Possible means of increasing resolution toward the contract objective of 1500 TV lines/inch are discussed.</p> <p>Electron gun resolution, measured at high velocity, was nearly doubled during the year. Improvement was achieved by modifying the shield current cathode coating.</p> <p>The procedure used to process targets is explained in detail.</p> <p>Toward the end of 1962 the procedure used to process targets was revised. These revisions resulted from the gradual evaluation of testing and methods procedures. The revised procedure is explained in detail.</p> <p>The processing procedure for "unlabeled pure targets" is explained in detail.</p> <p>Image fabricated with internal non plug type targets made with Philips resist showed a considerable reduction in dark current. The processing procedure of targets made with Philips resist is explained in detail.</p>	<p>1. Camera Tube 2. Electron Gun 3. Electron Beam 4. Storage Target, Aluminum Oxide Film</p> <p>I. AFSC Project A156, Task A156C II. Contract AF33(65)76-59 III. Radio Corporation of America, Lancaster, Pennsylvania IV. Gray, S. et al V. In D.D.C. Collection</p>
<p>Aeronautical Systems Division, AF Avionics Laboratory, Electronic Technology Division, Wright-Patterson AFB, Ohio. Rpt. No. ASD-TDR 63-433, APPLIED RESEARCH ON HIGH RESOLUTION CAMERA TUBES Technical Documentary Report, March 1963, 115 pages including illustrations, tables, references.</p> <p>Unclassified Report</p> <p>Image cathodes with structured targets were tested using a new cyclot test set which separates the functions of exposure and read-out by a selected time interval. Resolution of image cathodes, when cycled in a manner corresponding to slow scan read-out, has exceeded 50 percent diameter response at 500 TV lines/inch. Possible means of increasing resolution toward the contract objective of 1500 TV lines/inch are discussed.</p> <p>Electron gun resolution, measured at high velocity, was nearly doubled during the year. Improvement was achieved by modifying the shield current cathode coating.</p> <p>The procedure used to process targets is explained in detail.</p> <p>Toward the end of 1962 the procedure used to process targets was revised. These revisions resulted from the gradual evaluation of testing and methods procedures. The revised procedure is explained in detail.</p> <p>The processing procedure for "unlabeled pure targets" is explained in detail.</p> <p>Image fabricated with internal non plug type targets made with Philips resist showed a considerable reduction in dark current. The processing procedure of targets made with Philips resist is explained in detail.</p>	<p>1. Camera Tube 2. Electron Gun 3. Electron Beam 4. Storage Target, Aluminum Oxide Film</p> <p>I. AFSC Project A156, Task A156C II. Contract AF33(65)76-59 III. Radio Corporation of America, Lancaster, Pennsylvania IV. Gray, S. et al V. In D.D.C. Collection</p>	<p>Aeronautical Systems Division, AF Avionics Laboratory, Electronic Technology Division, Wright-Patterson AFB, Ohio. Rpt. No. ASD-TDR 63-433, APPLIED RESEARCH ON HIGH RESOLUTION CAMERA TUBES Technical Documentary Report, March 1963, 115 pages including illustrations, tables, references.</p> <p>Unclassified Report</p> <p>Image cathodes with structured targets were tested using a new cyclot test set which separates the functions of exposure and read-out by a selected time interval. Resolution of image cathodes, when cycled in a manner corresponding to slow scan read-out, has exceeded 50 percent diameter response at 500 TV lines/inch. Possible means of increasing resolution toward the contract objective of 1500 TV lines/inch are discussed.</p> <p>Electron gun resolution, measured at high velocity, was nearly doubled during the year. Improvement was achieved by modifying the shield current cathode coating.</p> <p>The procedure used to process targets is explained in detail.</p> <p>Toward the end of 1962 the procedure used to process targets was revised. These revisions resulted from the gradual evaluation of testing and methods procedures. The revised procedure is explained in detail.</p> <p>The processing procedure for "unlabeled pure targets" is explained in detail.</p> <p>Image fabricated with internal non plug type targets made with Philips resist showed a considerable reduction in dark current. The processing procedure of targets made with Philips resist is explained in detail.</p>	<p>1. Camera Tube 2. Electron Gun 3. Electron Beam 4. Storage Target, Aluminum Oxide Film</p> <p>I. AFSC Project A156, Task A156C II. Contract AF33(65)76-59 III. Radio Corporation of America, Lancaster, Pennsylvania IV. Gray, S. et al V. In D.D.C. Collection</p>